SPREADING OF CHEMICALS ON ICE AND SNOW

by

Peter Kawamura
Donald Mackay
Michael Goral
University of Toronto
Toronto, Ontario

This report has not undergone detailed technical review by Conservation and Protection and the content does not necessarily reflect the views and policies of Environment Canada. Mention of trade names or commercial products does not constitute endorsement for use.

This unedited version is undergoing a limited distribution to transfer the information to people working in related studies. This distribution is not intended to signify publication and, if the report is referenced, the author should cite it as an unpublished report of the Directorate indicated below.

Any comments concerning its content should be directed to:

Environment Canada
Environmental Protection Directorate
River Road Environmental Technology Centre
Ottawa K1A 0E7

EE-79

December 1986

SPREADING OF CHEMICALS ON ICE AND SNOW

Peter Kawamura
Donald Mackay
Michael Goral

Department of Chemical Engineering
and Applied Chemistry

University of Toronto

Report for Environment Canada
March 1986
DSS Contract KE 145-5-147
M. Fingas - Scientific Authority

ABSTRACT

A relatively simple, liquid spill behaviour model has been developed which includes terms for the extent and rate of spreading, as well as absorption, evaporation and snow and ice dissolution. Experiments were performed on snow and ice surfaces to determine the spreading behaviour and characteristics and the general phenomena which occur when various chemicals are spilled on these surfaces. The chemicals studied were: m-xylene, n-pentanol, bayol (white mineral oil), and light and heavy mineral oils.

The final spill area and the spreading rate results were correlated with the spill volume, chemical viscosity and snow depth and properties, in dimensional and dimensionless form. These correlations can be viewed as comprising part of the general spreading model, and are believed to enable predictions to be made of the spreading behaviour for most chemicals under actual spill conditions.

To document the extent to which a chemical interacts with, or dissolves snow and ice, a classification system was developed. Chemicals were categorized into one of three groups, based on the solubility of water/ice in the chemical. Most of the liquid chemicals on Environment Canada's list of Priority Hazardous Materials were classified into one of three groups by combining the solubility data from the literature and by performing simple experimental solubility measurements.

It is hoped that the results of this study will form the basis for future research into the various simultaneous processes which occur when chemicals are spilled on these and other surfaces.

RÉSUMÉ

On a élaboré un modèle relativement simple du comportement des matières liquides déversées qui tient compte du degré et de la vitesse d'étalement, de l'absorption, de l'évaporation et de la dissolution de la neige et la glace. Pour ce, on a déterminé au moyen d'expériences le comportement et les caractéristiques d'étalement de divers produits chimiques déversés sur des surfaces de neige et de glace ainsi que les phénomènes généraux se produisant alors. Les produits qui ont été étudiés sont le m-xylène, le n-pentanol, le "bayol" (huile minérale blanche), et des huiles minérales légères et lourdes.

On a mis en corrélation les résultats pour l'étendue finale de la nappe du liquide déversé et la vitesse d'étalement avec les données sur le volume déversé, la viscosité du produit et l'épaisseur ainsi que les propriétés de la neige, de façon dimensionnelle et non dimensionnelle. Les corrélations établies peuvent être considérées comme faisant partie du modèle général de l'étalement, et on croit qu'elles permettent de faire des prévisions concernant le comportement d'étalement de la plupart des produits chimiques en conditions réelles.

On a élaboré un système de classification pour rendre compte de la façon dont un produit chimique interagit avec la neige et la glace ou dissout la neige et la glace. Les produits ont été classés en trois groupes d'après la solubilité de l'eau/glace dans chacun. On a classé la plupart des produits chimiques liquides figurant dans la liste des matières dangereuses d'intérêt prioritaire d'Environnement Canada dans trois groupes après avoir examiné les données publiées sur la solubilité et effectué des mesures expérimentales simples de la solubilité.

On espère que les résultats de cette étude pourront servir à d'autres recherches sur les divers phénomènes se produisant simultanément lorsque des produits chimiques sont déversés sur la neige et la glace ainsi que sur d'autres surfaces.

LIST OF FIGURES

Figure		Page
3.1	Interfacial Tensions Which Influence Spreading (after Chen and Charles, 1976)	10
3.2	Transport of Chemicals in Snow Media	12
4.1	Contact Angle Experiment: Heavy Mineral Oil on Ice Surface	26
4.2	Artificially Prepared Rough Ice Surface	26
4.3	Experimental Apparatus for Small-Scale Ice Experiments	27
4.4	Spill of 50 mL of Xylene on Rough Ice Surface	27
4.5	Ice Surface for Outdoor Experiments	28
4.6	Release of Chemical Onto Ice Surface	28
4.7	Set-up for Outdoor Ice Experiments	29
4.8	Spill of Pentanol on Ice	29
4.9	Snow Spreading Apparatus	30
4.10	Snow on Ice Spreading Apparatus	30
4.11	Spill of Bayol on Snow	31
4.12	Spill of Ethanol on Snow	31
5.2.1	Plot of Cos θ_e on Glass vs. Liquid Surface Tension	38
5.2.2	Plot of Cos θ_e on Ice vs. Liquid Surface Tension	39
5.3.1	Effect of Viscosity on Final Spill Depth on Glass	41
5.4.1	Effect of Viscosity on Final Spill Depth on Ice	43
5.4.2	Effect of Spill Volume on Final Spill Depth	45
5.4.3	Correlation of Final Spill Area on Ice	47
5.4.4	Effect of Viscosity on the Spreading Time Constant (Smooth Ice)	51
5.4.5	Effect of Viscosity on the Spreading Time Constant (Average of Two Rough Ice Surfaces)	52

Figure		Page
5.4.6	Spill Area-Time Profile for Bayol and Pentanol on Smooth Ice	53
5.4.7	Effect of Spill Volume on Spreading Time Constant	54
5.4.8	Correlation of Ice Spreading Time Constant	56
5.4.9	Spreading Kinetics of Bayol on Smooth Ice	58
5.4.10	Spreading Kinetics of Xylene on Rough Ice	59
5.4.11	Spreading Kinetics of Light Mineral Oil (Outdoor Ice Experiment)	60
5.5.1	Spill of Bayol On Snow	62
5.5.2	Cross-Section Profile of Snow Experiment	62
5.5.3	Effect of Spill Volume on Snow Final Spill Depth	63
5.5.4	Effect of Snow Bulk Density on Final Spill Depth	65
5.5.5	Effect of Snow Depth on Final Spill Depth	66
5.5.6	Cross-Section Profile: Snow Depth 30 cm	67
5.5.7	Cross-Section Profile: Snow Depth 4 cm	67
5.5.8	Effect of Viscosity on Final Spill Depth in Snow	69
5.5.9	Surface Spreading of Heavy Mineral Oil on Snow	70
5.5.10	Channelling Effect of Heavy Mineral Oil	70
5.5.11	Cross-Section Profile of Heavy Mineral Oil	71
5.5.12	Correlation of Snow Final Spill Area	74
5.5.13	Effect of Snow Depth and Spill Volume on Time Constant	76
5.5.14	Effect of Snow Bulk Density on Time Constant	77
5.5.15	Effect of Chemical Viscosity on Snow Time Constant	78
5.5.16	Correlation of Snow Spreading Time Constant	80
5.5.17	Snow Spreading Kinetics of Pentanol	81
5.5.18	Snow Spreading Kinetics of Heavy Mineral Oil	82

Figure		Page
5.5.19	Spreading Kinetics of Bayol at Snow-Ice Interface	83
5.5.20	Spill of Ethanol Immediately After Discharge	88
5.5.21	Cross-Section Profile of Ethanol in Snow	88
5.5.22	Spreading of Ethanol at the Snow-Ice Interface	89
5.5.23	Cracks in the Underlying Ice Surface	89

LIST OF TABLES

Table		Page
2.1	Densities of Snowcover	5
3.1	Permeability of Various Media	13
4.1	Experimental Conditions for Snow Spreading Experiments Involving Insoluble Chemicals	24
4.2	Conditions for Snow Spreading Experiments Involving Water-Soluble Chemicals	25
5.1	Classification of Chemicals Based on Solubility	32
5.2	Solubilities of Ice in n-Propanol at Various Ice Mass Fractions	35
5.3	Experimental Contact Angles and Interfacial Energies for Various Chemicals on Ice	36
5.4	Interfacial Tension and the Final Spill Depth	40
5.5	Effect of Roughness on the Final Spill Depth	42
5.6	Drainage of Bayol at Different Snow Depths	64
5.7	Effect of Snow Crystal Type on Final Area	72
5.8	Snow Density Parameter	73
5.9	Temperature of Group 3 Chemicals After Spill Onto Snow	85
5.10	Constants for Equations 5.6 and 5.7.	86

TABLE OF CONTENTS

ABSTRACT		i
RESUME		ii
LIST OF FIGURES		iii
LIST OF TABLES		vi
CONCLUSIONS		ix
1	INTRODUCTION	1
2	PROPERTIES OF SNOWCOVER AND ICE	3
2.1	Snowcover Distribution in Canada	3
2.2	Snowcover Properties	3
2.3	Snow and Ice on Lakes	6
3	SPREADING MODELS AND THEORY	8
3.1	Existing Spreading Models	8
3.2	Theory of Spreading	9
3.3	Behaviour of Chemicals on Snow and Ice	11
3.4	Development of a General Spreading Model	15
4	EXPERIMENTAL	18
4.1	Solubility Studies	18
4.2	Spreading on Ice	18
4.2.1	Spreading Experiments on Glass	19
4.2.2	Contact Angle Measurements	20
4.2.3	Spreading on Artificially Prepared Ice Surfaces	20
4.2.4	Outdoor Ice Spreading Experiments	21
4.3	Spreading Experiments on Snow	22
4.3.1	Snow-on-Glass Spreading Experiments	22
4.3.2	Snow-on-Ice Spreading Experiments	23
5	RESULTS AND DISCUSSION	32
5.1	Solubility Studies	32
5.2	Contact Angles	36
5.3	Spreading of Chemicals on Glass	40
5.4	Spreading on Ice Surfaces	42
5.4.1	Effect of Chemical Viscosity on the Final Spill Area	42

5.4.2 Effect of Spill Volume on the Final Spill Area 44
5.4.3 Correlation of the Final Spill Area on Ice 46
5.4.4 Kinetics of the Spreading on Ice 49

5.5 Spreading on Snow 61

5.5.1 Spills of Insoluble Chemicals on Snow 61
5.5.2 Effect of Spill Volume on the Final Area 61
5.5.3 Effect of Snow Properties on the Final Area 64
5.5.4 Effect of Chemical Viscosity on the Final Area 68
5.5.5 Correlation of the Final Spill Area on Snow 68
5.5.6 Kinetics of Spreading on Snow 75
5.5.7 Spreading Behaviour of Water Soluble Chemicals 84

5.6 Application of This Study to an Actual Spill Situation 90

5.7 Sample Calculations 92

NOMENCLATURE 96

REFERENCES 98

ACKNOWLEDGEMENTS 101

APPENDIX A: SOLUBILITY DATA 102

APPENDIX B: CONTACT ANGLE DATA ON GLASS 104

APPENDIX C: EXPERIMENTAL DATA - ICE EXPERIMENTS 105

APPENDIX D: EXPERIMENTAL DATA - SNOW EXPERIMENTS 106

CONCLUSIONS

Spreading behaviour of chemicals on two surfaces, snow and ice, was studied. Spreading experiments were conducted on these surfaces, using various chemicals. It was found that the extent and the rate of the spreading of chemicals on an ice surface is dependent mostly on the spill volume and the chemical viscosity. Under experimental conditions, the time of spreading was in the order of minutes to hours, for most chemicals. For a spill on snow surfaces, the snow depth and its properties were also found to be important. The spreading time in this medium was found to be in the order of hours to days. Furthermore, results of experiments involving water miscible chemicals on ice and snow covered ice surfaces revealed that cracking, and subsequent migration of the chemical through these cracks can occur.

The experimental data, in particular the final spill areas (subsurface spill area for snow) and the spreading rates were correlated in both dimensional and dimensionless form. These correlations are believed to be applicable for chemicals in which water is not completely soluble but can be used with caution for water-soluble chemicals for spills on ice.

These correlations form part of the general spreading model which was also developed in this study. The model is relatively simple, and contains terms for evaporation, absorption and snow and ice dissolution. It is recommended that further studies be conducted to quantify the effect of snow dissolution, evaporation from snow, and absorption characteristics in snow media.

Finally, a simple three-group classification system was proposed to categorize chemicals based on their ability to dissolve ice and snow. By conducting experiments and obtaining data from the literature, most of the liquid chemicals on Environment Canada's list of Priority Hazardous Materials were classified into one of three groups.

1. INTRODUCTION

When planning for, or responding to, chemical spills, it is useful to know the likely spreading characteristics of the chemical. In particular, it is helpful if the final spill area and the time necessary to reach that area can be predicted. Any special or unusual spill characteristics of the chemical such as tendency to react, or evaporate rapidly should also be known in advance. This study explores the spreading and behaviour of chemicals when spilled onto snow and ice, a common ground surface in much of Canada for much of the year.

The spill area, aside from quantifying the area of contamination, is required in the evaluation of the evaporation rate of the chemical, which in turn controls atmospheric concentrations. Possible hazard, or evacuation distances can be calculated based on the comparisons of the chemical atmospheric concentration to the toxic or flammable hazard concentrations. In addition, estimating the final spill area for spills on snow and ice is particularly important since the spill area is difficult to detect by eye for most liquid chemicals. On a snow surface, the chemical may penetrate downward in the snow and spread invisibly along the bottom of the snowcover.

Various models, such as that of Kawamura and Mackay (1986) have been developed to estimate the evaporation rate from a pool of chemical. The atmospheric chemical concentration can be determined from well established atmospheric dispersion models. On the other hand, there has been little study of the terrestial spreading behaviour of chemicals, especially on snow and ice surfaces.

There are additional effects that must be considered in the event of a chemical spill on snow and ice covered surfaces, as opposed to a spill on a ground surface. The most important is the extent to which the chemical interacts with, or dissolves snow/ice. For example, chemicals which are completely miscible with water, such as low molecular weight alcohols, will readily dissolve snow and ice, which results in an increase in spill volume. These chemicals, if spilled on or near a snow or ice covered body of water, may "eat through" the snow and ice to the underlying water. Furthermore, a strong acid may release sufficient heat on contact with ice to melt an appreciable quantity.

Examples of major chemical spills on snow and ice include the release of approximately 70 000 litres of vinyl chloride monomer onto snow covered ground as a result of a train derailment near Macgregor, Manitoba. This accident has been referred to as "The Macgregor Derailment". A full inquiry was held following this accident by the CTC (1980). More recently, a train derailment south of Parry Sound, Ontario resulted in the

leakage of sulphuric acid from seven cars, one of which dischaged most of its contents (50 000 L) in a small frozen lake (Toronto Star, Feb. 13, 1986).

This study is concerned with the understanding and the prediction of the behaviour of chemicals when spilled on snow and ice. The general objectives of this study are:

i. to describe the general phenomena which occur when various chemicals are spilled on ice and snow,

ii. to categorize chemicals according to the extent to which they can dissolve snow and ice,

iii. to provide methods to estimate the final spill area as a function of spill volume and other properties (This study is concerned with instantaneous spills, or spills in which a finite volume of chemical is released rapidly, as opposed to a continuous leak spill.),

iv. to estimate the time of spreading, and

v. to develop a model of general spill behaviour.

2. PROPERTIES OF SNOW AND ICE

In order to describe or model the spreading behaviour of chemicals on snow and ice, various properties and characteristics of snow/ice should be identified and known. The following sections describes briefly the properties and processes that occur within the ice and snowcover during the winter months. The facts and figures in this section are from Gray and Male (1981) unless otherwise stated.

2.1 Snowcover Distribution in Canada

Most of the surface area of Canada is covered by snow or ice during the winter months. The actual amount and the period during which the ground is covered by snow will vary greatly depending on the location, local land features, and atmospheric conditions.

For example, in Canada, the mean date of snowcover formation and disappearance vary from Dec 1/Apr 1 in southern Ontario to Sept 15/July 1 in the Arctic. Snowcover during the winter usually reaches the greatest depths in snowbelt areas to the lee of open waters and on windward slopes. The months of maximum snowcover for most regions are February and March, in which the mean maximum depth of snow may be as little as 30 to 70 cm in southern Ontario, the Prairies and the Arctic to as much as 160 cm in parts of Quebec, Newfoundland and British Columbia. Data on actual snow depths can be obtained from measurements conducted by synoptic observing weather stations. Monthly snow depth summaries are also published by individual agencies and all climate stations.

The type of ground surface also affects the snowcover depth. Kuz'min (1960) has determined the snow retention coefficients for various surfaces relative to virgin soil. This coefficient is a measure of the extent to which snow accumulates on different surfaces, with a reference value of 1.0 for virgin soil. The greatest local snowcover depth is likely to be in the vicinity of river beds, rushes, forest cutting and edge of forests, with a retention coefficient of 3.0-3.4. On the other hand, open ice has a coefficient of 0.4-0.5, which indicates that the snow depth is likely to be half that of local snowcover on soil. Although the magnitude of the coefficients depend on wind speed and other factors, this type of information, along with historical snow survey data may be useful in estimating the depth of snowcover when actual measurements are not available.

2.2 Snowcover Properties

The snowcover is formed by the deposition of snow crystals, which can have a large variety of sizes and

crystalline structure. Diameter of individual snow crystals can have a difference of two orders of magnitude, ranging from 50 microns to 5 mm. Magono and Lee (1966) have classified almost all types of natural snow crystals, which in their classification, total eighty. During and after the formation of the snowcover, the snow crystals are modified continuously by wind action and by a process known as metamorphism.

Wind action influences the packing arrangement of the snow crystals, which commonly results in hard packed snow and snow drifts. These effects are marked by an increase in snowcover density.

Metamorphism is a very complex phenomena which alters the snow particle shapes. In general, this process involves the transformation of the snow particle from a crystal structure to more or less rounded grains of ice. The size of these crystals can either increase or decrease, depending on the temperature gradient of the snowpack and external conditions. In thermodynamic terms, this is a spontaneous process, in which the snow crystals minimize their free energy by minimizing the ratio of surface area to volume.

The metamorphic process can also occur as a result of external energy sources, such as from an increase in pressure due to the weight of the upper snowcover and from thaw-freeze cycles. It is by repetition of these externally-aided metamorphic processes that forms high strength, high density (0.70-0.83 g/mL) ice-like snowcover. Although relatively large grains of ice can form strictly as a result of the change in free surface and internal energy of the crystals, it cannot match the density and strength of the snowcover produced by thaw-freeze and pressure metamorphism.

Classification of the crystalline nature of the snowpack has been difficult because each metamorphic process tends to produce a distinct snow particle. Existing classification systems, such as that of Klein et. al (1950) included parameters such as grain size, free water content, density and hardness. The National Research Council of Canada (1954) has classified grain shape into five broad categories:

Class a: Freshly deposited snow, excluding ice pellets, graupel (snow pellet) and hail
Grain Size: <0.5 mm (but crystals size can be as as large as 5 mm)

Class b: Settled snow, that has lost most of its crystalline character but fairly soft.
Grain Size: 0.5 - 1 mm.

Class c: Irregular or rounded grain shape as a result of thaw-freeze cycle. Dull appearance, fairly soft

when wet but very hard when frozen.
Grain Size: 1 - 2 mm.

Class d: Irregular shaped grains with facets, as a result of transformation under temperatures well below freezing. Sparkles under sunlight. Almost all of the settled snow in the Arctic falls into this category. Usually fairly hard.
Grain Size: 2 - 4 mm.

Class e: This snow is termed depth hoar. Hollow cup-shaped crystals. Produced under a long and uninterrupted cold period. Found mostly in the lower part of the snowcover.
Grain Size: >4 mm.

The grain sizes quoted above are estimates, and may fall outside of this range, depending on factors such as wind speed, temperature, the type of metamorphic process and external conditions.

Porosity of the snowcover, which is related to the density, is a property often used by engineers and scientists to describe a snowcover. This property, again, can vary greatly depending on factors listed earlier, and therefore cannot be associated strictly with grain shape or size. Nevertheless, typical values are listed in Table 2.1, compiled from Gray and Male (1981).

Table 2.1 Densities of Snowcover

Snow Type	Density (g/mL)
Settling Snow	0.07 - 0.09
Average Wind Toughened Snow	0.28
Hard Wind Slab	0.35
New Firn* Snow	0.4 - 0.55
Advanced Firn Snow	0.55 - 0.65
Thawing Firn Snow	0.6 - 0.7

* snow consolidated partly into ice.

Additional complexities arise when properties such as type and size of crystal, temperature, and density vary with depth in a snowpack. This is especially true in regions of heavy and frequent snowcover. Although type "a" and "b" crystals, which have a relatively low density are found close to the surface of the snowcover, "c, d and e" crystals may exist in any order,

depending on the nature of the previous snowfalls and the preceeding transformation processes.

The type of metamorphic process that occurs within the snowcover is determined largely by the presence and magnitude of the temperature gradient in the snow. In isothermal snowcover, destructive metamorphic processes usually take place to produce rounded, small grains of relatively high density. If a temperature gradient is present, (>0.1 deg C/cm) constructive metamorphism occurs which involves the redistribution of mass within the snowcover. This results in the growth of relatively large grains. An example is the type "e" or depth hoar snow crystals which are frequently found at the base of a snowcover. Temperature gradients within the snow usually occur in very thin snowcover and under extremely cold air temperatures.

Both types of metamorphic processes can occur in the same snowcover at different depths. Therefore, at the end of the winter, a snowcover which did not experience periods of snow melt may consist of light snow crystals on top, followed by dense products in the middle, and less dense, looser crystals at the base. However, a region which experiences frequent snowfalls, occurring under varying meteorological conditions will have a highly stratified snowcover. Stratification refers to the ice layers within the snowcover which are formed by either: surface melt, usually as a result of radiation, which is then refrozen; or the addition of freezing rain, which can produce thick ice lenses. In both cases, the ice layers can be covered by new snow. Stratification of the snowpack, in general, tends to be spatially heterogeneous and not horizontally uniform.

2.3 Snow and Ice on Lakes

Ice cover during the winter months can occur as a result of freezing, after a period of snow melt or rainfall or more commonly, freezing of natural bodies of water, such as lakes and rivers. In Canada, approximately 8% of the surface area is covered by freshwater, with the majority covered by ice and or snow for a significant period each year.

The most common ice cover over lakes is composed of columnar crystals, which are oriented in the vertical direction, known as columnar or black ice. It is the organization of these crystals and the impurities in the crystal boundaries that determine the strength, melting, and breaking properties of the ice sheet. The density of black ice depends on the rate at which freezing occurs. Under rapid ice growth, the ice formed may have a density of 0.895 g/mL or less due to greater air bubble entrapment. This is less than the maximum density of 0.917 g/mL for "pure" ice.

In regions with low snowfall and very cold temperatures,

black ice may grow to a depth of 3 m. However, snowcover on the ice tends to slow down the formation of the ice cover due to its insulating effect. Black ice can usually withstand winter's load of snow without cracking but cracking may be induced by rapid changes in air temperature. Water may flow up through the cracks by capillary action in the snowcover to produce a layer of slush on top of the ice surface. This slush then usually freezes to produce a new layer of solid ice on top of the original ice sheet. The new ice layer is granular and opaque, and is called white ice. White ice may also be produced by flooding on the snow, which occurs as a result of rain.

Although white and black ice may have different properties, both are relatively impermeable, effectively suppressing exchange of gases and other masses.

Snowcover on lakes is characterized by significant temperature gradients, which promote constructive metamorphic processes. Therefore, the snowcover is usually distinguished by large grains and relatively low density. Snowcover on lakes is generally thinner than regional snowcover on land, mainly due to redistribution and compaction by wind.

3. SPREADING MODELS AND THEORY

3.1 Existing Spreading Models

Spreading and behaviour of chemicals, especially crude oils on water surfaces have received extensive study by a number of researchers such as Fay (1969). In comparison, studies of the spreading on solid surfaces have received little attention.

Raisbeck and Mohtadi (1974) developed a model for crude oil spreading from a continuous leak on permeable and impermeable surfaces. Although simple equations were presented to estimate the spreading rate and thickness of the oil film, the applicability of this study to instantaneous, or rapid leak rate spills is uncertain. In addition, one of the input parmeters required for this model is the value of the chemical contact angle but no procedure or equations are presented with which to estimate this angle. Experimental measurements of the contact angles on a specific surface could be made but this approach becomes impractical for a general model involving many chemicals and variably rough surfaces.

There have been several studies concerning the spreading and behaviour of crude oils in the Arctic environment. McMinn (1972), in estimating the final spill area on snow and ice, employed a term called the effective roughness height of the spill surface as criteria for termination of spreading . Hoult et al. (1975) used a statistical approach to determine the range of effective roughness heights in Arctic areas of high spill potential. The drawback of these approaches is that the model should rely on parameters which are well established, such as physical-chemical properties of the chemical, instead of depending heavily on the nature of the spill surface, which is usually unknown.

Chen et al.(1974) and Chen and Charles (1976) studied the rate of spreading of crude oil on an ice surface for two of the three spreading stages known to exist. These spreading stages are identified in Section 3.2. Chen's studies correlated the data in dimensionless form, for the latter two spreading regimes. Combining these results into a general spreading model proved to be difficult since the initial spreading stage, the time of transition of the stages that follow and the time of cessation of spreading were not addressed.

Currently, Belore et al. (1986) are attempting to model the simultaneous processes of evaporation, infiltration and spreading of chemicals on hard packed clay and grass surfaces. Their approach involves solving the equations of motion in a multidimensional matrix by a numerical computer model. Experiments are also being conducted to validate this model.

3.2 Theory of Spreading

When a spill occurs, in which a certain volume of chemical is released rapidly onto an impermeable surface such as ice, the spill dimensions increase rapidly during the period immediately after the discharge. The force which promotes spreading is due to gravity, and is countered by inertial and viscous forces. The actual rate of spreading will depend mainly on the spill rate and the chemical viscosity.

As the spill proceeds, the rate of spreading decreases until spreading finally stops. It has been established by several workers, such as Fay (1969) that the spreading process can be divided into three distinct stages. In each of these stages, one spreading force is balanced by one retarding force. The three stages are: gravity-inertia, gravity-viscous, and surface tension-viscous. Chen's studies involved plotting the log of the spill area or radius versus log time in the expectation that three linear regions, corresponding to the three spreading stages, will be obtained. Specifically, plotting log area versus log time will yield a slope of 0.4 in the gravity-viscous regime and (1-b)/2 in the surface tension-viscous stage, where b is a constant.

The third stage of spreading is the most complicated and least understood. In this stage, the spreading rate is determined by the combination of chemical-air, chemical-solid, and solid-air interfacial tensions, as well as the chemical viscosity, the nature of the solid surface (eg. the type of solid and its roughness), the rate of evaporation of the chemical and wind speed. The latter effect on spreading will be most significant for chemicals of low viscosity.

The three interfacial tensions and the viscous force, Fv, which influence spreading are illustrated in Figure 3.1 for an ice surface. It can be seen that the three forces act to produce a net spreading force of:

$$\Delta\sigma = \sigma_i - (\sigma_{ic} + \sigma \cos\theta) \qquad (3.1)$$

where $\Delta\sigma$ is the net spreading force, σ_i is the air-solid interfacial tension, or the solid surface tension; σ_{ic} is the liquid-solid interfacial tension, and σ is the liquid-air interfacial tension, or the liquid surface tension; and θ is the contact angle. The contact angle is the angle at which the chemical contacts the ice surface. The magnitude of this angle depends on the relative values of the three interfacial tensions.

During the surface tension-viscous spreading stage, the contact angle and the net spreading force decrease in magnitude to an equilibrium value, and to a value of zero, respectively.

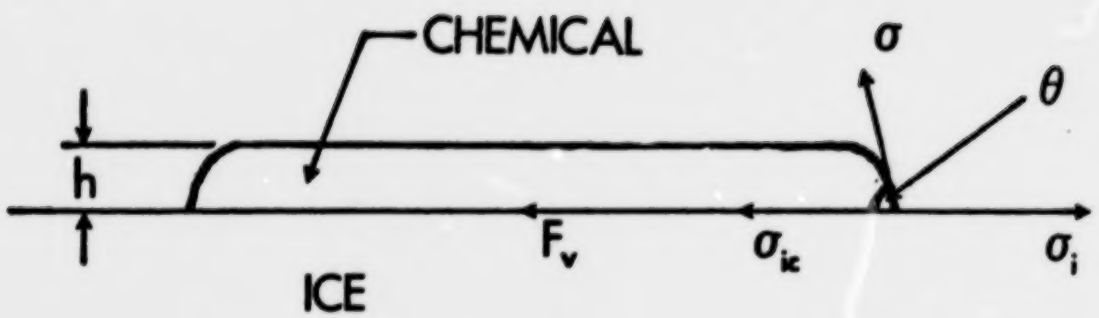

Figure 3.1 Interfacial Tensions Which Influence Spreading (After Chen and Charles, 1976)

At equilibrium, the interfacial tensions and the contact angle are related by:

$$\sigma_i = \sigma_{ic} + \sigma \cos \theta_e \qquad (3.1a)$$

where θ_e is the equilibrium contact angle.

The equilibrium contact angle is a property of the chemical and the solid surface, and is often used as an indication of the wettabillity of the solid surface. The smaller the equilibrium contact angle, the higher the wettabillity, or "spreadability". Banerji (1981) has proposed a term called the degree of spreading, which is the ratio of the solid-liquid adhesion energy and the cohesive energy of the liquid.

$$\text{Degree of spreading} = (1 + \cos \theta_e)/2 \qquad (3.2)$$

Thus, a chemical with an equilibrium contact angle of zero degrees (degree of spreading equal to 1) will spread completely on the solid surface, while a chemical with a degree of spreading of zero, or an angle of 180 degrees will not wet or spread on the solid. It is possible, if the solid-liquid adhesion energy exceeds the energy of cohesion, to have a case where there is "no contact angle". The rate of spreading will be very rapid, and is expected to depend on the magnitude of the difference of the two energies. Equations 3.1a and 3.2 do not apply to this situation since the system is not in equilibrium.

3.3 Behaviour of Chemicals on Snow and Ice

It is expected that most chemicals will have a fairly high degree of spreading on ice. This is based on the relatively high value of the ice-air interfacial tension, which was determined to be 80.2 dynes/cm by Spelt et al.(1982). One characteristic of high energy solids, such as ice, is their high wettabillity to most fluids. Thermodynamically, surface tension, or interfacial tension can be thought of as being a form of free energy. Since the tendency for all systems is to minimize their free energy, many solid surfaces achieve this by allowing a liquid to spread. The extent of spreading for a certain volume of liquid is, in general, greater for a high energy solid than for a solid with a lower surface tension.

Liquid chemical spills on snow surfaces are more complex than on impermeable surfaces such as ice. The processes include spreading on the surface (if any), absorption into the snow, dissolution of the snow (for water soluble chemicals) and spreading on and possible infiltration into the underlying surface. The transport of a chemical in the snow media is illustrated in Figure 3.2.

Snow has the ability to absorb a substantial amount of fluid. Table 3.1 shows that snow has a relatively high porosity

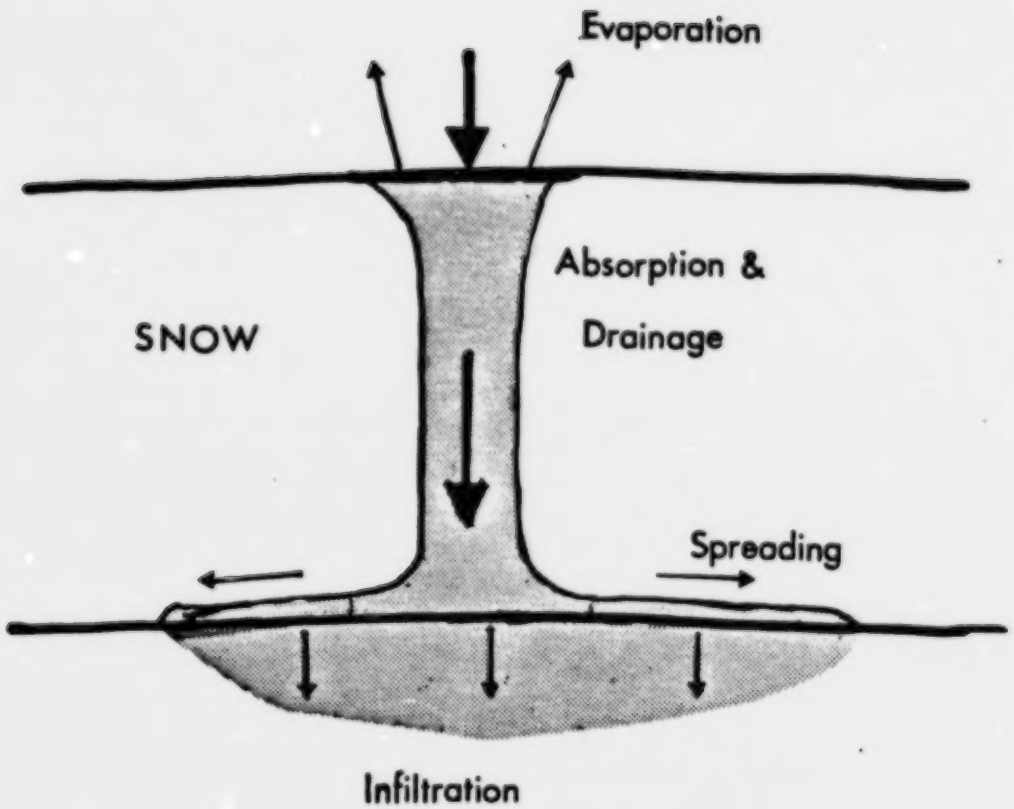

Figure 3.2 Transport of Chemicals in Snow Media

compared to other porous media. Permeability, which is also shown in Table 3.1, can be thought of as the "fluid conductivity" of the porous medium. The actual infiltration rate of liquids into the snow may be determined using Darcy's Law, as outlined by Collins (1961).

The variables which determine whether the spilled chemical occurs as a pool at the surface of the snow (or any porous surface) are the chemical leak rate per unit area of the spill area and the transmissive capacity of the snow, which is the Darcy flux for saturated conditions. Zukovs et al. (1986) state that a pool of chemical will form if the ratio of the chemical leak rate and the pool area is greater than the transmissive capacity of the snow. Under these conditions, the pool will increase in size until the two controlling variables are equal in magnitude.

Table 3.1 Porosity and Permeability of Various Media (Collins, 1961)

Substance	Porosity	Permeability (Darcys)
Loose Sand	0.37 - 0.50	20 - 180
Soils	0.43 - 0.54	29 - 140
Limestone	0.04 - 0.1	2 E-04 - 4.5 E-02
Snow	0.5 - 0.9+	0.01*

+ from current study
* from Overall, 1976

Note: 1 Darcy = 9.9 E-05 cm2

However, this principle is difficult to employ with reasonable accuracy under actual spill conditions since the transmissive capacity of the snow is highly dependent on snow properties such as crystal size, structure, and compaction, which can vary by an order of magnitude, as described in Section 2. Further, the leak rate is not always known. Therefore, instead of focusing on the surface of the snowcover, this study concentrates on the movement of chemicals within the snowcover, which is thought to be of greater importance.

The spilled chemical moves downward in the snow mainly by gravity force. This movement continues until the leading front reaches the bottom of the snowcover. At this time, the chemical front may spread radially along the bottom of the snowcover, while the remaining chemical continues to drain downward. In addition, some of the chemical may migrate upwards within the snow, from the bottom of the snowcover, by capillary action. Infiltration into the underlying ground cover may also occur. However, it is not uncommon during the winter months for the

ground to consist of a surface layer of frozen melt water or frozen water in the pores of the soil, which would prevent or slow down the infiltration rate into the ground. Another common underlying material is a sheet of ice, which is impermeable to most chemicals.

The actual radial spreading rate within the snowcover will probably depend on properties and characteristics of the snow cover, and properties of the chemical, such as viscosity, density and surface tension. Variables such as the chemical discharge rate and the depth of snowcover may also influence spreading.

Another property which will influence spreading is the ability of the chemical to dissolve ice and snow. Chemicals which can dissolve a significant amount of snow/ice will incur a change in their physical-chemical properties. An increase or decrease in temperature of the water-chemical-snow/ice mixture may also occur depending on the rate of snow/ice dissolution and the heat of dissolution. Completely water soluble chemicals, such as sulphuric acid and ethanol, may dissolve snow/ice until:

i. there is no more snow and ice;

ii. the concentration of water in the chemical reaches a point such that the surrounding temperature equals the freezing point temperature of the water-chemical mixture, at which point the mixture may freeze;

iii. the system can no longer draw sufficient heat from the surroundings to obtain the required heat of dissolution.

The extent to which the chemical dissolves snow and ice may be estimated by the determination of the solubility of ice/water in the chemical, which is the maximum amount of snow/ice that dissolves in the chemical at a specific temperature. This is the solubility of ice/water in the chemical and is different from the usual measurement of solubility, which is the solubility of chemical in water. The solubilities of water in various chemicals are reported in the literature, but the list is relatively small. One of the objectives of this study is to classify chemicals based on the amount of snow/ice they dissolve. This procedure is described in Section 4.

It should be noted that for water miscible chemicals such as ethanol, there is no distinction between the two types of solubilities, ie. the water-in-chemical and the chemical-in-water solubilities are identical. In addition, the terms "soluble" and "miscible" are used interchangably in this report.

3.4 Development of a General Spreading Model

The spreading behaviour of a chemical on snow, ice or absorbing terrain is a very complex phenomena. Thus, it is likely that several models will be devised, each with a desired level of accuracy. It is believed that progress is best made in this subject area by postulating models, subjecting them to peer review and criticism in the expectation that the better and more useful models survive and are modified by other investigators. In this study, a novel general model is introduced which includes absorption, evaporation and snow and ice dissolution.

In this model, a basic area-time relationship is proposed of the form:

$$A = A_f \, (1-\exp(-(t/\gamma)^x)) \qquad (3.3)$$

where A is the area, A_f is the final area at infinite time (t) and γ and x are constants. Regardless of the value of x, the area is 63% of the final area when t equals γ. γ is thus a "spreading time constant". Increasing x slows down the initial spreading and accelerates the later spreading. It controls the slope of the A-t graph when t equals γ, a large value of x giving a large slope.

The final area, A_f, is estimated from the initial spill volume (V), the volume change (until spreading stops) due to evaporation, absorption, etc. (ΔV), and a final equilibrium spill depth on the surface (h_f), such that

$$V - \Delta V = A_f \, h_f \qquad (3.4)$$

ΔV is estimated as the algebraic sum of three terms:

$$\text{Loss due to evaporation} = h_e \, A_f \qquad (3.5a)$$

$$\text{Loss due to absorption in soil} = h_a \, A_f \qquad (3.5b)$$

$$\text{Gain due to dissolution of snow} = h_s \, A_f \qquad (3.5c)$$

$$\text{Therefore,} \quad \Delta V = A_f \, (h_e + h_a - h_s) \qquad (3.6)$$

In all cases the h terms represent mean values which apply at the time of cessation of spreading. For evaporation, it is postulated that

$$h_e = C_e \, K_e \, (Pv/RT) \, \gamma \qquad (3.7)$$

where C_e is a dimensionless constant, K_e is a mass transfer coefficient, (Pv/RT) is the dimensionless ratio of chemical concentration in air to concentration in the chemical phase, in which P is vapour pressure, v is molar volume, R is the gas

constant and T is absolute temperature. The time term is γ and C_e thus "corrects" for the change in area with time.

Similary for absorption we postulate,

$$h_a = C_a K_a \gamma \qquad (3.8)$$

where K_a is an absorption velocity controlled by the soil porosity.

For snow dissolution,

$$h_s = \phi H_s \qquad (3.9)$$

where ϕ is the volume fraction of water in the snow and H_s is the mean snow depth dissolved.

It follows that

$$A_f = V / (h_f + h_e + h_a - h_s) \qquad (3.10)$$

The final equation is:

$$A = \frac{V\,(1-\exp(-(t/\gamma)^x))}{h_f + [C_e K_e (Pv/RT) + C_a K_a]\gamma - \phi H_s} \qquad (3.11)$$

The advantage of this equation is that it is simple and contains terms for absorption, evaporation, and snow or ice dissolution. The constants which must be determined by experiment are as follows:

- γ - spreading time constant, which is expected to be primarily a function of viscosity
- x - slope term
- C_a - absorption constant
- C_e - evaporation constant
- h_f - final spill thickness which is expected to depend on the surface, viscosity and interfacial tension.

The terms K_a, P, V, T, K_e, ϕ, and H_s can be estimated directly from spill conditions and chemical properties, and are not adjustable.

The spreading time can be approximated by determining the time when the area equals 99% of the final area, using equation 3.3. The spreading time, t_f is:

$$t_f = (4.605)^{\frac{1}{x}} \gamma \qquad (3.12)$$

In this study, the final spill area and the spreading rate for chemicals on ice and snow were investigated. In particular, the experimental data were gathered to correlate the final spill

thickness, h_f, (or A_f, with h_e, h_a, h_s equal to zero), and the spreading time constant, with parameters such as the spill volume, chemical viscosity and snow properties. The experimental slope value, x, was also determined.

4. EXPERIMENTAL

4.1 Solubility Studies

The purpose of this study was to determine the solubility of ice/water in various chemicals. These results could then be used to classify chemicals according to the extent to which they can dissolve snow and ice. This investigation focused mainly on the liquid chemicals on the Environment Canada's list of priority hazardous materials.

A literature search was initially performed to obtain water-in-chemical solubility data. For chemicals of interest, in which the solubility data were not available, a simple experiment was conducted to measure this solubility.

The experimental procedure involved contacting an ice cube made from distilled water with a known volume of chemical in a sealed glass bottle for a 24 hour period. Prior to the commencement of the experiment, the ice cube, chemical and the glass container were allowed to reach an equal and constant temperature, which ranged between -5 and -20 deg C. This study was carried out in a cold room, which maintained a constant temeprature throughout the experiment. The initial mass of the ice cube and the initial chemical volume ranged between 4 and 8 grams and 6 and 12 mL, respectively, for most experiments. At the end of the experiment, the ice cube remaining in the container was carefully dried and weighed. The solubility of the ice in the chemical was calculated from the difference in mass of the ice cube before and after the 24 hour period, and from the initial volume of the chemical.

A slightly different approach was taken for chemicals which are completely soluble in water. The chemical studied was n-propanol. For this chemical, several trials were conducted using different initial mass ratios of ice and chemical. The mass ratio for the first trial was set at 0.35, and the amount of ice relative to the chemical was increased in succeeding experiments until some of the original ice cube remained after the experimental duration. This set of experiments was performed at -5 deg C.

The solubility data obtained from the literature and experiments were combined. In total, 48 out of 55 liquid chemicals on the priority list, as well as 5 additional chemicals of interest were studied and data obtained. These liquids were then classified into one of three groups, as discussed later.

4.2 Spreading on Ice

Initial spreading experiments involved spilling various

solutions on a smooth glass surface. This was followed by small scale spreading experiments on artificially prepared smooth and rough ice surfaces. Finally, several large spills on ice were conducted under outdoor conditions.

4.2.1 Spreading Experiments on Glass

Two sets of experiments on smooth glass surface were performed on a 91x91 cm glass sheet. The glass was placed on a plastic sheet, with 1 cm markings in four directions, from the centre. The glass and the plastic sheet were placed horizontally on the floor. The surface of the glass was carefully cleaned before each experiment.

All experiments involved spilling 50 mL of an aqueous solution or a chemical, with red dye added, from a 2.2 cm ID by 20 cm glass tube at room temperature. A rubber ring was attached to one end of the glass tube and the rubber end of the tube was placed firmly against the glass surface. A pre-determined volume of liquid was then poured into the tube. Time was recorded with a stopwatch, which was started, when the tube containing the liquid, was lifted.

The first set of experiments were performed to determine the effect of viscosity on the final spill depth (or area). The following aqueous solutions were used:

	Viscosity (cp)
Glycerol Solutions:	
36% (by wt)	3.1
46	5.0
60	10.2
65	15.5
Ethylene Glycol Solutions:	
60	5.2
100	21.0
Water	1.0

The time of spreading and the final spill dimensions were recorded for all experiments.

In the second set of experiments, the role of interfacial tension in the spreading process was investigated. Three aqueous solutions and one chemical were used, all having the same viscosity (5.2 cp) but varying surface tensions (25.5 - 74 dynes/cm). The liquids used were: 38% sucrose solution, 47% glycerol, 60.5% ethylene glycol (all in water) and pure n-pentanol. The final spill dimensions and the time of spreading were again recorded for this experiment.

4.2.2 Contact Angle Measurements

As described in Section 3.2, spreading is influenced by the combination of three interfacial tensions. However, the direct measurement of these forces, with the exception of the surface tension of the liquid, is difficult. On the other hand, the contact angle, which forms as a result of these interfacial forces, is relatively easy to measure.

In this study, equilibrium contact angles for various chemicals and aqueous solutions were measured on both glass and smooth ice surfaces. The procedure involved taking magnified photographs of a bead of chemical, consisting of approximately two average-sized drops, onto clean glass or ice surface. Sufficient time was allowed for the liquid to stop spreading before the picture was taken. The angle was then determined from the picture by using the arc-tangent method described by Neumann and Good (1979).

These angles were used in an attempt to correlate and explain the spreading behaviour of various chemcials. A sample photograph of heavy mineral oil on ice is presented in Figure 4.1.

4.2.3 Spreading on Artificially Prepared Ice Surfaces

Small-scale spreading experiments were performed on artificially prepared smooth and rough ice surfaces. Preparation of these surfaces proved to be difficult at first, but after several attempts, a relatively simple method was developed.

A 61x61 cm square piece of plywood, which was painted with white latex paint acted as the base for the ice formation. One cm markings were drawn, on the painted surface, similar to the grid prepared for the spreading experiments on glass. Distilled water was poured onto the painted surface and a rigid vinyl sheet with the same dimensions was carefully placed on top of the water surface. The problem of pockets of air between the vinyl sheet and the painted plywood surface was eliminated by the continuous addition of water during the placement of the vinyl sheet. This system was allowed to freeze at -5 deg C. After freezing, the vinyl sheet was lifted to produce a smooth ice surface, free from cracks or apparent roughness. The thickness of the ice produced was approximately 2 mm.

Rough ice surfaces were prepared by allowing ice crystals of a certain size to fall from a sieve onto a smooth ice surface, which was prepared as just described. Ice surfaces of two different surface roughness were constructed, consisting of ice crystals ranging from 0.5-1 mm in diameter for one and 1-2 mm for the other. The area covered by the ice crystals relative to the total base area was approximately 70%. The ice crystals

were produced by forcing crushed ice through a steel mesh sieve. By "sifting" the ice crystals using sieves with different mesh sizes, the desired diameter range of crystals was obtained. Before the start of the experiment, the ice crystals on top of the smooth ice surface were allowed to partially melt and were refrozen to firmly attach these crystals onto the underlying ice surface.

The chemicals selected for this study were m-xylene, n-pentanol, heavy USP mineral oil (viscosity: 1500 cp at -5 deg C), and a white mineral oil called Bayol 35 (8 cp at -5 C deg C). These chemicals were chosen on the basis of low solubility of ice, small evaporation rate, a relativly non-hazardous nature and their wide range of viscosities (0.9 - 1500 cp). The volume of chemical used was 25 and 50 mL for spills on smooth ice and 50 mL for each chemical on each of the two rough ice surfaces. A new ice surface was prepared and used for each spill.

The chemicals were spilled in the same manner as described in Section 4.2.1, and all experiments were conducted at a temperature of -5 deg C in a temperature-controlled cold room. A video camera was used to record the spreading and the stopwatch readings. At the termination of spreading, the final spill dimensions were recorded. Photographs of the experimental apparatus and the rough ice surface are presented in Figures 4.2 and 4.3. A spill of 50 mL of xylene on this surface is seen in Figure 4.4.

4.2.4 Outdoor Ice Spreading Experiments

Large-scale outdoor spreading experiments on ice were conducted in a residential area in Scarborough, Ontario in February, 1986. A 2.4x2.4 m plastic-sealed wooden platform was constructed, and water was poured onto this platform to produce an ice surface approximately 1.5 cm thick.

The ice surface was "marked off" at 10 cm intervals in eight directions from the centre, as shown in Figure 4.5. In total, six experiments were performed, using five different chemicals. The chemicals and the volume spilled were: m-xylene, 450 mL and 1 L; n-pentanol, 1L; Bayol, 700 mL; light mineral oil (viscosity 450 cp at -5 deg C), 2L; and ethylene glycol, 750 mL.

The discharge of the chemical onto the ice surface involved pouring the chemical into a large funnel, with a flexible plastic tube attached to the end. The discharge end of the tube was positioned a few cm above the centre of the ice surface. The discharge time for most of the chemicals spilled was less than five seconds. This apparatus and procedure can be seen in Figures 4.6 and 4.7.

During the initial period of spreading, the dimensions of the spill were recorded with a video camera, but after several

minutes, the spill distances were recorded by hand. The initial chemical and air temperatures, as well as the general meteorological conditions were also noted and recorded. After each experiment, the ice surface was wiped clean and additional water was added to form a new layer of ice. The ice surface was relatively smooth for most experiments, although several "rough" (<1 mm) areas were observed for some experiments, which may have been due to wind effects during freezing. A few cracks in the ice were also present. Results from a spill of 1 L of pentanol is presented in Figure 4.8.

4.3 Spreading Experiments on Snow

The snow spreading experiments involved the use of two impermeable surfaces, glass and ice, to act as a base for the snowcover. The spreading rate and characteristics were observed and quantified with respect to these surfaces.

4.3.1 Snow-on-Glass Spreading Experiments

As stated in Section 3.3, it is believed that there are many variables which affect the spreading of chemicals in snow media. In this study, experiments were performed to determine the effect of the following variables on the final spill area and spreading rate: spill volume, chemical viscosity, snow density, snow depth and the type of snow. Due to time limitations, and the assumption that the spill is released instantaneously, experiments to determine the effect of spill release rate were not performed. However, the five variables studied are believed to be the major parameters which determine the spreading characteristics.

Bayol (white mineral oil) was the chemical used in all of these experiments with the exception of the chemical viscosity experiments, which involved four other insoluble chemicals. In each of the five sets of experiments, an attempt was made to keep all other experimental conditions constant.

The apparatus consisted of a 91 x 91 cm smooth glass sheet in which a grid consisting of 1 cm markings originating from the centre was drawn in eight directions. This glass sheet was placed grid-side down on a wooden frame and the glass on this frame was supported by two, one metre high tables. The snow was placed on top of the glass, and the spreading of chemicals (which were dyed red) was observed from a mirror positioned at an angle under the glass. This set-up is shown in Figure 4.9. These experiments were performed on the roof of the chemical engineering building at the University of Toronto.

The experimental conditions for the five sets of experiments are summarized in Table 4.1. Unlike the ice experiments, the spreading rate was slow enough such that all spill dimensions were recorded by hand at regular time

intervals. In addition, the penetration time, which was defined as the time for the chemical to penetrate to the bottom of the snowcover, and the extent of spreading on the surface of the snow were recorded. Snow and air temperatures were also monitored throughout the experiment. After each experiment, a cross section profile of the chemical in the snow was made and observations, such as the amount of drainage, and chemical snow "slush" depths were recorded. Samples of the snow-chemical mixture were taken near the surface and at the bottom of the snowcover for some experiments.

These experiments were followed by several experiments using water-soluble chemicals. The same experimental procedure was followed for these experiments. Details of these experiments are listed in Table 4.2.

4.3.2 Snow on Ice Spreading Experiments

Two spreading experiments on snow covered ice surfaces were conducted on the same ice surface that was used in the large-scale ice experiments, as described in 4.2.4. Instead of a grid to mark the dimensions of the spill, wooden sticks (approx diameter 1 cm, length 15 cm) were stuck into the snow at 10 cm intervals, as shown in Figure 4.10. The chemicals were discharged onto the snow in the same manner as in the large-scale ice experiments.

The first experiment involved spilling 3 L of Bayol on to 9 cm of snow. A photograph is presented in Figure 4.11. The extent of spreading on the underlying ice surface was determined by checking for red-dyed Bayol-snow mixture by using the wooden sticks as a "dipstick". The spreading was assumed to have stopped after 3 hours into the experiment in which 5 cm advancement of the spill did not occur in either of the four directions during the last 1.5 hours of the experiment. The final spill area was then accurately determined by removing the snow. Additional experimental conditions are listed on Table 4.1, under experiment no. 18.

The second experiment involved spilling 1 L of 85% ethanol onto 11 cm of snow. The area of discharge on the snow can be seen in Figure 4.12. The wooden sticks were again used to determine the extent of spreading but they were tested for the smell of ethanol instead of the red dye. In addition to the spreading rate, the temperatures and general observations of the ethanol-water-snow mixtures were recorded. The spreading was allowed to proceed to completion by allowing the experiment to continue overnight. On the morning of the next day, a cross section of the snowcover was made and the state of the snow and ice surface, as well as the final spill area was observed and noted. Further experimental details are listed in Table 4.2.

Table 4.1 Experimental Conditions for Snow Spreading Experiments Involving Insoluble Chemicals

Experiment	Exp. No.	Vol. (L)	Ave. Temp. (c)	Pour Rate (L/min)	Snow Density (g/ml)	Snow Depth (cm)	Snow Properties: Crystal + Type	Snow Properties: Age (days)	Snow Properties: Wetness
Volume	1	0.5	-6	1	0.25	3	a, b	1	D
	2	1	-8	1	0.25	3	a, b	1	D
	3	2	-8	1	0.25	3	a, b	1	D
	4	3	-3	1	0.24	3	a, b	1	D
Snow Depth	5	2	-6	1	0.27	4	b	2	D
	6	2	-6	1	0.27	9	b	2	D
	7	2	-9	1	0.26	15	b	2	D
	8	2	-4	1	0.25	30	a, b	1	D
Snow Density	9	1	-4	1	0.12	10	a, b	1	D
	10	1	-1	1	0.25	10	b	3	W
	11	1	-1	1	0.42	10	b	3	W
Chemical Viscosity	12	1	-2	1	0.25	10	b	2	D
	13	1	-3	1	0.25	10	b	2	D
	14	1	-5	1	0.25	10	b	2	D
	15	1	-6	1	0.24	10	b	2	D
	16	1	-3	1	0.25	10	b	3	D
Snow Type	17	3	-2	1	0.41	3	c, e**	10	D
	18	3	-3	1	0.34	9	c*	7	D

\+ See section 2 for definitions
* Grain size: 1 mm
** Grain size: 2 - 4 mm
Wetness: D - Dry, W - Wet
Note: Exp. 18 was performed with ice as a base for snow cover
Bayol was the chemical used for exp. no. 1 - 11, 13, 17 and 18
Other chemicals used were xylene (exp. 12), n-pentanol (exp. 14), light mineral oil (exp. 15) and heavy mineral oil (exp. 16)

Table 4.2 Conditions for Snow Spreading Experiments Involving Water-Soluble Chemicals

Chemical	Exp. No.	Vol. (ml)	Ave. Temp. (c)	Snow Density (g/ml)	Snow Depth (cm)	Snow Properties Crystal Type	Age (Days)	Wetness
Sulfuric Acid (97%)	19	100	-1	0.42	10	b	2	W
Ethylene Glycol	20	200	0	0.32	10	a, b	1	W
Ethanol (85%)	21	200	0	0.32	10	a, b	1	W
Ethanol (85%)	22	1000	0	0.34	11	c*	7	D

* Grain Size: 1 mm

Note: Exp. 22 was performed with ice as base for snow cover
See Table 4.1 for explanation of symbols

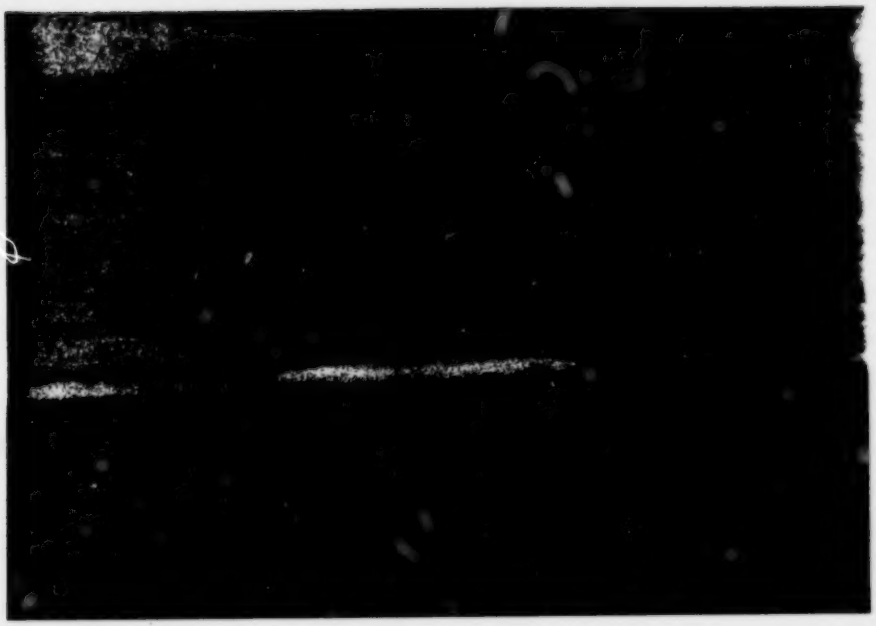

Figure 4.1 Contact Angle Experiment: Heavy Mineral Oil on Ice Surface

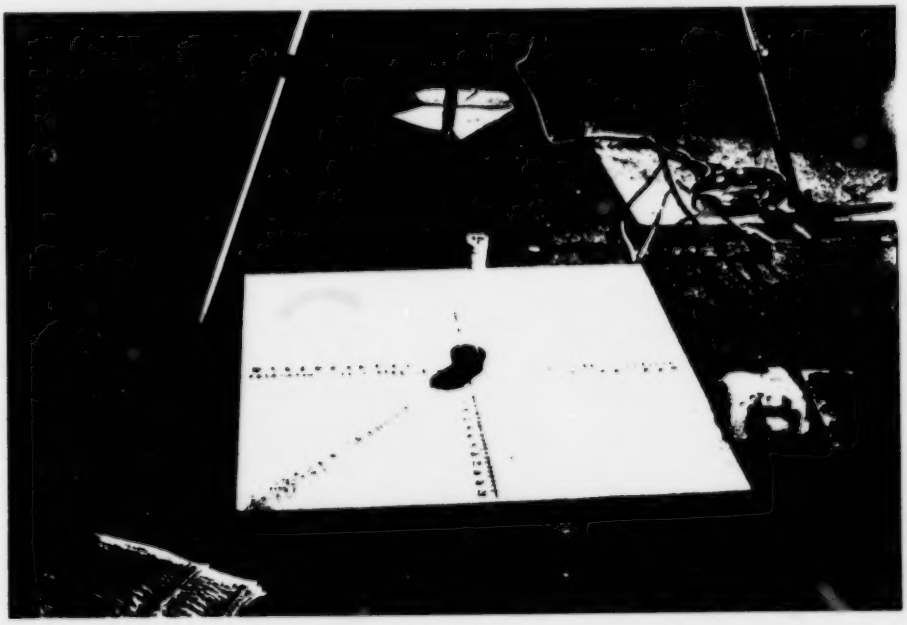

Figure 4.2 Artificially Prepared Rough Ice Surface

Figure 4.3 Experimental Apparatus for Small-Scale Ice Experiments

Figure 4.4 Spill of 50 mL of Xylene on Rough Ice Surface

Figure 4.5 Ice Surface for Outdoor Experiments

Figure 4.6 Release of Chemical Onto Ice Surface

Figure 4.7 Set-up for Outdoor Ice Experiments

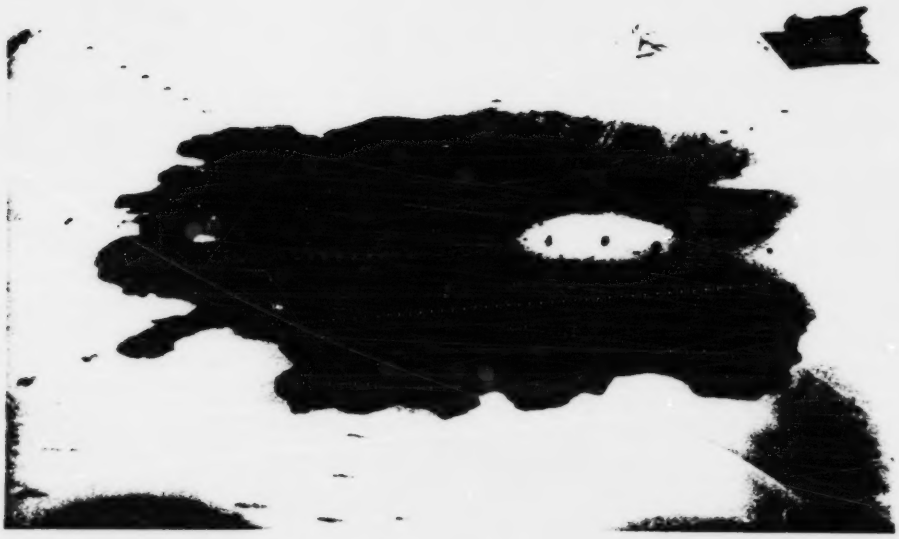

Figure 4.8 Spill of Pentanol on Ice

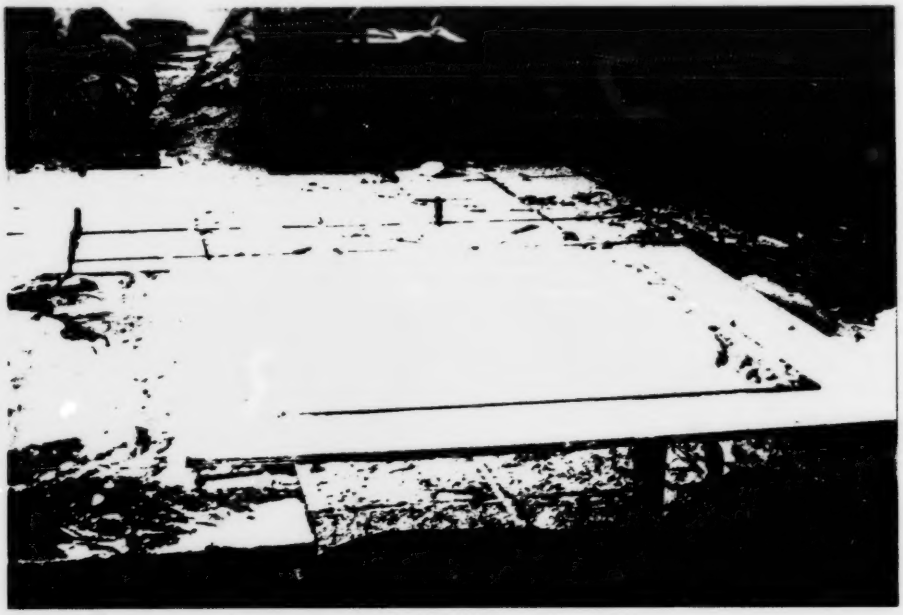

Figure 4.9 Snow Spreading Apparatus

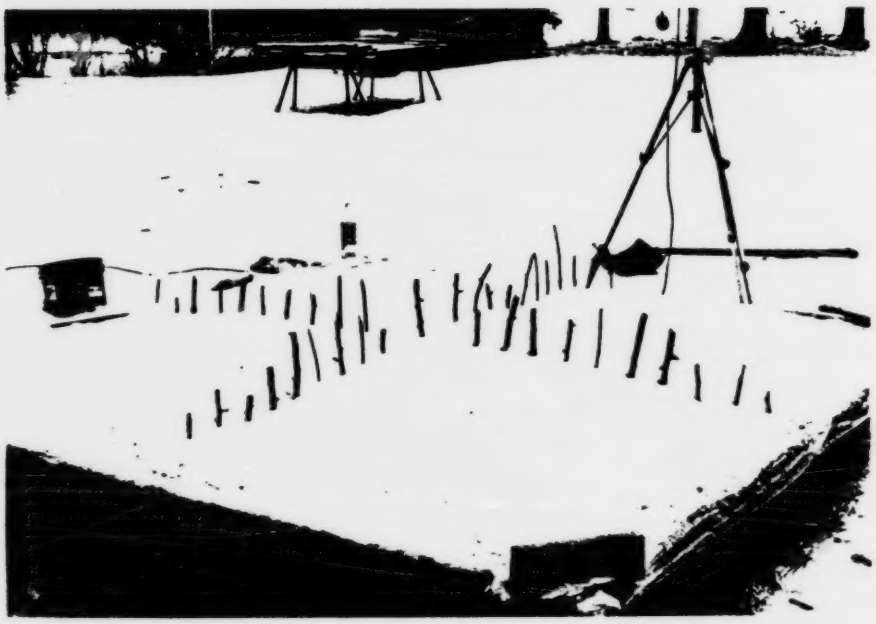

Figure 4.10 Snow on Ice Spreading Apparatus

Figure 4.11 Spill of Bayol on Snow

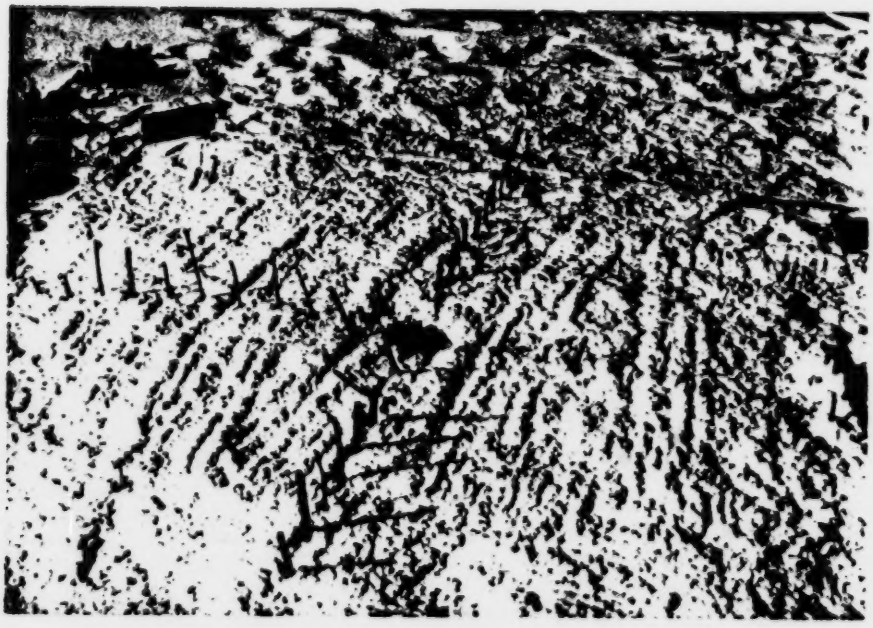

Figure 4.12 Spill of Ethanol on Snow

5. RESULTS AND DISCUSSION

5.1 Solubility Studies

The solubility data from the literature and experiments were used to classify these chemicals into one of three groups. The criteria for classification was arbitrarily chosen, based on the following values of the solubility of water/ice in the chemical:

Group 1: less than 5% solubility by weight;
Group 2: greater than 5% but not completely soluble;
Group 3: completely soluble.

Table 5.1 lists the classification of the chemicals studied. The actual solubility data are listed in Appendix A. Although most of the literature solubility data were based on temperatures greater than 0 deg C, these results were still used for classification purposes since solubility of water in chemical decreases with temperature for most chemicals. For example, the American Petroleum Institute (1970) lists the solubility of water in Naptha solvent (54.3 deg API) as 4.5 mole % at 150 deg C. This information was used to classify this liquid as a Group 1 chemical since the solubility will probably be less than 4.5 mole %, and hence less than 5 weight %, at sub-zero temperatures.

Table 5.1 Classification of Chemicals Based on Solubility

GROUP 1

Aniline
1,3 Butadiene
Butylene
Carbon Tetrachloride
Chloroform
1,2 Dichlorobenzene
Dichlorofluoromethane (Freon 21)
Ethyl Acetate
Ethyl Benzene
Ethylene Dichloride
Gasoline
Isopropyl Benzene
Methyl Isobutyl Ketone
Methylene Chloride
Methyl Methacrylate
Mineral Oil (white, USP heavy)
Naptha Solvent
n-Hexane
1-Hexanol
Perchloroethylene

Styrene
Toluene
1,1,1 Trichloroethane
Trichlorofluoromethane (Freon 11)
Turpentine
m-xylene
o-xylene

GROUP 2

Butanol
Methyl Ethyl Ketone
Pentanol
Propylene Oxide

GROUP 3

Acetic Acid (aq - aqueous solution)
Acetone
Acrylonitrile
Ethanol
Ethylene Glycol
Ethylene Oxide
Formaldehyde (aq)
Hydrazine (aq)
Hydrochloric Acid (aq)
Hydrofluoric Acid (aq)
Hydrogen Fluoride
Hydrogen Peroxide
Methanol
Methylamines (di, tri)
Nitric Acid (aq)
Oleum
Phosphoric Acid (aq)
Propanol
Propylene Glycol
Sulfuric Acid
Sulfuryl Chloride

Based on this classification system, Group 1 chemicals have a common property of small or negligible solubility of water in the chemical. (Most of the Group 1 chemicals listed in Table 5.1 have a solubility of less than 1%) If the initial temperature of these chemicals is below 0 deg C, spills of these chemicals onto snow may be difficult to detect visually, since no appreciable dissolution of snow will occur.

Chemicals in the second group are able to dissolve a greater amount of ice/snow (>5%) but are only partially soluble. The number of chemicals in this group is relatively small but

these chemicals, under certain conditions, may melt but not completely dissolve the ice. This results in the formation of two liquid phases, consisting of a water rich phase with a certain amount of dissolved chemical, and a chemical rich phase with some dissolved water. This phenomenon was observed experimentally for methyl ethyl ketone, 2-butanol and propylene oxide at -5 deg C. Although no analysis was done for dissolved water in the chemical, these three chemicals were classified in the second category, since it is believed that heat given off during the dissolution process was the reason for the melting of the ice cube.

In addition, the solubility of the chemical in the melted ice cube must be high enough to lower the freezing point of the water phase to below the surrounding temperature. Although the exact conditions associated with this phenomenon are uncertain, a combination of high mutual solubilities and mild surrounding temperatures is thought to favor this occurance.

Group three chemicals are characterized by the ability to completely dissolve water in all proportions. However, for snow and ice, the extent of dissolution is governed by factors such as the surrounding temperature, heat of dissolution (which includes the effects of heats of fusion and mixing), and the relative amounts of chemical and snow/ice and their contact area. Spill behaviour of Group three chemicals are described in Sections 3.3 and 5.5.7.

The results of the solubility test for n-propanol at varying ice mass fractions are listed in Table 5.2. The results indicate that complete dissolution of the ice cube took place at ice mass fractions less than 0.85. Yet, at an ice fraction of 0.91 and 0.96, three phases were observed at the end of the experiment. The three phases consisted of an original ice cube, a liquid solution and a frozen alcohol-water mixture. The relative amount of the original ice cube remaining at the end of the experiment was greater at 0.96 ice fraction, and is indicated by the lower solubility. Partial freezing of the liquid alcohol-water solution can be explained by the fact that the concentrations of n-propanol in melted ice water, which were calculated to be 10% for ice mass fraction 0.91, and 11% for 0.96 are less than the concentration of 14%, which freezes at -5 deg C (CRC, 1983).

The results show that there is a limit to the amount of snow/ice which a chemical of a certain volume can completely dissolve. For n-propanol at -5 deg C, this limit was observed at concentrations between 0.85 and 0.90 ice mass fraction.

Table 5.2 Solubilities of Ice in n-Propanol at Various Ice Mass Fractions

Ice Mass Fraction	Solubility (g ice/mL chemical)
0.35	∞
0.42	∞
0.85	∞
0.91	7.1
0.96	6.7

When dealing with spills on snow and ice, it should be noted that chemicals which are normally thought of as gases, such as butane and propylene oxide are liquids at winter temperatures and "liquid" chemicals such as benzene and cyclohexane are solids. Therefore, prior to classifying these chemicals, their melting and boiling points were checked. Appropriately, chemicals on the priority list of hazardous materials were either included or omitted from the list of candidates for the solubility studies, as required.

5.2 Contact Angles

The measured equilibrium contact angles are presented in Figures 5.2.1 for glass and 5.2.2 for an ice surface, as a plot of cosine of the equilibrium contact angle versus liquid surface tension. It can be seen from the figures that a linear relationship may exist for alkanes and alcohols on ice and possibly for aqueous ethylene glycol and glycerol solutions on glass. However, a general correlation, which is applicable for all liquids does not seem to exist. This is in agreement with Good's (1979) review of the treatment of contact angle data that a linear relationship may exist for homologous chemicals, and Gardon's (1963) observation that different contact angle behaviour can occur for non-homologous liquids.

Although a general prediction of the contact angle was not obtained, the results confirm the expectation that most chemicals have a high degree of spreading on ice. This is seen by the relatively small contact angles for the liquids studied. These angles and the liquid surface tensions from the ice surface results were used to calculate the ice surface tension and the liquid-ice interfacial energies, using the equations of state developed by Gerson (1982). These energies are listed in Table 5.3. Appendix B gives the experimental contact angles on glass surface.

Table 5.3 Experimental Contact Angles and Interfacial Energies (dynes/cm) for Various Chemicals on Ice.

Chemical	Equil. Contact Angle (deg)	Chemical Surface Tension	Ice Surface Tension	Chemical-Ice Interfacial Tension
m-xylene	14	32	31	-0.04
bayol	10	27	26	-0.23
mineral oil	27	32	29	+0.21
toluene	15	33	32	+0.05
n-butanol	14	27	26	+0.002
n-pentanol	15	28	27	-0.02
n-octanol	22	29	27	+0.13
n-pentane	10	19	19	-0.01
n-hexane	11	21	21	+0.06
n-octane	12	24	24	-0.02
n-nonane	12	25	27	+0.06
n-dodecane	14	28	27	+0.06

The results suggest that the calculated ice surface tensions are not constant. Furthermore, their values differ greatly from Spelt et al. 's (1982) value of 80.2 dynes/cm. A possible explanation is that the ice surface tensions in Table 5.3 are not the true surface tensions but are rather measures of

an apparent or effective surface tension. The true value of 80.2 dynes/cm is applicable only for pure ice, without the presence of chemicals or other substances. Neumann (1986) has suggested that since ice is a high energy solid, it will lower its surface tension in the presence of impurities or chemicals by either contact with the liquid or with the vapour from the liquid. Therefore, the apparent surface tensions of ice in Table 5.3 differ from the "true" value and are probably the surface tensions which are applicable in a chemical spill situation.

Another property of high energy solids, which was verified in this experiment is its relatively small liquid-solid interfacial energy. This again, is due to the high degree of spreadability on ice of most chemicals. There are many studies of interfacial tensions, contact angles, and wettabillity characteristics of solids surfaces in the presence of liquids. However, there are, at present, no simple models or equations which can be used to predict the degree of spreading for any liquid and further consideration in this area is beyond the scope of this study. These results will instead be used to describe or explain some of the results obtained in the ice spreading experiments.

Figure 5.2.1 Plot of Cos θ_e on Glass vs. Liquid Surface Tension

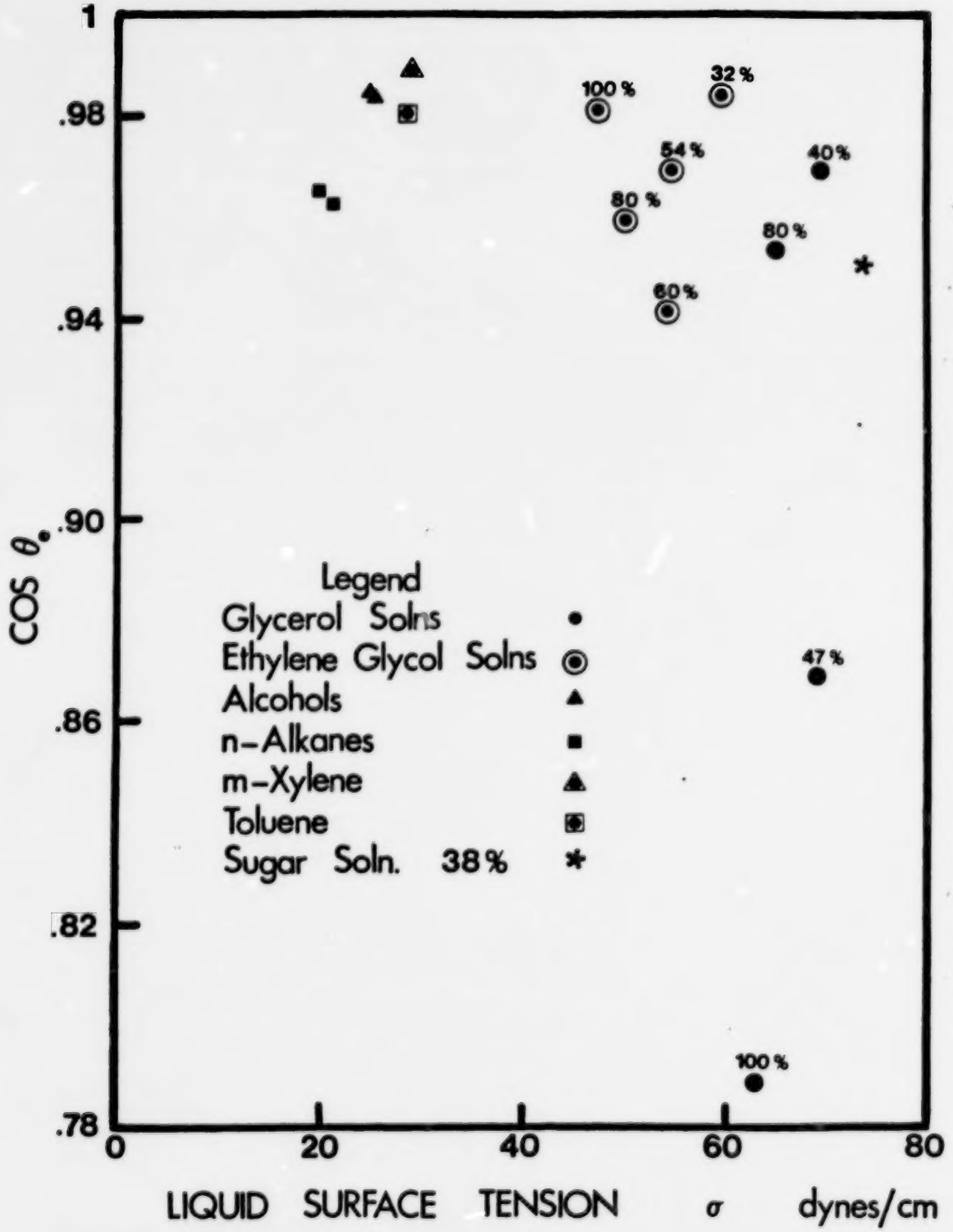

Figure 5.2.2 Plot of Cos θ_e on Ice vs. Liquid Surface Tension

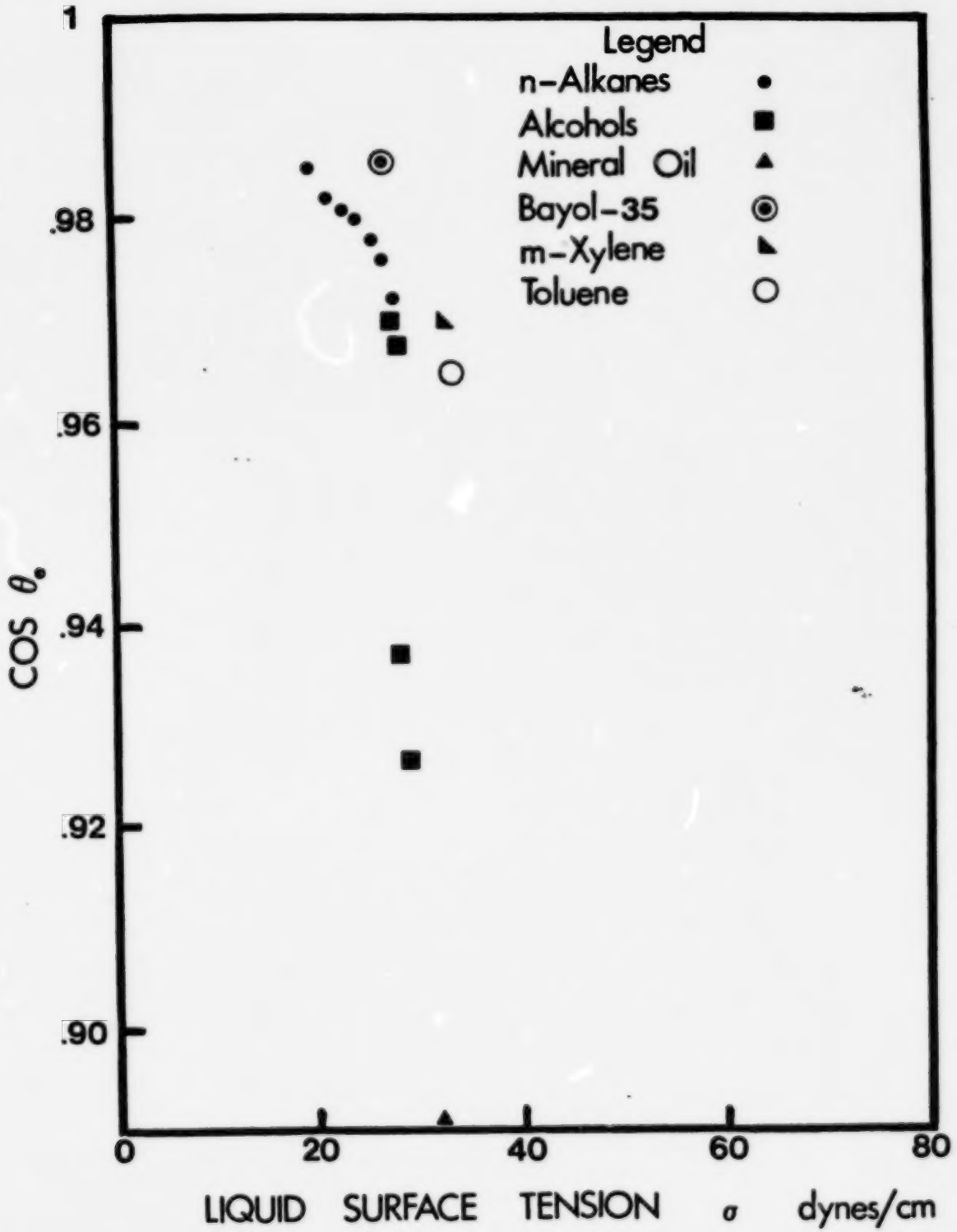

5.3 Spreading of Chemicals on Glass

The final spill dimensions for all glass spreading experiments were gathered and final spill depths calculated. These equilibrium spill depths were plotted (on a log scale) against the liquid viscosity for the first set of experiments, which involved the spreading of various glycerol and ethylene glycol solutions. This graph is presented in Figure 5.3.1.

The results indicate a general trend of an increase in spill depth (decrease in final spill area) with increasing liquid viscosity. Although an "average" line could be drawn through the experimental data, it is apparent that a much better correlation could be obtained by using only the data from the glycerol solutions. This seems to indicate that the final spill area is dependent on factors other than the liquid viscosity, such as the type of chemical and its wetting characteristics.

The results for the second set of experiments, which studied the effect of interfacial tension using four liquids of identical viscosity are listed in Table 5.4. Despite the maximum of only 22% difference in the final spill depths for the four liquids studied, the results were used to search for a correlation between the final spill depth and the liquid surface tension; or a combination of liquid surface tension and the equilibrium contact angle on glass. Various combinations such as h_f vs. θ_e, $\cos\theta_e$, $(1-\cos\theta_e)$, etc., were tried but no correlation was found. This seems to indicate that there may be additional factors, such as surface interaction (adsorption, absorption), in addition to the interfacial energies, that influence the spreading. However, these effects appear to be relatively small compared to the viscosity effect. It is also possible that the differences in the final spill depths are not truly significantly different.

Table 5.4 Interfacial Tension and the Final Spill Depth

	h_f (cm)	σ (dynes/cm)	$\cos\theta_e$
38% sucrose	0.055	74.0	0.95
47% glycerol	0.065	69.0	0.87
60.5% ethy. glycol	0.053	54.0	0.94
n-pentanol	0.059	25.5	0.98

Figure 5.3.1 Effect of Viscosity on Final Spill Depth on Glass

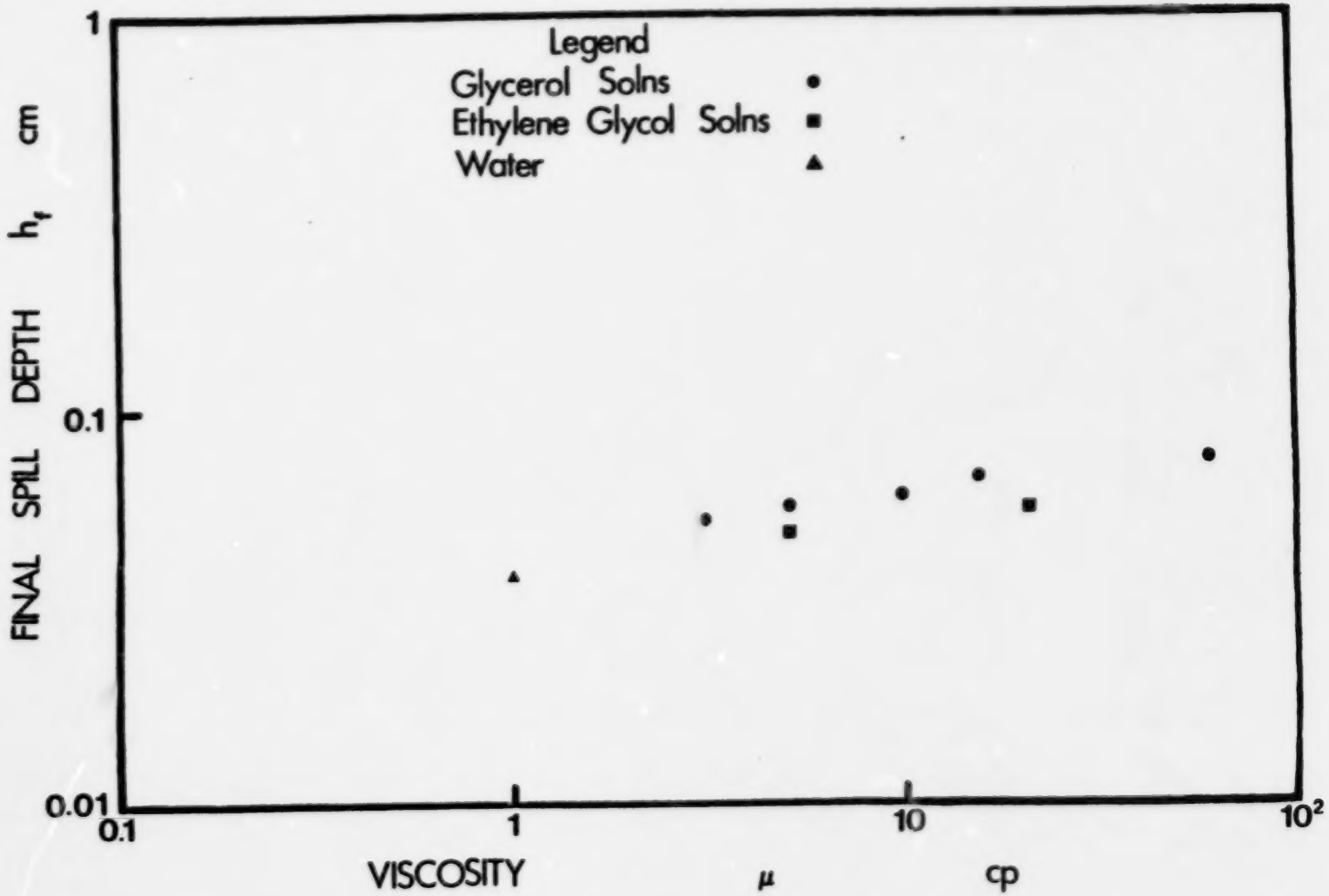

5.4 Spreading on Ice Surfaces

The results of the spreading experiments on artificially prepared smooth and rough ice surfaces and large scale outdoor experiments were combined to describe the spreading characteristics with properties of the chemical and the spill volume. Specifically, the final area, A_f, the spreading time constant, γ, and the slope term, x, were correlated using the data obtained. The development of these correlations and their significance are described in the following sections. The results are presented here in graphical form where possible. These and other numerical results are presented in Appendix C.

5.4.1 Effect of Chemical Viscosity on the Final Spill Area

Based on the results of the glass spreading experiments, only the chemical viscosity, among the various properties of the chemical, was considered in the correlation of the final spill depth (or area). The final spill depths for all experiments with a spill volume of 50 mL were plotted (on a log scale) against the viscosity, as shown in Figure 5.4.1.

It can be observed that the final spill depth for a particular chemical is dependent on the roughness of the ice surface. Table 5.5 lists the final spill depths for the four chemicals studied.

Table 5.5 Effect of Roughness on the Final Spill Depth

Chemical	Final Spill Depths (cm)		
	Smooth Ice	Rough Ice Surface 0.5-1 mm	1-2 mm
m xylene	0.034	0.032 (-6%)	0.031 (-9%)
bayol	0.045	0.032 (-29%)	0.036 (-20%)
n pentanol	0.081	0.068 (-16%)	0.064 (-21%)
heavy min. oil	0.177	0.129 (-27%)	0.215 (+21%)

(% difference relative to smooth ice)

The final spill depths for three of the four chemicals; xylene, bayol, and pentanol, decreased for rough ice surfaces, relative to the smooth ice depths. For heavy mineral oil, a decrease in spill depth was observed for the 0.5-1mm rough ice but an increase was noted for the 1-2 mm rough surface. The effect of roughness on the spreading is believed to be dependent on the roughness height, relative to the height of the final chemical pool, and on the wettabillity of the chemical to the ice surface.

Figure 5.4.1 Effect of Viscosity on Final Spill Depth on Ice

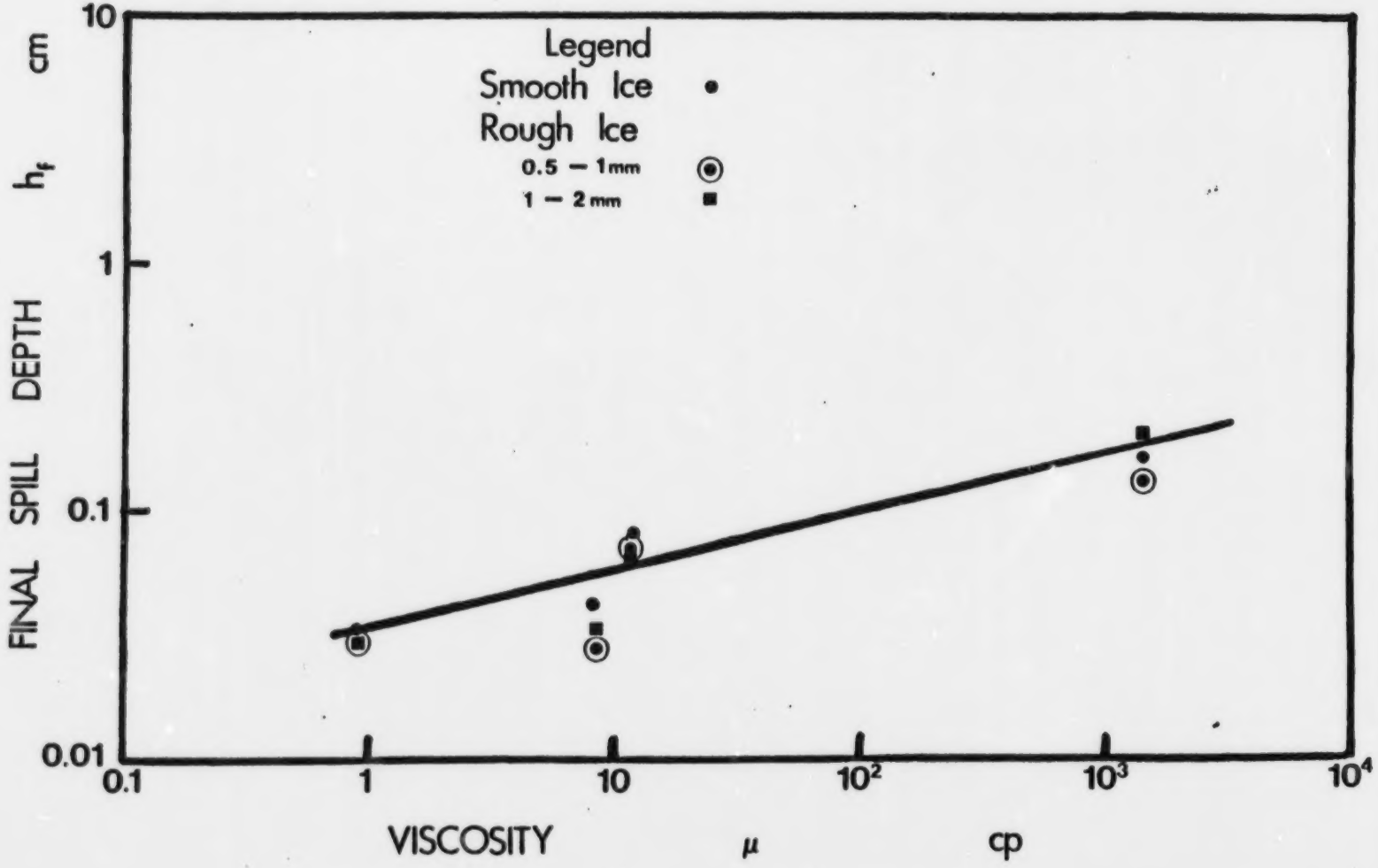

A decrease in final spill depth (increase in spill area), relative to smooth ice may occur when the final spill height is approximately equal to or less than the height of roughness, as was the case for xylene, bayol and pentanol. For these chemicals, it was observed during the latter stages of spreading, that the chemical travelled around the rough elements. This action is a result of interfacial forces, which influence the net spreading effect. This effect is larger for rough ice surfaces due to the larger contact area between the chemical and the ice than for smooth ice surfaces. The roughness elements thus behaved like "islands" in the pool, the areas of which are included in the total area.

The effect of roughness on the spreading behaviour of mineral oil was different than the other three chemicals. It can be seen from Table 5.5 that the spreading terminated for both rough surfaces when the final spill depth was just slightly greater than the roughness height. This is attributed to the high viscosity of mineral oil and its relatively low degree of spreading on ice (it has a higher contact angle on ice, 27 deg, than the other three chemicals; <15 deg), which prevented the chemical from spreading around the rough surfaces once the spill depth reached the roughness height. If the roughness takes the form of pits or holes, it is likely that the spill area is reduced and the final thickness is increased.

It is clear from these results that surface roughness affects the spreading behaviour of chemicals. However, it can be seen from Figure 5.4.1 and Table 5.5 that the effect of roughness is relatively small. In addition, due to the nature of the interaction between the roughness height and the chemical, which involves the wettabillity of the chemical on ice and the actual roughness height, both which are often unknown, an "average" of the results for the three surfaces was used for the data correlation.

Therefore, a best fit line in Figure 5.4.1 was drawn through the "roughness-averaged" experimental data and the slope was determined to be 0.24. This indicates that the final depth is proportional to chemical viscosity to the power of 0.24.

5.4.2 Effect of Spill Volume on the Final Area

To determine the effect of spill volume on the final spill depth, the results of the experiments on both artificially prepared smooth ice surfaces and the large scale outdoor experiments were utilized. The final spill depths are plotted (log scale) against the spill volume in Figure 5.4.2. The results of the experiments involving the two rough ice surfaces were not used since they were conducted only at one spill volume (50 mL). The ice surfaces for the outdoor experiments were considered to be "smooth" for the purposes of this study.

Figure 5.4.2 Effect of Volume on Final Spill Depth
(Slopes Indicated Above Lines)

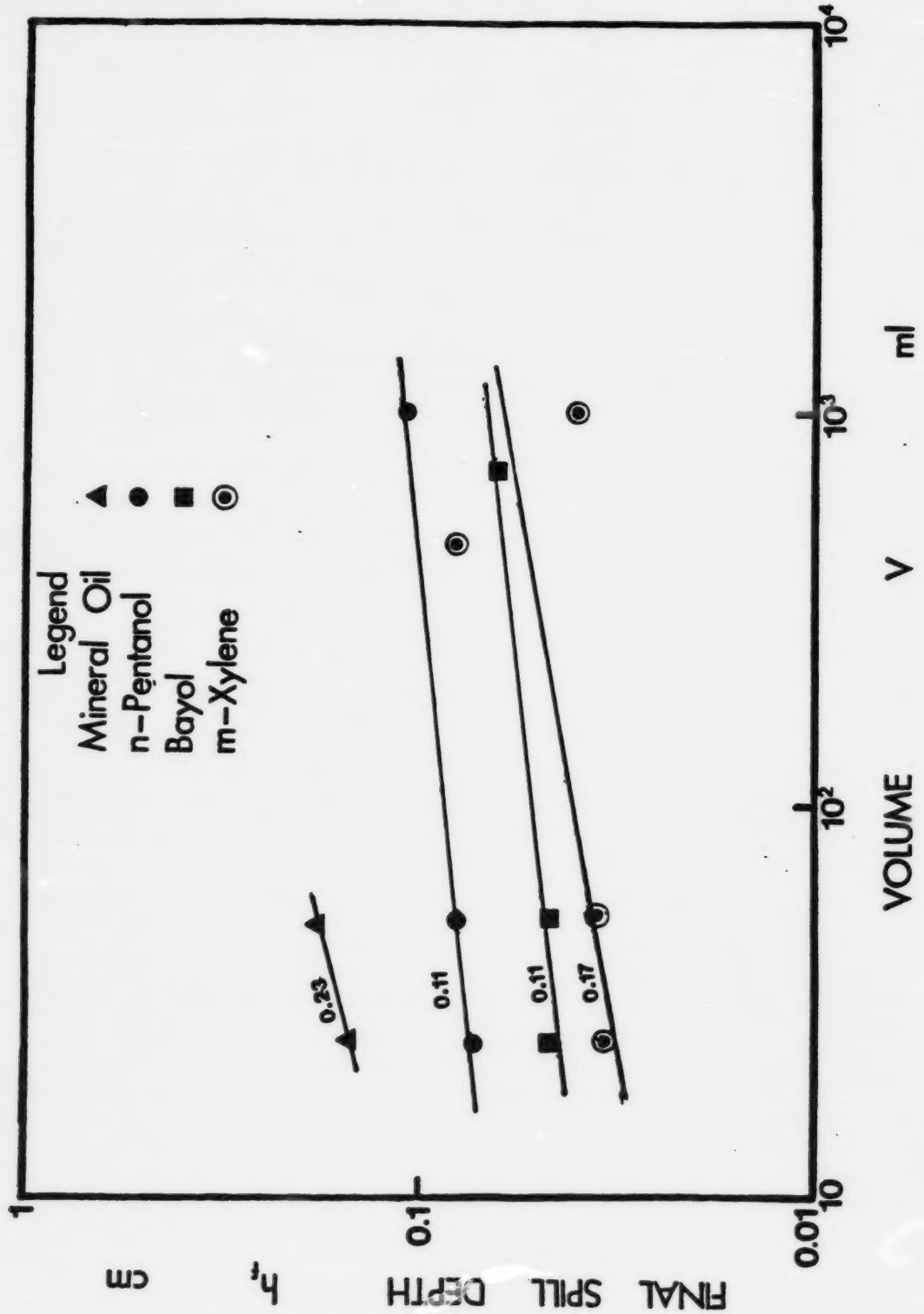

Despite some inconsistency in the experimental data, there is a general trend of an increase in spill depth with increasing spill volume. The low spill depth for the 1 L xylene spill is attributed to the effect of strong winds which were not present or did not significantly affect the pool dimensions for the other outdoor experiments. The wind effect is discussed further in Section 5.4.3.

A best fit line was drawn for each chemical. The slopes for these lines ranged between 0.11 for bayol and pentanol to 0.23 for mineral oil. An average of 0.15 was used in the overall correlation of the data.

5.4.3 Correlation of the Final Spill Area on Ice

The results from Sections 5.4.1 and 5.4.2 were used to obtain a correlation for the final spill area. The results obtained thus far is:

$$h_f \propto V^{.15} \mu^{.24}$$

or, in terms of the final spill area:

$$A_f \propto V^{.85} \mu^{-.24}$$

where μ is the chemical viscosity, and V is the spill volume. The above expression for A_f was non-dimensionalized by introducing the chemical density (ρ_c), liquid surface tension (σ) and the gravitational constant, (g), to produce the following equation:

$$\frac{A_f}{V^{2/3}} = K \frac{V^{.18} \rho_c^{.33} g^{.21}}{\mu^{.24} \sigma^{.09}} \qquad (5.1)$$

It is important to note that the powers of the chemical density and the liquid surface tension are a result of the non-dimensionalizing process and were not obtained from the results of this study. This does not introduce a serious error because the power on surface tension is small and liquid densities vary over a relatively narrow range. A plot of equation 5.1 and the experimental data is presented in Figure 5.4.3. A line with a slope of 1.0 was drawn, and this line was used to determine the constant, K, in equation 5.1. This value was found to be 6.0. Therefore, the final equation for the final spill area, can be written as:

$$\frac{A_f}{V^{2/3}} = 6.0 \frac{V^{.18} \rho_c^{.33} g^{.21}}{\mu^{.24} \sigma^{.09}} \qquad (5.2)$$

Figure 5.4.3 Correlation of Final Spill Area on Ice

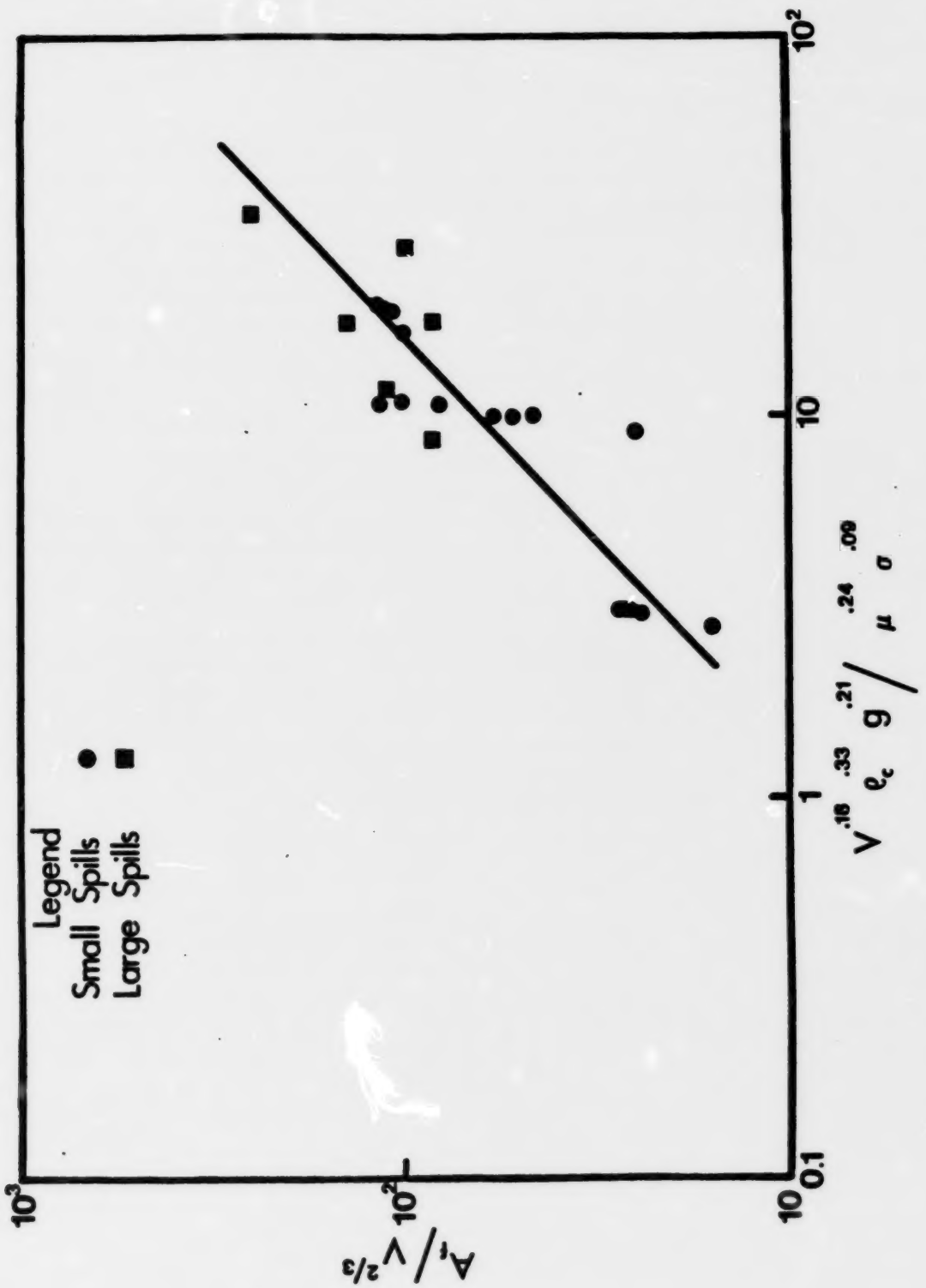

An algebraically equivalent expression for the final spill depth, h_f, is:

$$h_f = 0.008 \; V^{.15} \mu^{.24} \qquad (5.2a)$$

where h_f has units of m; V, m^3; and μ, kg/m s. Note that the above correlation is not dimensionless and is dependent on the units used. Since ρ_c and σ do not vary greatly for most chemicals, similar results will be obtained by using either equation 5.2 or 5.2a.

It can be seen from Figure 5.4.3 that equation 5.2 is able to correlate the experimental data with reasonable accuracy. The two outdoor experiments (light mineral oil and ethylene glycol), in which their results were not used in the development of this correlation also showed good agreement. It is therefore proposed that equations 5.2 and 5.2a (equation 5.2 was developed from the results of 5.2a) can be used to obtain a reasonable estimate of the final spill area for Group 1 and 2 chemicals and with caution for Group 3 chemicals. The difference between the experimental spill areas and the areas predicted by equation 5.2 ranged between 2 and 50%, with an average difference of 23%.

It should be noted that equations 5.2 and 5.2a were correlated from the data obtained under varying wind speeds, and this equation does not explicitly include the effect of wind speed in determining the final area. Although quantitative measurements of the wind speeds were not recorded, it was observed from the outdoor experiments that spreading of low viscosity chemicals, such as xylene (viscosity 0.9 cp), which was significantly affected by strong winds.

The effect of similar wind speeds did not influence the spreading of pentanol (11 cp) in comparison with xylene, and had no noticable effect for light mineral oil (450 cp). (The other experiments were performed when the winds were calm.) For the pentanol spill, an interesting spreading behaviour occurred. The winds were sufficiently calm during the first few minutes of the spill, which allowed the spill to spread in a circular manner. This period was followed by strong gusts of wind, which caused one side of the spill to advance. However, at the same time, the other side "receeded", at approximately the same rate as it advanced. Therefore, the wind caused a change in the overall location of the pool but did not significantly affect the final area.

The inclusion of the surface tension in equation 5.2 also deserves attention. Even though the surface tension and its power of -0.09 was introduced strictly to produce a dimensionless equation, its negative power is in agreement with the principles of the role of interfacial tensions in the spreading process. It can be observed from equation 3.1 that

the net spreading force in the latter stages of spreading, $\Delta\sigma$, is aided by a smaller liquid surface tension and a larger transient contact angle. Thus, a decrease in the product of the liquid surface tension and the cosine of the contact angle, with other variables constant, will increase $\Delta\sigma$, which favor an increase in the final spill area. This agrees with the negative power for the surface tension in equation 5.2. The proper term to be included in this equation is the product of the liquid surface tension and the cosine of the contact angle. However, the lack of a model to predict this angle and the failure to quantify the interfacial effects were the reasons for this approach.

Although only a single experiment involving Group 3 chemicals was performed, the assumption that for instantaneous spills, the dissolution process during its relatively short spreading time does not significantly alter the spreading characteristics appeared to hold true. The viscosity of these chemicals can either increase or decrease as a result of dissolution of ice, depending on the relative viscosities of the chemical and water. Yet, when ethylene glycol was discharged, cracking sounds were heard. An inspection of the ice surface at the end of the experiment revealed several cracks in the ice, through which some of the chemical drained. The cracking was most likely due to a temperature drop of the ice surface, induced by the decrease in chemical temperature as a result of absorption of heat required for dissolution of ice. It is thought that the volume increase from ice dissolution was offset somewhat by the loss of chemical through cracks in the ice. It is therefore suggested that caution be exercised when using equation 5.2 for Group 3 chemicals until further experiments are conducted.

5.4.4 Kinetics of the Spreading on Ice

The spill area versus time profiles for the ice spreading experiments were determined from the analysis of the video pictures taken during the experiment. For the 25 and 50 mL spills, the pictures were analyzed frame by frame up to the first half-second after the spill, and time zero was identified by extrapolating the spill areas from each video frame (a frame is recorded every 1/35 th of a second) backwards in time until the spill area equalled zero.

From these profiles, the spreading time constant, which was defined as the spreading time to necessary to reach 63% of the final area, was correlated with the chemical viscosity and spill volume.

The experimental spreading time constants for the 50 mL spills were plotted against the chemical viscosity. Two graphs were constructed: one for experiments on smooth ice (Figure 5.4.4) and the other representing the average of the two rough

ice surfaces (Figure 5.4.5). From the two figures, it can be observed that the spreading time constant is greater for rough ice than for smooth ice. There is also a general trend for increase in time constant with the chemical viscosity.

However, both graphs show a large difference in the time constant for two chemicals of similar viscosity (Bayol, 8 cp; Pentanol, 11 cp). The source of this difference is apparant from the experimental spreading rates of these chemicals, which is presented in Figure 5.4.6. It can be seen from the graph that the spill areas for both chemicals increased rapidly in the initial stage of spreading, but after 60 seconds, pentanol has virtually stopped spreading while bayol continued to spread for another two minutes. The reason for this may be due to the higher degree of spreading of bayol (contact angle: 10 deg) compared to pentanol (15 deg), but this alone cannot explain the large difference. It is believed that surface interaction(s) between the chemical and the ice, such as absorption and adsorption are responsible for this behaviour. However, further investigations into these effects were not conducted.

A best fit line was drawn in Figures 5.4.4 and 5.4.5, and their slopes were determined to be 0.69 and 0.37 respectively. An approximate average of these slopes, 0.5, was used in the correlation of the spreading time constant with the chemical viscosity.

The spill volume effect on the time constant is presented in Figure 5.4.7. The data shown in this graph are from small-scale smooth ice and large-scale outdoor ice spreading experiments. The error bars shown in Figure 5.4.7, as well as in Figures 5.4.4 and 5.4.5 give estimates of the uncertainty in determining the experimental time constant. These uncertainties were based on the error involved in either: measuring the spill area with time (+/- 5%); or the measurement of the actual time after commencement of the experiment (+/- 0.2s). The former applied to all of the outdoor experiments and the indoor experiments in which the experimental spreading constant was greater than one second, while the latter referred to experiments in which the time constant was less than one second.

A best fit line was drawn for each of the four chemicals in Figure 5.4.7, and their slopes measured. The average of the slopes was 1.0. Therefore, the data indicates that the spreading time constant was, on the average, found to be directly proportional to the spill volume.

These results were combined to yield the following relationship:

$$\gamma \propto \mu^{.5} V$$

This was used to produce the following dimensionless equation

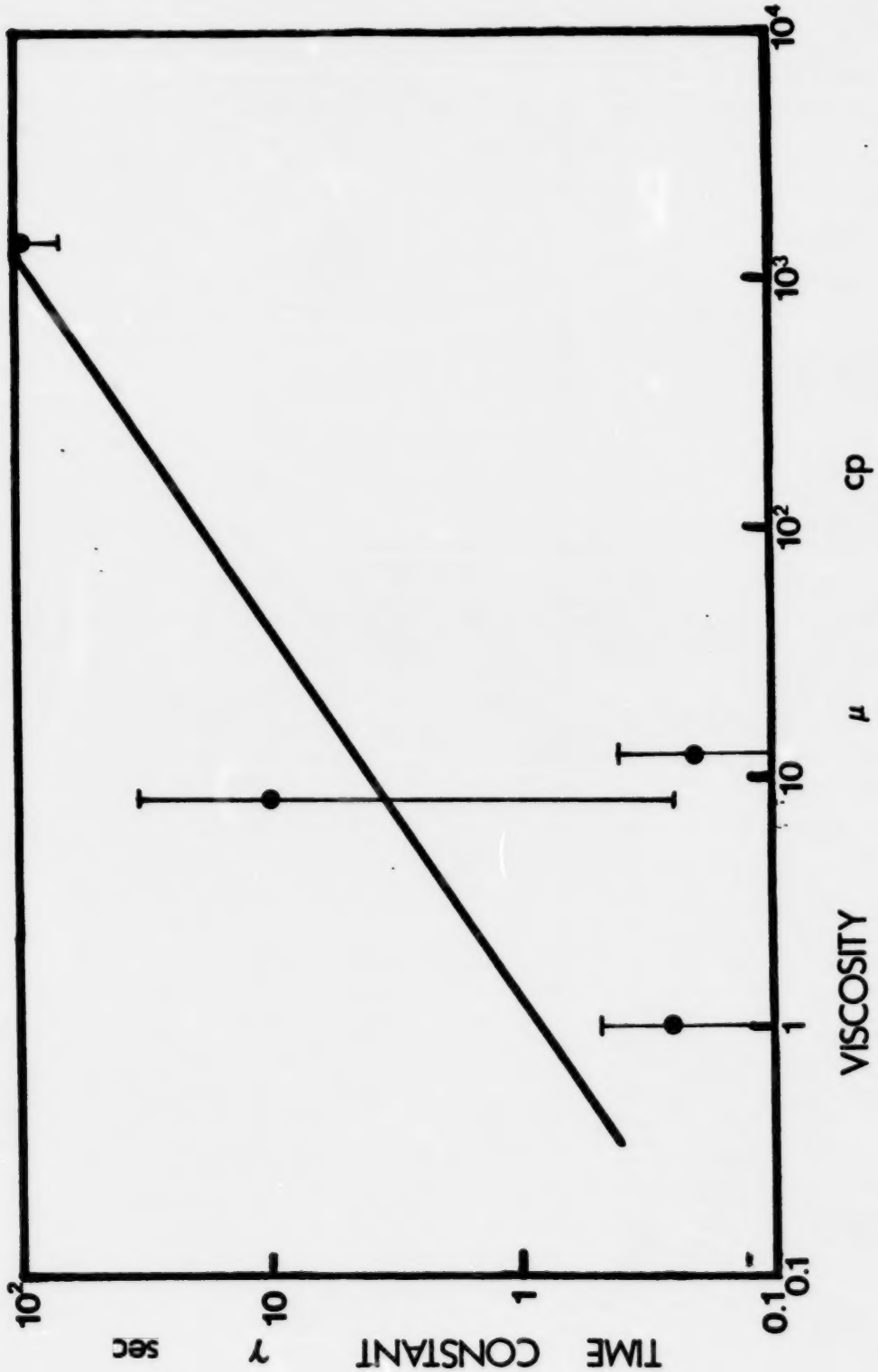

Figure 5.4.4 Effect of Viscosity on the Spreading Time Constant (Smooth Ice)

Figure 5.4.5 Effect of Viscosity on the Spreading Time Constant
(Average of Two Rough Ice Surfaces)

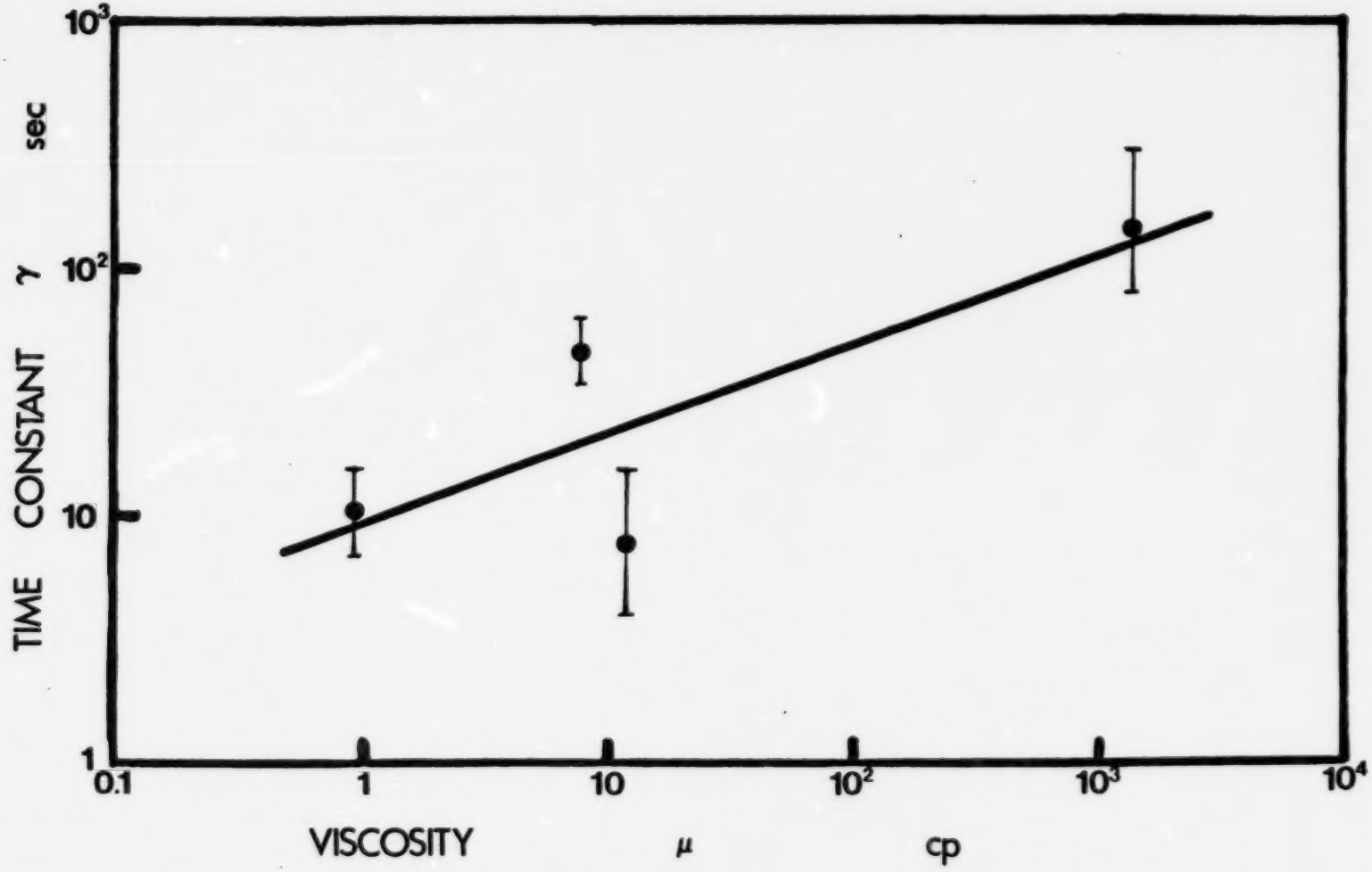

Figure 5.4.6 Spill Area-Time Profile for Bayol and Pentanol on Smooth Ice

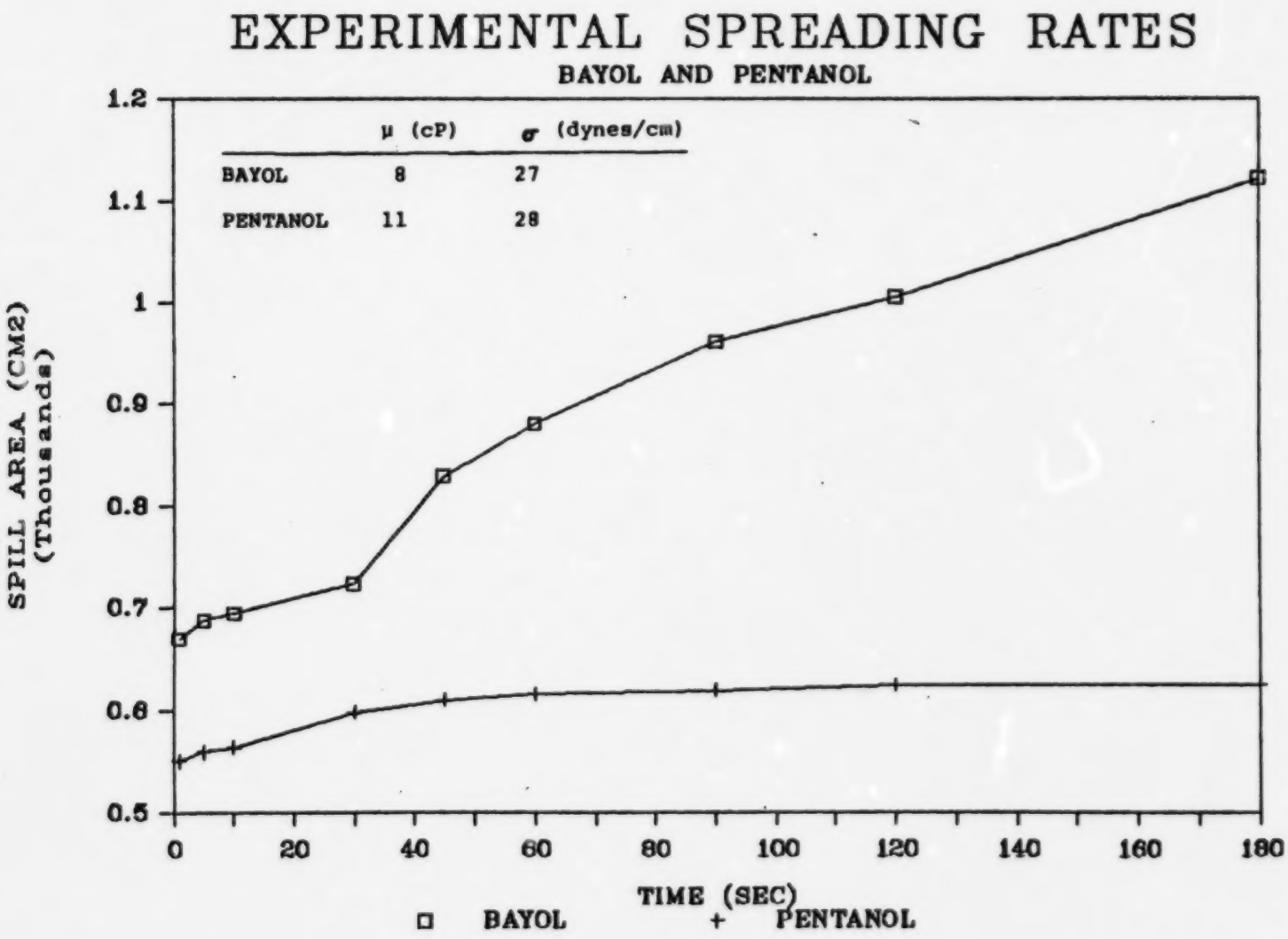

Figure 5.4.7 Effect of Spill Volume on Spreading Time Constant (Slopes Indicated Above Lines)

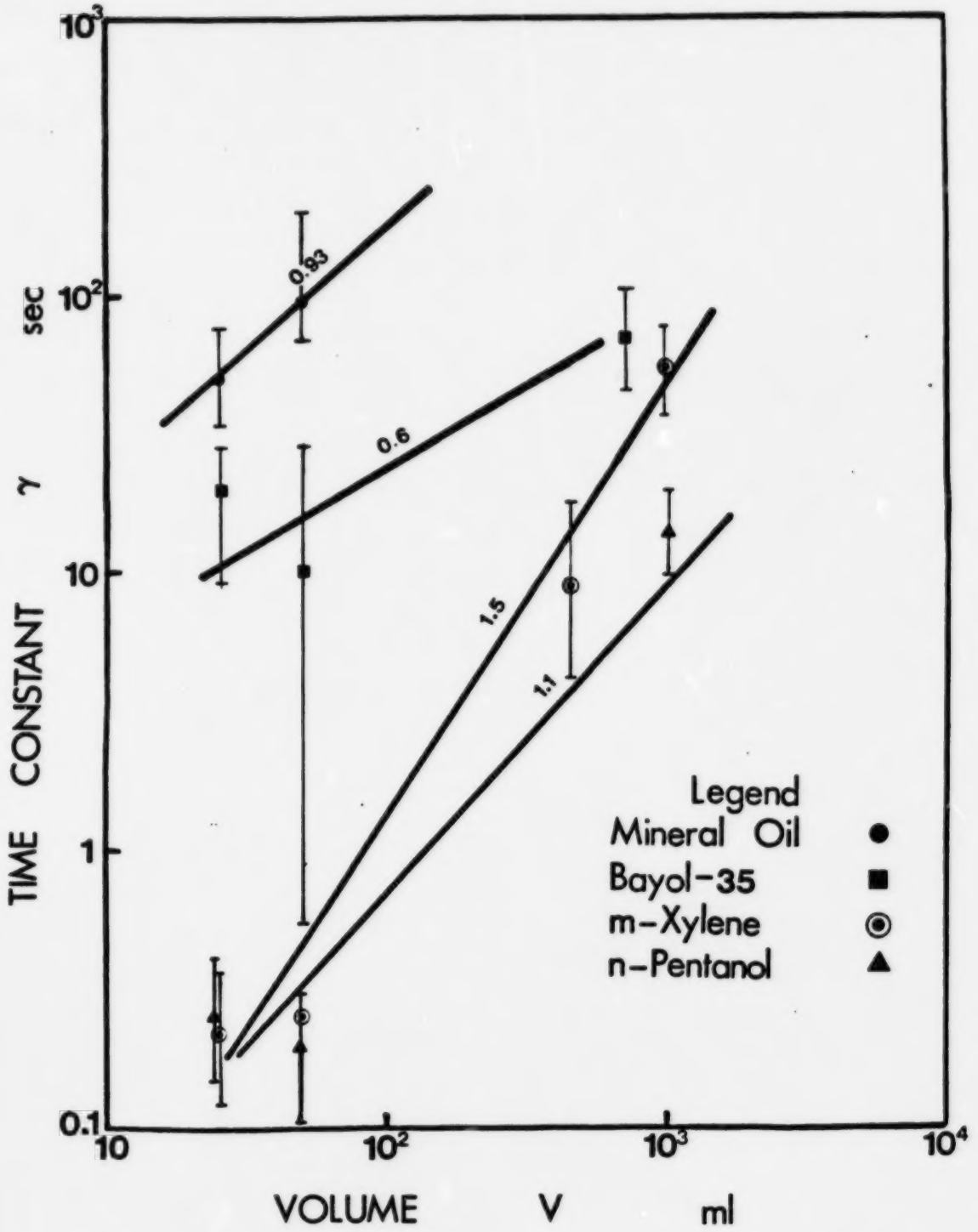

for the spreading time constant:

$$\frac{\gamma V^{1/6}}{g^{.5}} = 2.5\ E\text{-}05\ \frac{V^{2/6}\ \mu^{.5}\ \rho_c^{1.625}\ g^{1.875}}{\sigma^{2.125}} \qquad (5.3)$$

The non-dimensionalization, and the constant, 2.5 E-05, was determined as described in Section 5.4.3. Equation 5.3 and the experimental data are shown in Figure 5.4.8.

A dimensional version can also be written:

$$\gamma = 5\ E\text{+}05\ V\ \mu^{.5} \qquad (5.3a)$$

in which γ has units of seconds, V, m^3; and μ, kg/m s. Although the method of discharge, and consequently the spill release rate differed for the small and large ice spreading experiments, this effect was not considered to significantly affect the spreading time constant in these experiments since the discharge time relative to the spill duration was very small in both cases. For the outdoor ice experiments, the ratio of the discharge time to the spreading time varied between 0.002 and 0.01. The actual discharge rates were estimated at values between 200 and 500 mL/s for most experiments.

From Figure 5.4.8, it can be seen that the spreading time constants predicted by equations 5.3 and 5.3a can, in extreme cases, overpredict or underpredict the actual time constant by an order of magnitude. Thus, caution should be exercised when applying these equations to determine the spreading rate for actual spills. Unlike the correlations developed to estimate the final spill area, in which the spill rate is not believed to significantly affect the extent of spreading, the discharge rate may play a significant role in the spreading time, especially for large volume spills. For example, the spreading duration for a 10,000 L spill, in which the discharge rate is 10 L/s (complete discharge time of 17 minutes) will probably be longer than at 100 L/s (2 min. discharge time). Furthermore, if the spill volume is very large and the spill rate small, such that the discharge time is very long, the time of discharge may exceed the spreading duration predicted by equations 5.3 or 5.3a and 5.4. It appears that a more accurate correlation cannot be developed without including effects of chemical-ice interaction, surface roughness, and the spill discharge rate.

The second phase of the spreading kinetics study focused on determining the value of the slope term, x, in equation 3.3. The method involved finding the value of x, using equation 3.3, which best matched the experimental spill area-time profiles for all ice spreading experiments. It was determined that the best value of x ranged between 0.3 and 0.7 for all but one experiment, with 0.5 being the best or next-to-best value for 14 out of the 21 ice experiments. Experimental spill area-time

Figure 5.4.8 Correlation of Ice Spreading Time Constant

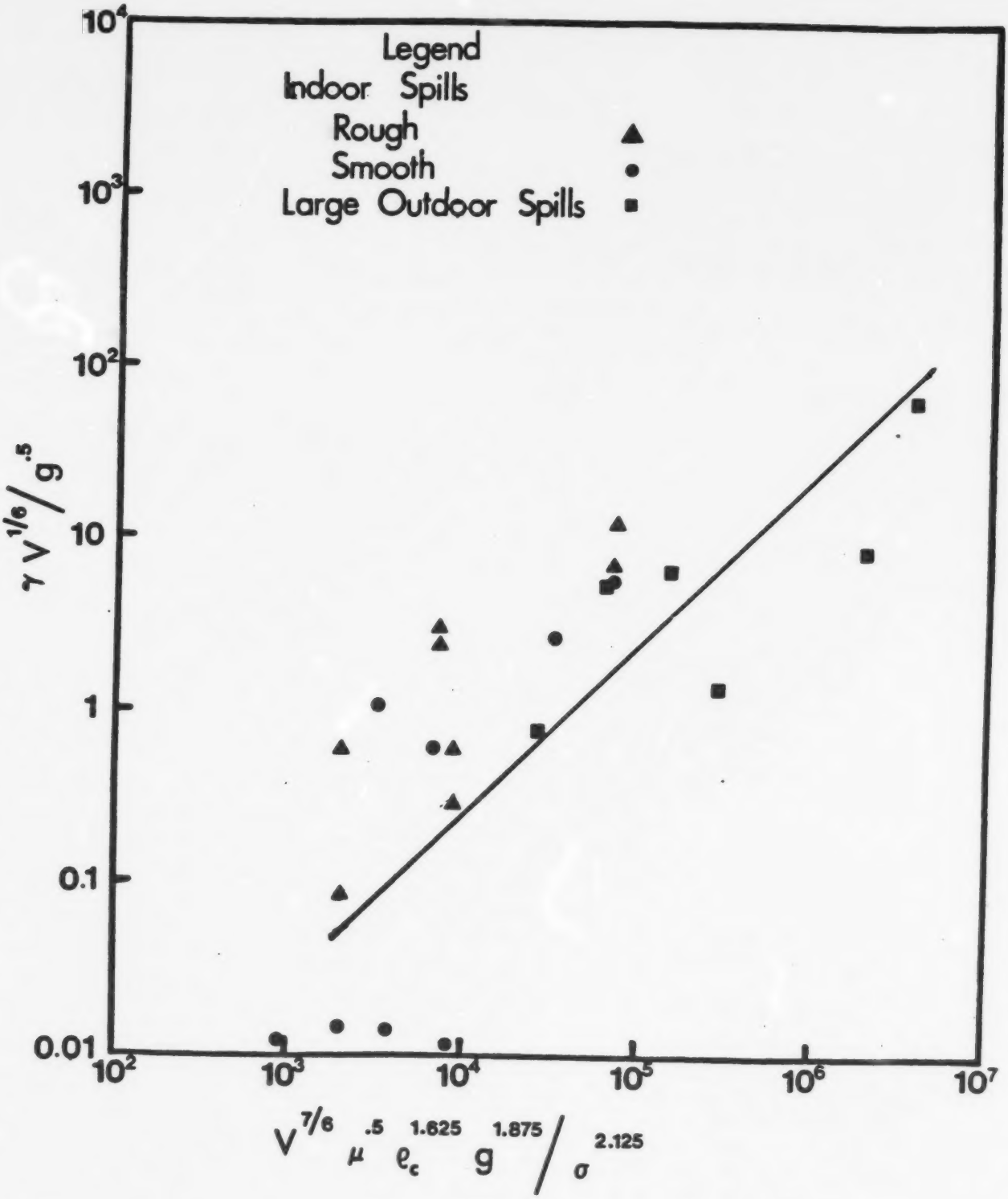

profiles and the profile predicted by equation 3.3, with x=0.5, using experimental A_f and γ values are presented in Figures 5.4.9, 5.4.10, and 5.4.11 for selected chemcials.

The only experiment in which the best x value did not fall in this (0.3 - 0.7) range was the 1 L outdoor xylene experiment, which had a best x of 1.0. This was due to the effect of strong winds, which accelerated the spreading. The effect of wind on the value of x for the higher viscosity chemicals was found to be negligible. This again, supports the observation (described in Section 5.4.4) that the wind effect is most prominent for low viscosity chemicals.

In spite of this result, it is believed that a value of x of 0.5 will adequately describe the kinetics of spreading for most chemicals under most conditions. The time of spreading can be estimated from equation 3.3 (with x=0.5) by setting the area to be 99% of the final spill area when spreading stops. The spreading time, t_f , is thus approximately:

$$t_f = 20\gamma \qquad (5.4)$$

Figure 5.4.9 Spreading Kinetics of Bayol on Smooth Ice

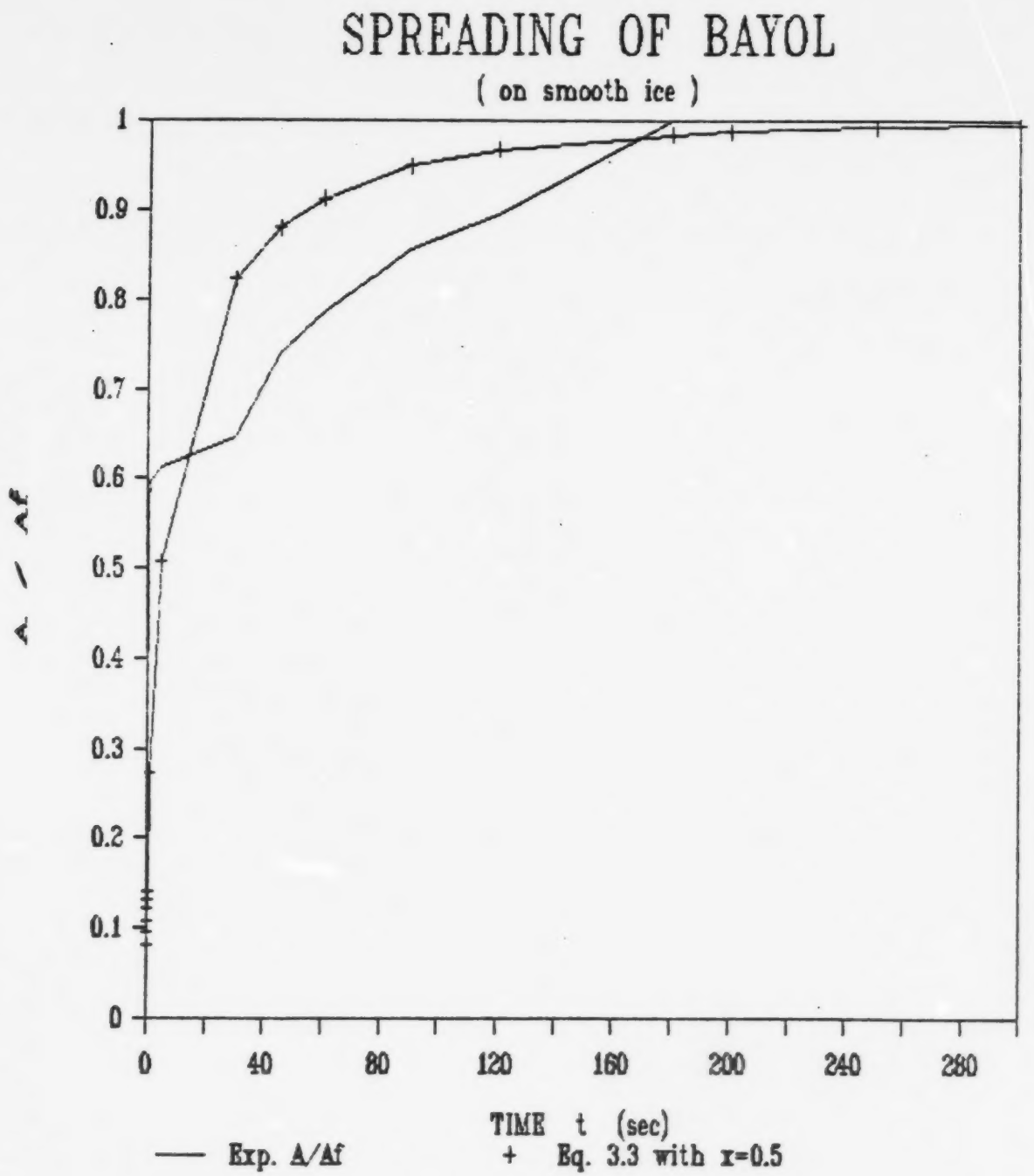

Figure 5.4.10 Spreading Kinetics of Xylene on Rough Ice

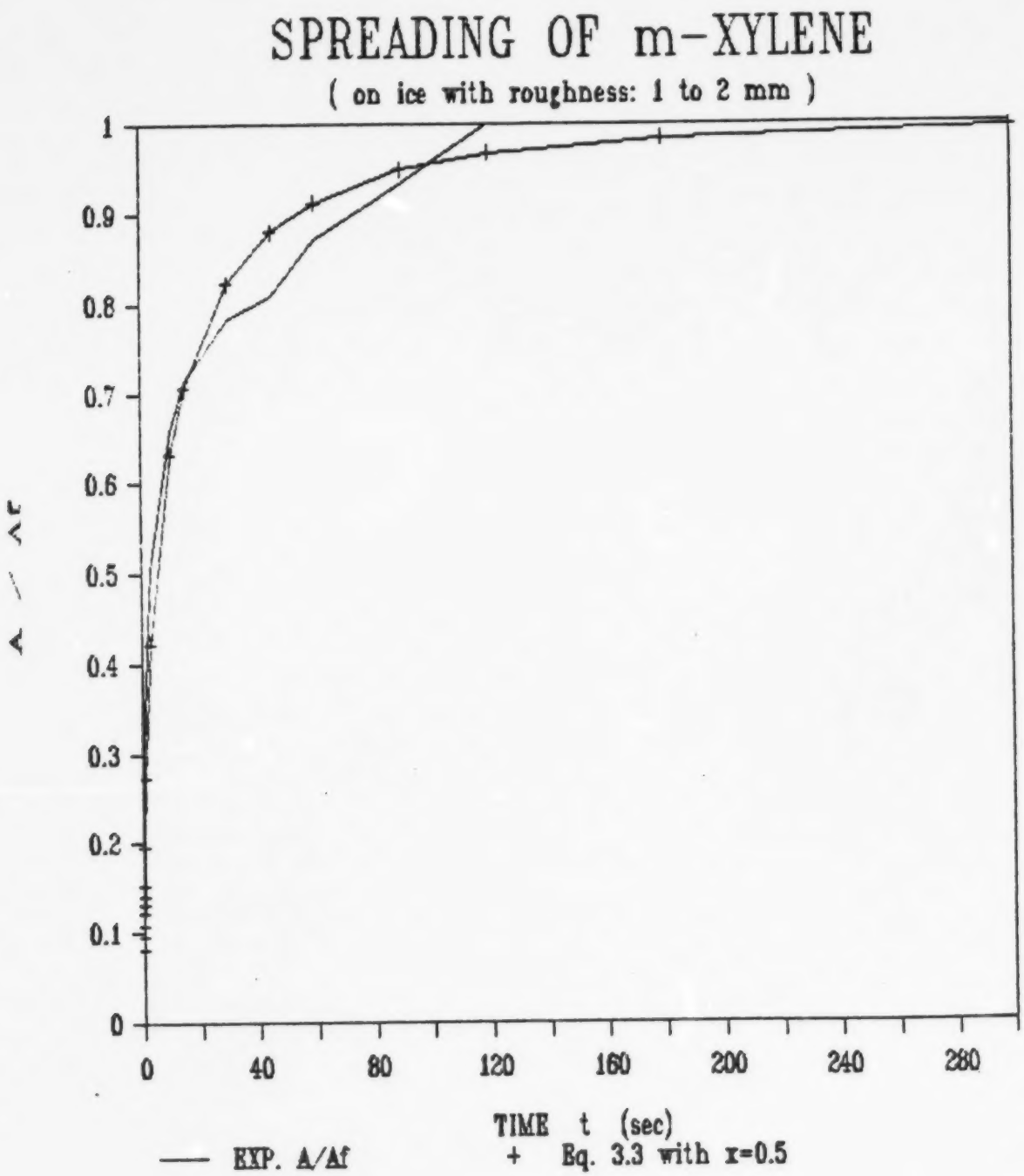

Figure 5.4.11 Spreading Kinetics of Light Mineral Oil
(Outdoor Ice Experiment)

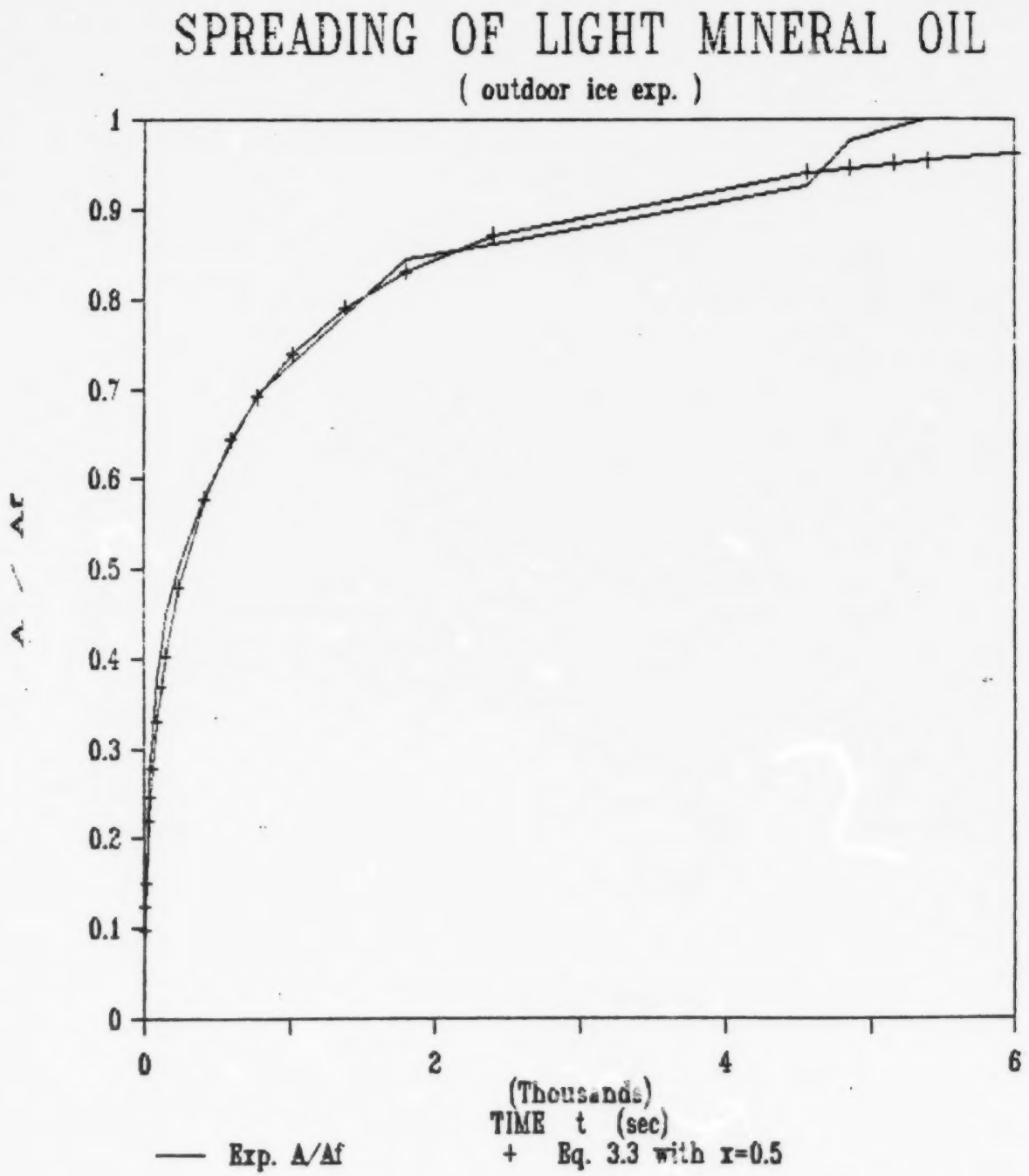

5.5 Spreading on Snow

5.5.1 Spills of Insoluble Chemicals on Snow

Results from the experiments involving insoluble chemicals (Group 1 and 2) on snow confirmed the expectation that the chemical is readily absorbed by snow and will spread radially along the bottom of the snowcover. This is seen in Figure 5.5.1, which shows that the spill area at the glass-snow interface is greater than the area on the surface of the snow. The extent of the surface spreading was minimal in most experiments, and its magnitude was found to depend mostly on the compaction of the snow and the chemical viscosity. Increase in either of these variables resulted in an increase in surface spill area. A cross section (Figure 5.5.2) of the snow reveals that there is no radial spreading of the chemical before the liquid reaches the bottom. These two photographs, (Figures 5.5.1 and 5.5.2), were taken from a spill of Bayol, but were representative of the general spreading behaviour of all experiments (experiment no. 1-18).

The data obtained from these experiments were used to correlate the final subsurface spill area and the rate of spreading. The actual surface and bottom areas, as well as other results not presented in the following sections are tabulated in Appendix D.

5.5.2 Effect of Spill Volume on the Final Area

The final bottom spill areas for the spill volume experiments (experiment no. 1-4) were used to determine the equivalent final spill depth, which was calculated by dividing the spill volume by the bottom spill area. These spill depths were plotted against the spill volume (log scale) in Figure 5.5.3.

The graph reveals a slight increase in the equivalent final spill depth with increasing volume of chemical spilled. The slope of the straight line drawn through the data was 0.13. Although this slope is smaller than the slope obtained from depth-volume experiments on ice, a similar trend was observed for both sets of experiments. It can be seen from Table 4.1 that the average temperature of these experiments varied by as much as 5 deg C. However, this effect is not believed to directly affect the spreading characteristics, except to alter the chemical viscosity. The viscosity effect on the spill area was found to be very small, and is discussed further in Section 5.5.4.

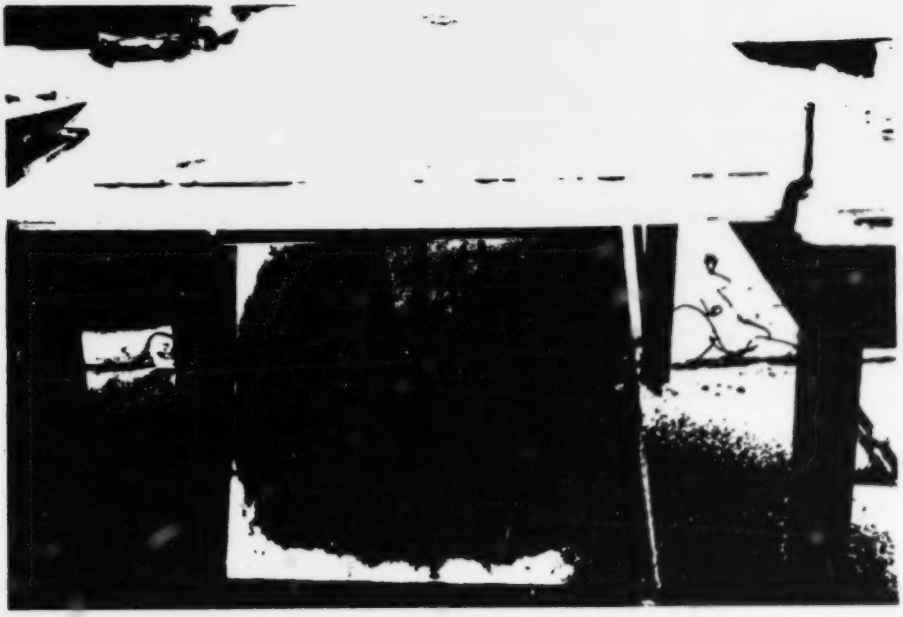

Figure 5.5.1 Spill of Bayol On Snow

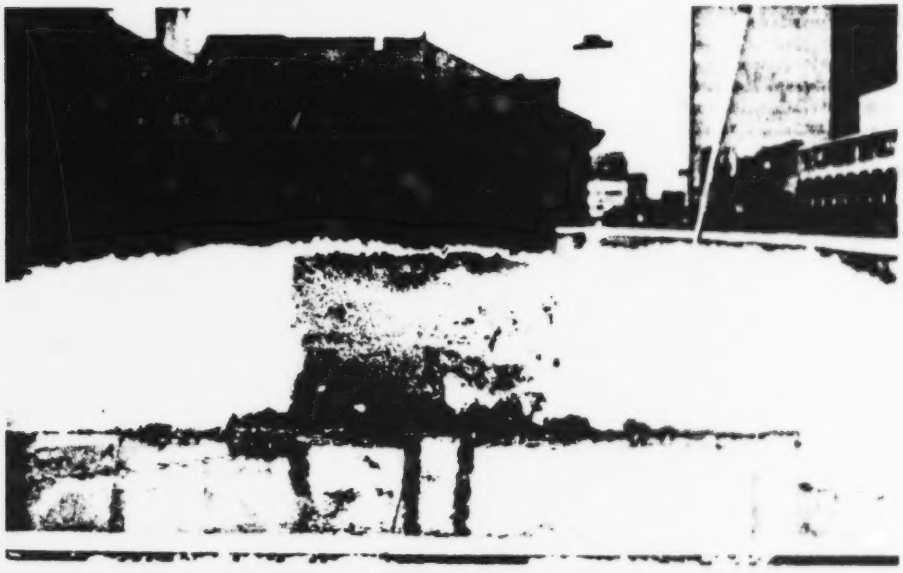

Figure 5.5.2 Cross-Section Profile of Snow Experiment

Figure 5.5.3 Effect of Spill Volume on Snow Final Spill Depth

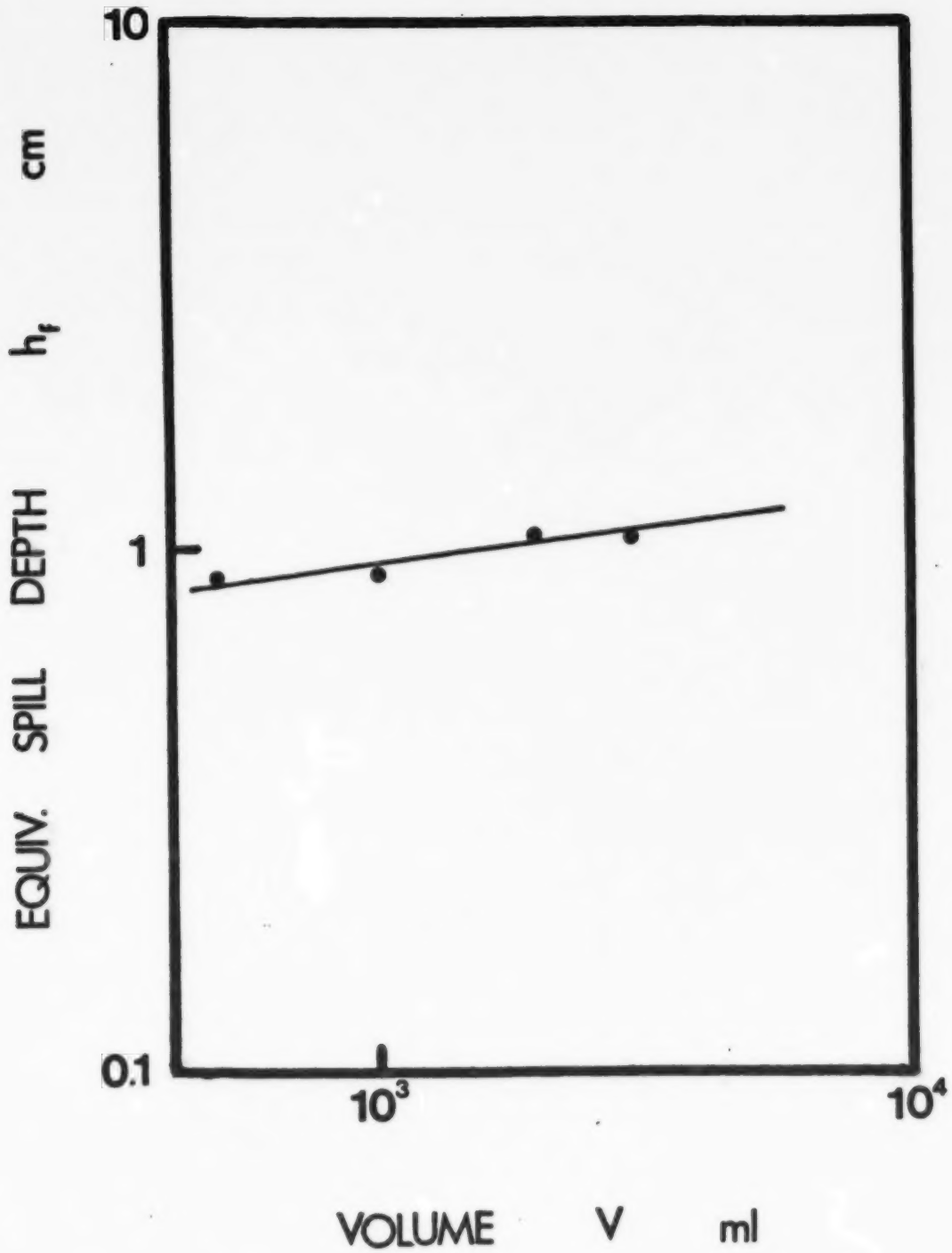

5.5.3 Effect of Snow Properties on the Final Area

The effect of snow bulk density and snow depth on the final equivalent spill depth were determined using the same method as described in the previous section. These graphs are presented in Figures 5.5.4 and 5.5.5.

The slopes of the best fit lines were found to be 0.48 for the snow density and -0.2 for the snow depth experiments. The slope of the snow density study indicates that as the snow density increases (snow porosity decreases), the final spill area decreases (final spill depth increases). This is due to the increase in resistance to the radial flow of the chemical, as a result of greater packing of snow crystals.

The snow depth result revealed that an increase in spill area occurred with increase in snow depth. To further investigate this unexpected result, cross sections of the snow were made at the end of these experiments. Photographs of the cross section from two of these experiments are shown in Figure 5.5.6 (snow depth 30 cm) and Figure 5.5.7 (4 cm). It is clear from these pictures that greater drainage of chemical occurred for the experiment with the greater snow depth. Table 5.6 tabulates the volume fraction of Bayol in the snow at two different regions: the upper "drained" region, and the bottom "near saturated" region, as well as the fraction of the total snow depth corresponding to the upper "drained" region.

Table 5.6: Drainage of Bayol at Different Snow Depths

Snow Depth (cm)	Volume Fraction Bayol "upper"	"lower"	Depth Fraction
30	0.22	0.67	0.93
15	0.22	0.56	0.68
9	0.27	0.64	0.56
4	0.46	0.56	0.25

The results from Table 5.6 show that the effect of gravity is best utilized in the drainage of the chemical at greater snow depths. The snowdepth of 30 cm is also associated with the greatest drainage efficiency, as indicated by the depth fractions. These effects are thought to result in a larger driving force for the outward spreading of the chemical, which would explain the results from these experiments.

The experiments performed to determine the effect of snow crystal type on the final spill area were not sufficient in number to determine an explicit relationship for the data

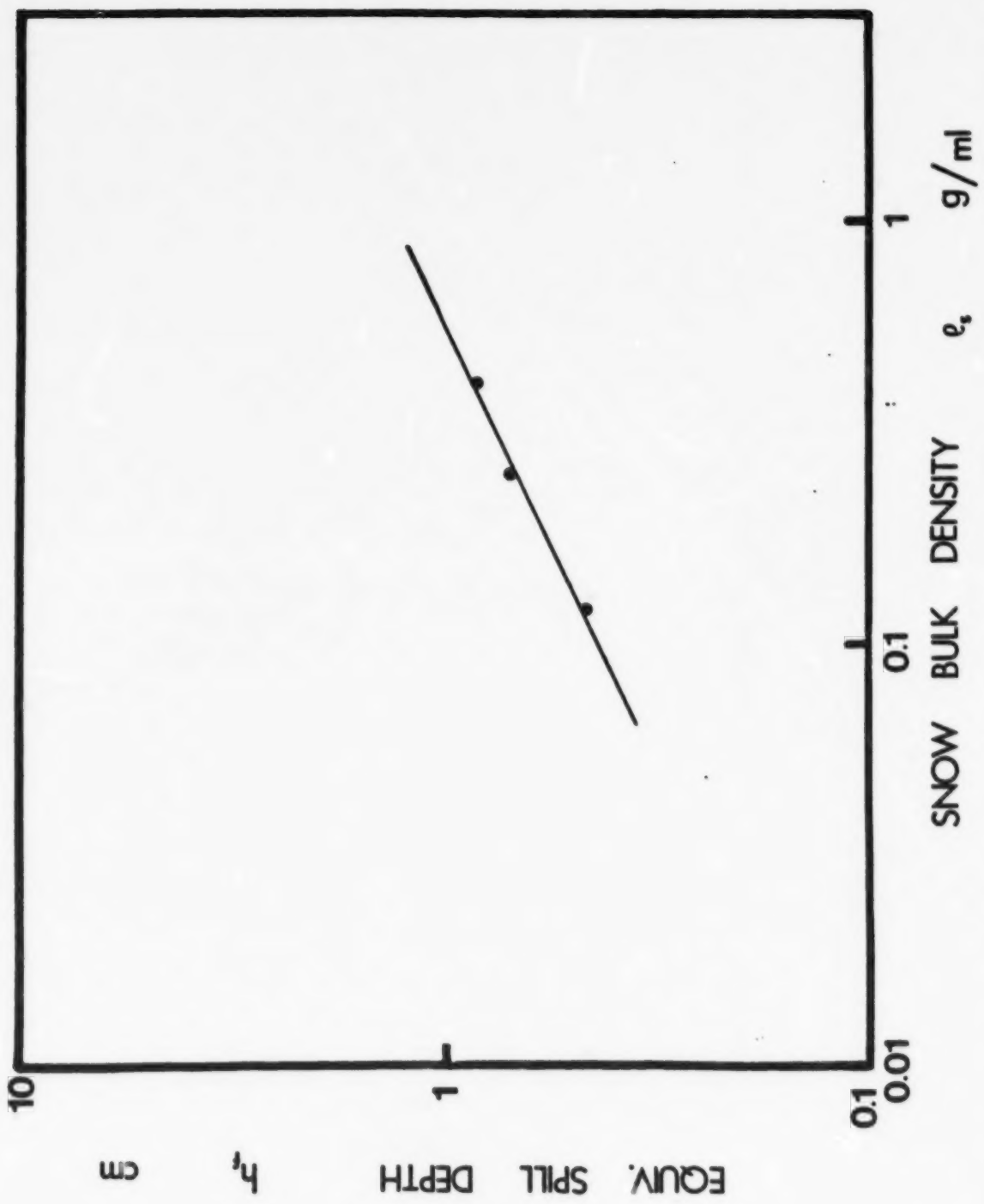

Figure 5.5.4 Effect of Snow Bulk Density on Final Spill Depth

Figure 5.5.5 Effect of Snow Depth on Final Spill Depth

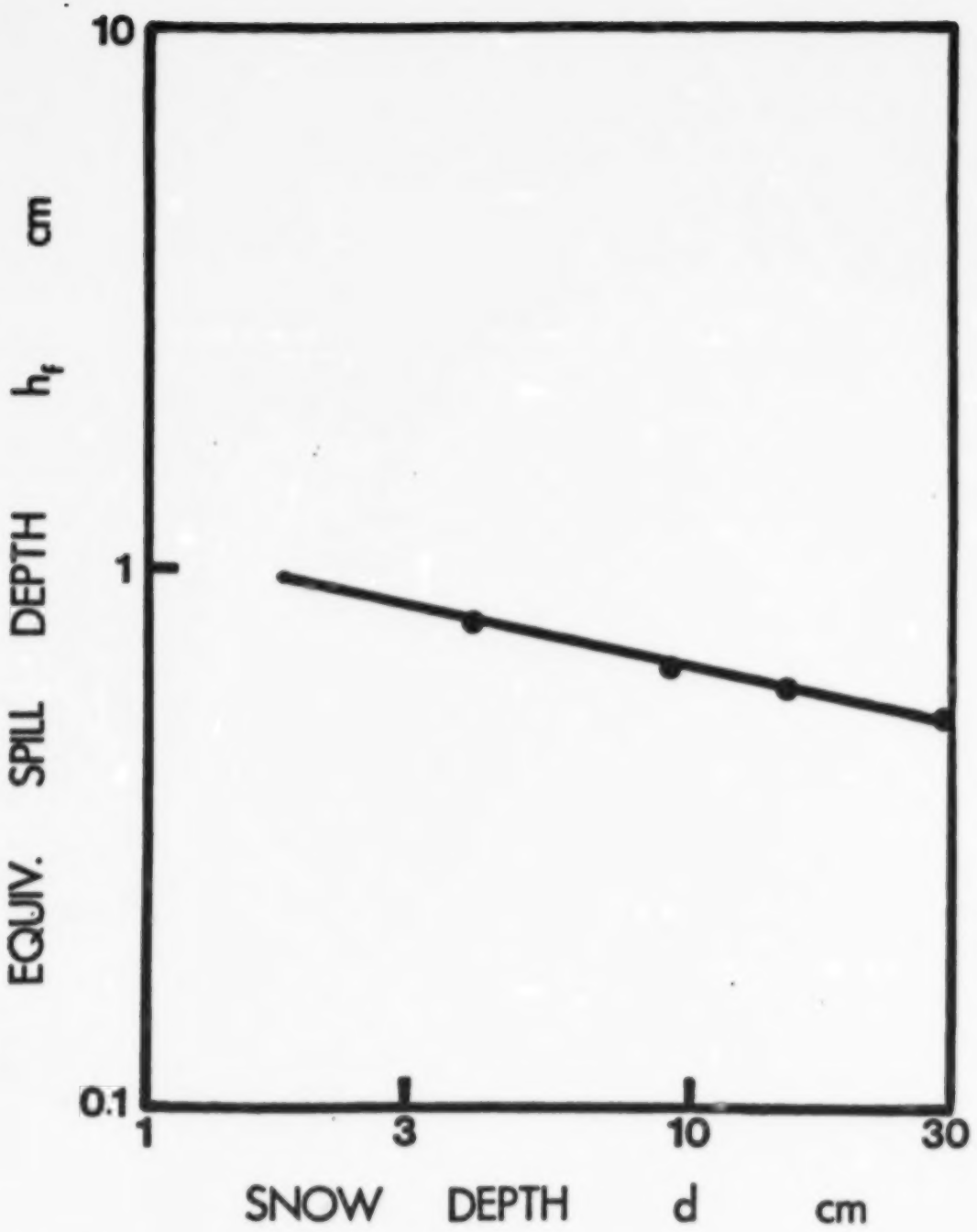

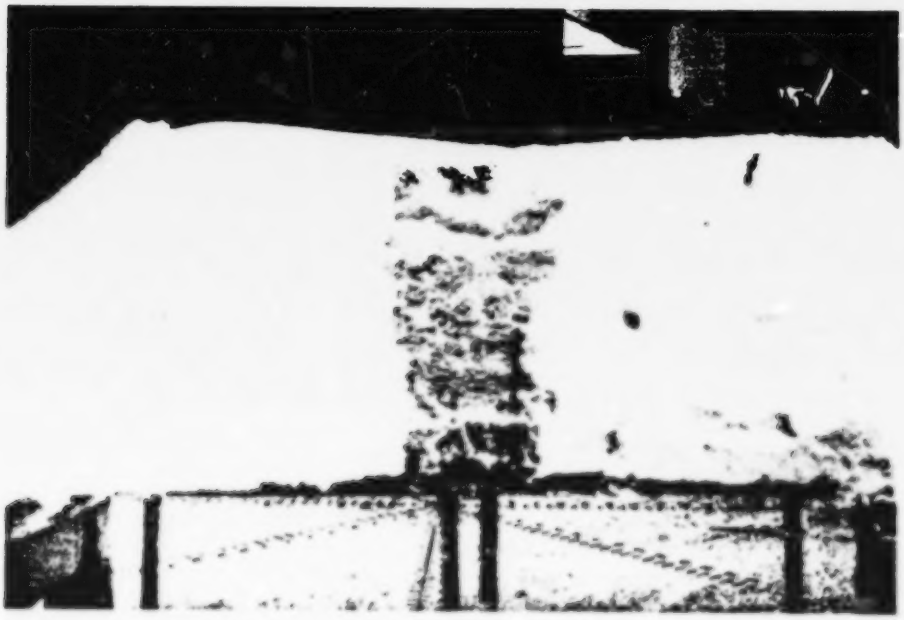

Figure 5.5.6 Cross-Section Profile: Snow Depth 30 cm

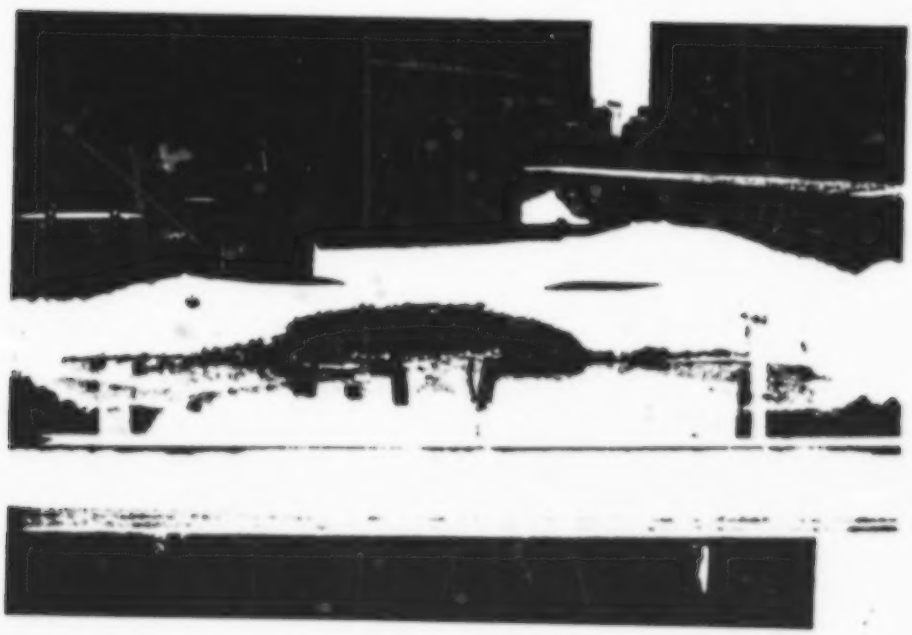

Figure 5.5.7 Cross-Section Profile: Snow Depth 4 cm

correlation. However, a snow density factor was introduced, based on the results of these experiments. This is further discussed in Section 5.5.5.

5.5.4 Effect of Chemical Viscosity on the Final Spill Area

The final equivalent spill depths were calculated and plotted against the chemical viscosity for the five experiments, numbers 12-16. As Figure 5.5.8 shows, there is a small (slope -0.05) but a definite trend of decrease in spill depth (increase in area) with increasing chemical viscosity. This trend is contrary to what was observed for the experiments on ice surfaces. It is believed that viscous chemicals, because they spread at a slower rate, and for a longer duration, are much more susceptible to variations in the surrounding temperature, solar insolation and other external factors which may influence the spreading. Furthermore, the upward capillary movement of the chemical, from the glass-snow interface were found to be smaller for viscous chemicals. Experimental measurements revealed that the actual thickness of the near-saturated chemical-snow mixture from the glass surface was 5 cm for xylene, 4 cm for bayol, 3 cm for pentanol and 2 cm for heavy mineral oil. That is, the thickness of the radial spill was found to be smaller for viscous chemicals. This effect is thought to allow more volume of chemical to be available for the outward spreading. Therefore, the combination of longer spreading duration and the smaller upward movement of the chemical in the snow are believed to be the reasons for the increase in spill area with the viscosity.

Although the effect of chemical viscosity on the final spill area is small, the spreading characteristics for highly viscous chemicals, such as heavy mineral oil (1500 cp) was noticably different than for chemicals with lower viscosity. Figure 5.5.9 shows the surface spreading of mineral oil, which is significantly greater than for bayol (Figure 5.5.1). It was observed that the radial surface spreading of mineral oil did not cease until the termination of the discharge onto the snow. In addition, the drainage of the chemical into the snow occurred in "channels", instead of as a saturated front. The channelling effect can be seen in the photograph (Figure 5.5.10), which was taken moments after penetration to the bottom. A cross section picture taken at the end of the experiment (Figure 5.5.11) shows this effect as well as a decrease in snow depth, which was probably due to the effect of solar insolation. Also visible is a layer of fresh snowfall on top of the original snowcover.

5.5.5 Correlation of the Final Spill Area on Snow

The results from Sections 5.5.2, 5.5.3 and 5.5.4 were combined to correlate the final bottom spill area with the chemical viscosity and snow properties. The results obtained thus far are:

Figure 5.5.8 Effect of Viscosity on Final Spill Depth in Snow

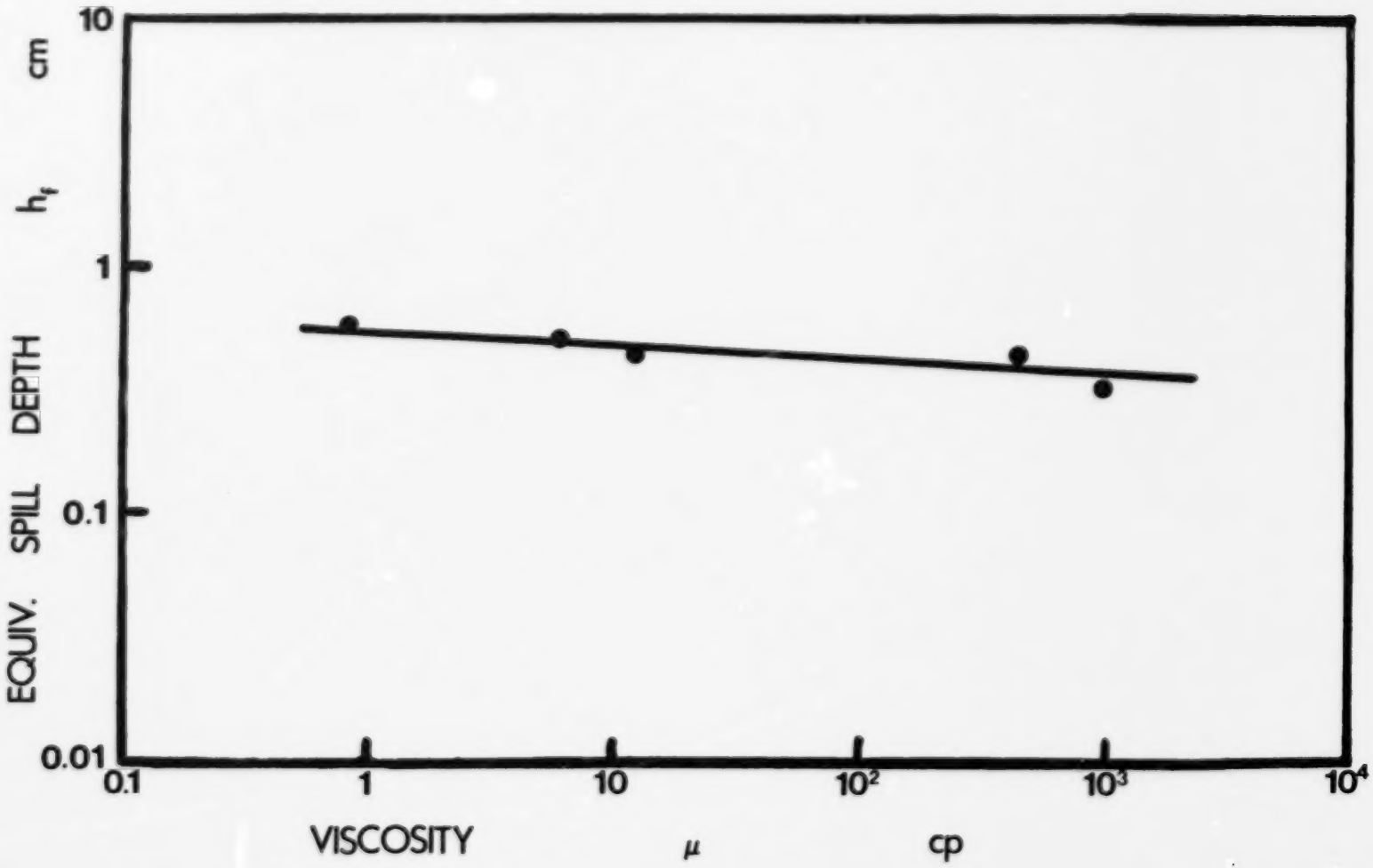

Figure 5.5.9 Surface Spreading of Heavy Mineral Oil on Snow

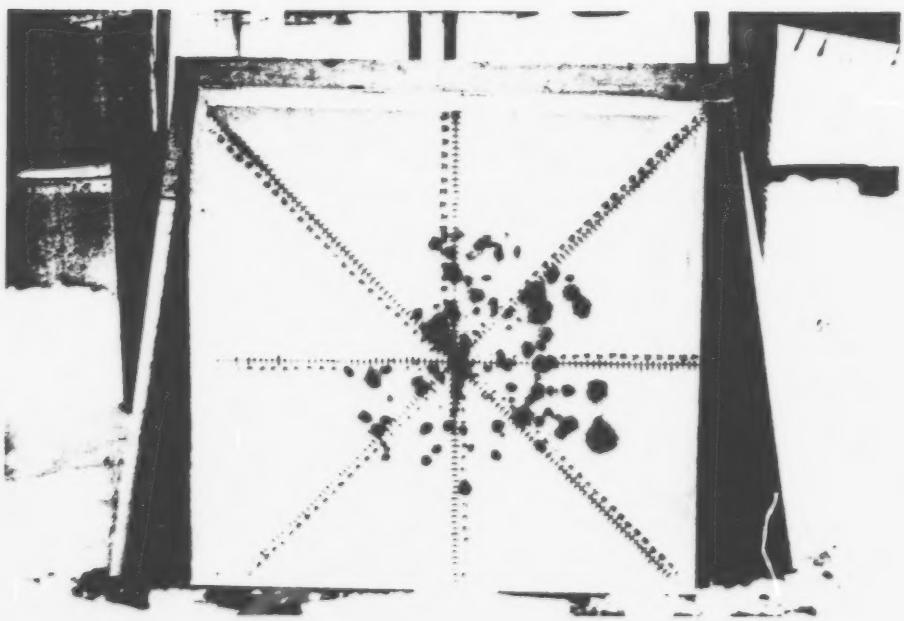

Figure 5.5.10 Channelling Effect of Heavy Mineral Oil

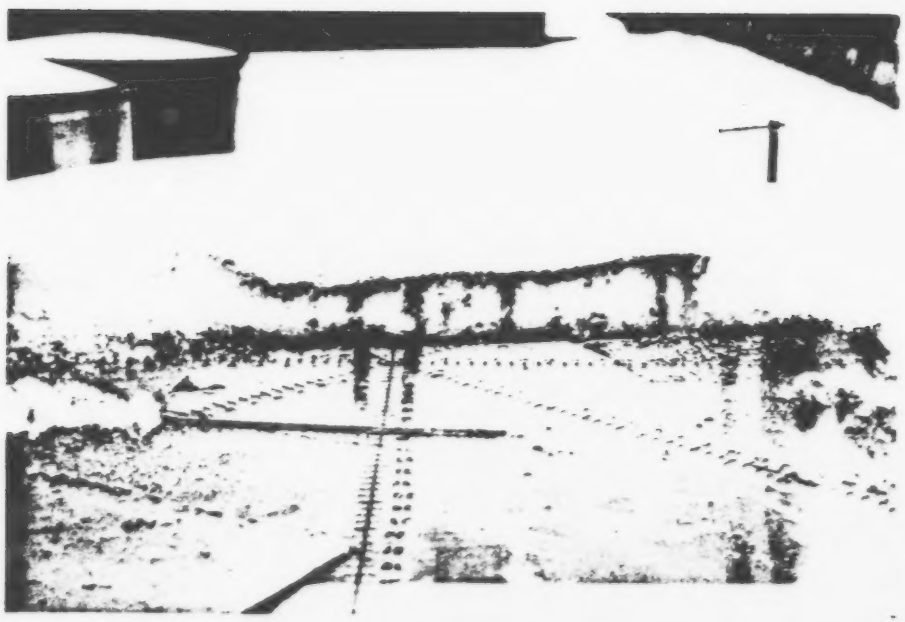

Figure 5.5.11 Cross-Section Profile of Heavy Mineral Oil

$$h_f \propto V^{.13}\, d^{-.2}\, \rho_s^{.48}\, \mu^{.05}$$

or:

$$A_f \propto V^{.87}\, d^{.2}\, \rho_s^{-.48}\, \mu^{.05}$$

where ρ_s is the density of the snowcover, and d is the snow depth. The relationship for A_f was non-dimensionalized by introducing the same variables and employing the same procedure as described in 5.4.3.

The above expression, in dimensionless form is:

$$\frac{A_f}{V^{2/3}} = K' \frac{V^{.2}\, d^{.2}\, \rho_c^{.8675}\, g^{.4125}\, \mu^{.05}}{\rho_s^{.48}\, \sigma^{.4375}} \qquad (5.5)$$

Experimental data were used to calculate the constant K' in equation 5.5. Table 5.7 lists these values along with the snow crystal properties for each experiment.

Table 5.7 Effect of Snow Crystal Type on Final Area

Exp. no.	K'	Crystal Type+	Age of Snow (days)	Surface Wetness
1	0.37	a,b	1	D
2	0.39	a,b	1	D
3	0.36	a,b	1	D
4	0.37	a,b	1	D
5	0.46	b	2	D
6	0.47	b	2	D
7	0.46	b	2	D
8	0.45	a,b	1	D
9	0.41	a,b	1	D
10	0.40	b	3	W
11	0.42	b	3	W
12	0.49	b	2	D
13	0.53	b	2	D
14	0.53	b	2	D
15	0.46	b	2	D
16	0.63	b	3	D
17	1.7	c,e**	>10	D
18	0.72	c*	7	D

* Grain size : 1mm D: dry
** Grain size : 2-4 mm W: wet
+ see Section 2 for definitions.

Since snow type was the only property which was not addressed in the development of equation 5.5, the effect of this property should be exhibited by the constant, K'. It can be seen from Table 5.7 that K' is fairly constant for snow crystal types a and b, (experiment no. 1-16) regardless of its wetness. However, for crystal types c and e, the constant is considerably greater than the average of 0.45 for experiments involving snow crystal types a and b. This led to the inclusion of a snow density parameter, φ . This parameter was introduced in the hope that the product of the snow density parameter and the snow bulk density will quantify the properties of the snow which affect the spreading. The results in Table 5.7 confirm that this objective cannot be attained by snow density alone. The values of the snow density parameter were calculated based on the constants in Table 5.7 and are listed in Table 5.8. It should be noted that these values were determined from single experiments and further experiments should be performed to verify or improve these values.

Table 5.8 Snow Density Parameter

Snow Description	Snow Crystal Type	φ
Fresh snow, wet or dry (crystalline structure still present)	a,b	1.0
Crusty firn (rounded) snow approx 1 mm in dia.	c	0.5
Advanced firn snow: 2-4 mm dia	c,e	0.1

Specifically, the snow density parameter reflects the degree of resistance to the radial, subsurface spreading of the chemical. The maximum value of 1.0 apply for snow crystals which still possess some crystalline structure, and this offers the greatest resistance to flow. As metamorphic processes, or thaw-freeze cycles convert these crystals to a more or less round shape, the resistance decreases, and is indicated by smaller φ values.

Equation 5.5 now becomes:

$$\frac{A_f}{V^{2/3}} = 0.45 \frac{V^{.2}\, d^{.2}\, \rho_c^{.8675}\, g^{.4125}\, \mu^{.05}}{(\varphi\, \rho_s)^{.48}\, \sigma^{.4375}} \qquad (5.6)$$

An expression for the equivalent final spill depth in snow is:

Figure 5.5.12 Correlation of Snow Final Spill Area

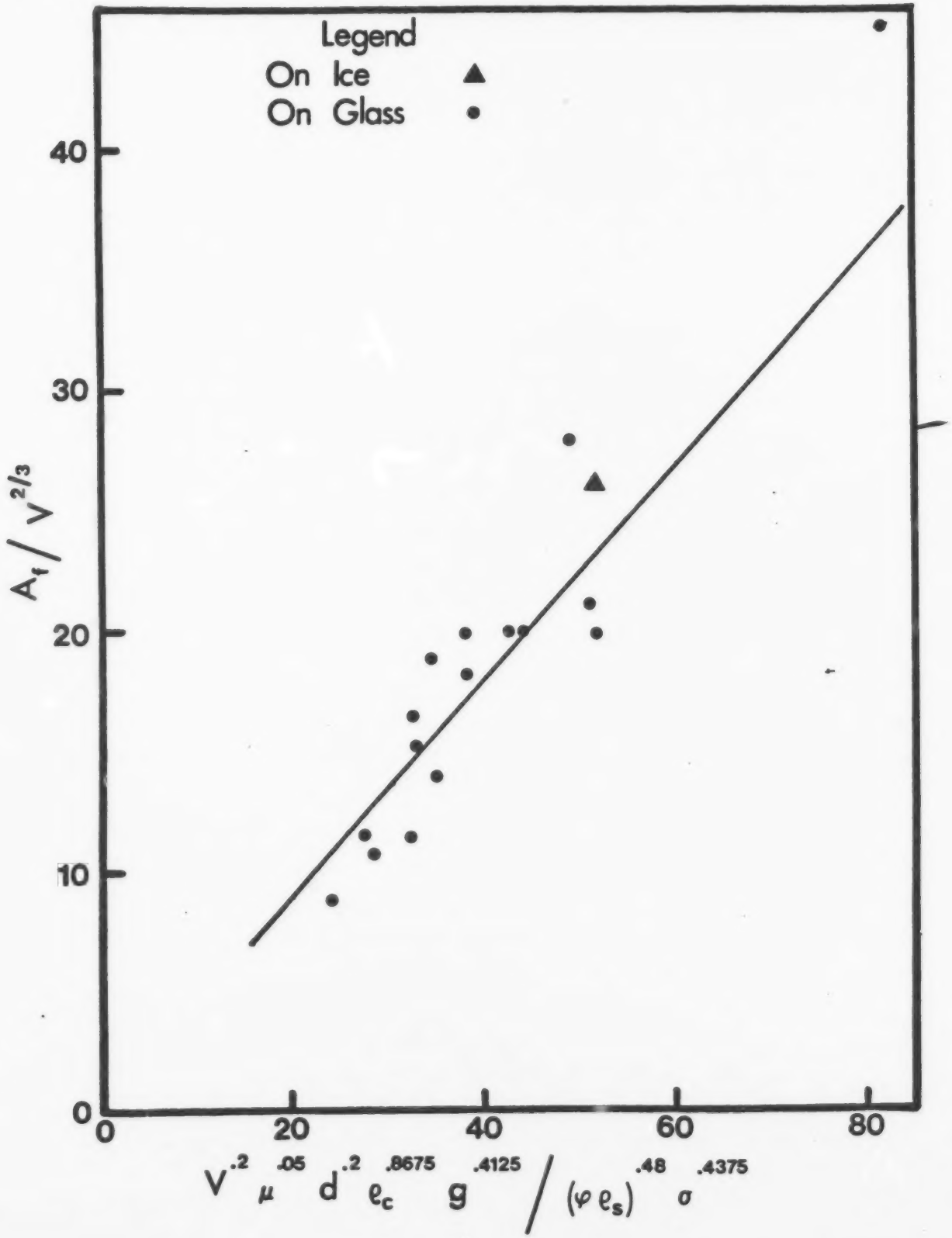

$$h_f = 5.3\ E\text{-}04\ \ V^{.13}\ d^{-.2}\ \mu^{-.05}\ (\varphi \rho_s)^{.48} \qquad (5.6a)$$

where h_f is in m, V in m^3, d in m, μ in kg/m s, and ρ_s in kg/m^3.

The constant in equation 5.6 for experiments 17 and 18, after introducing the snow density parameter was 0.55 and 0.52, respectively, which is closer to the average of 0.45. A plot of equation 5.6 and the experimental data is presented in Figure 5.5.12. The difference between the experimental spill areas and the areas predicted by equation 5.6 ranged between less than 1% and 29%, with an average difference of 12%. Since this equation was able to correlate the experimental data with reasonable accuracy, it can be used to estimate the final bottom spill area of Group 1 and 2 chemicals.

However, one problem of using equation 5.6 or 5.6a in actual spill conditions is that the snow type and density are usually unknown. (The snow depth, as described in Section 2, can be obtained from weather stations or estimated from historical data.) Nevertheless, if the age of the snow and the area's overall climate are known, one can make an intelligent estimate for the value of these properties. Snowcover theory presented in Section 2 would be beneficial in this case. Even if an estimate cannot be made, average or typical values could be employed from Tables 2.1 and 5.8.

There are other variables that may be present in the environment which may influence the spreading behaviour, but were not investigated in this study. These include the presence of stratified snow or ice layers, non-horizontal and porous underlying surface, and the long term effect of spills. In the latter situation, the spill may begin to spread after the initial cessation of spreading due to temperature fluctuations and melt down of snow. Despite these uncertainties, the correlations presented in this study are believed to be able to give an order-of-magnitude estimation of the extent of the subsurface spreading of chemicals in snow.

5.5.6 Kinetics of Spreading on Snow

The spreading time constants for all spreading experiments involving Group 1 and 2 chemicals were determined from spill area vs. time profiles. For this study, time zero was taken as the time when the chemical was first observed at the bottom of the snowcover. These time constants were plotted, on log scale, against the variable being studied for each of the four sets of experiments. These graphs are presented in Figures 5.5.13 to 5.5.15.

By evaluating the slopes from each of the graphs, the following relationship was obtained:

$$\gamma \propto V^{.45}\ d^{.6}\ \rho_s^{1.1}\ \mu^{.78}$$

Figure 5.5.13 Effect of Snow Depth and Spill Volume on Spreading Time Constant

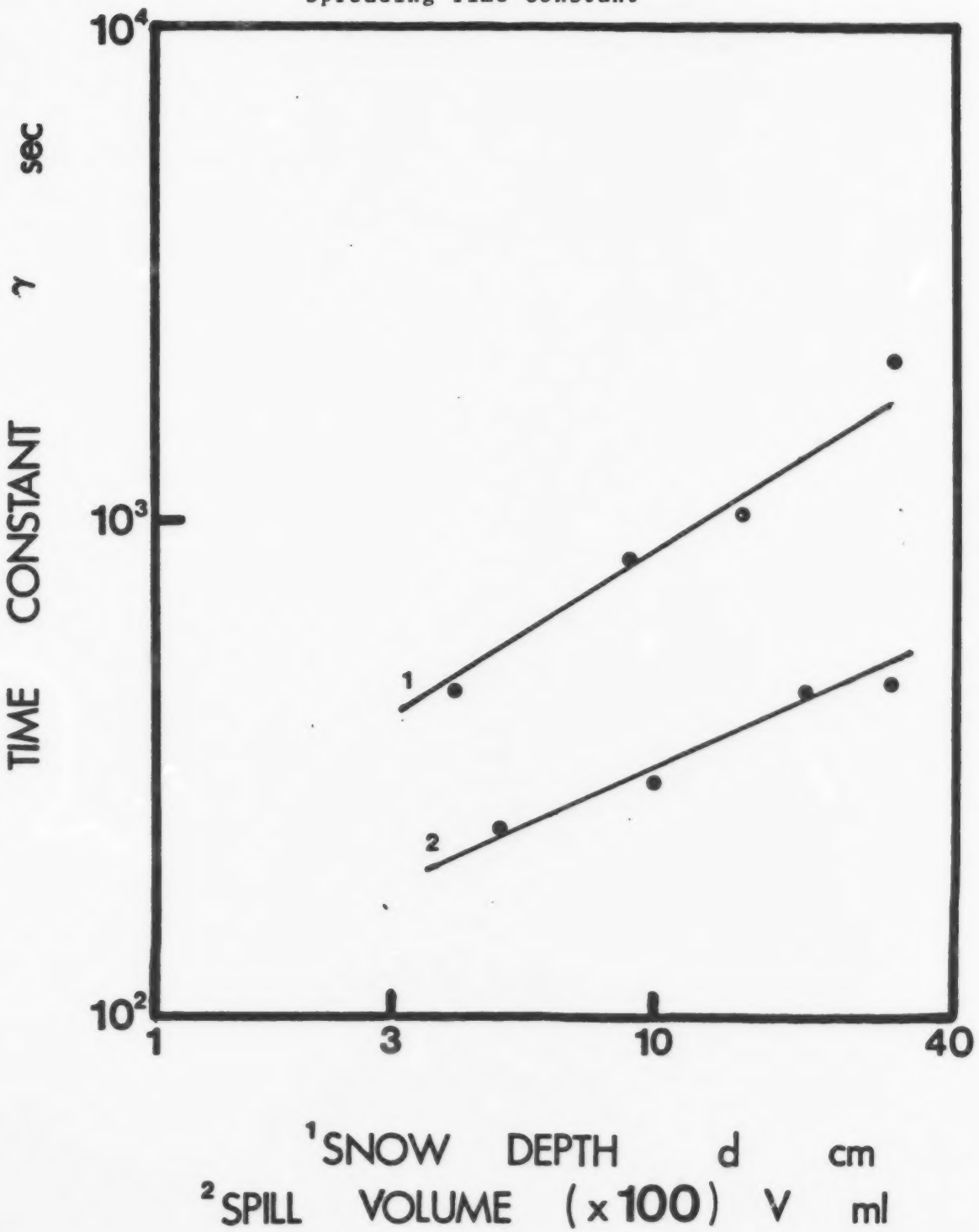

Figure 5.5.14 Effect of Snow Bulk Density on Time Constant

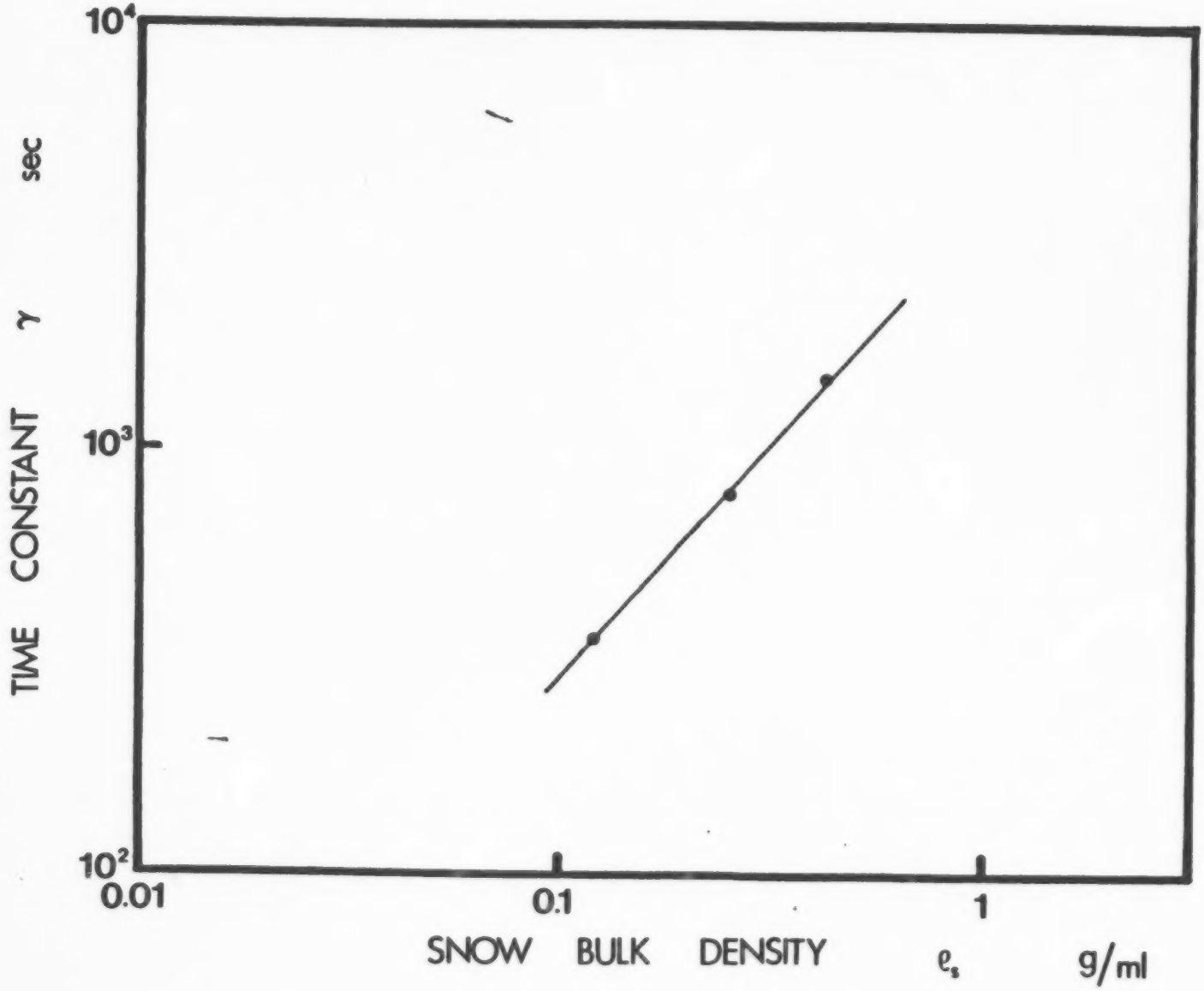

Figure 5.5.15 Effect of Chemical Viscosity on Snow Time Constant

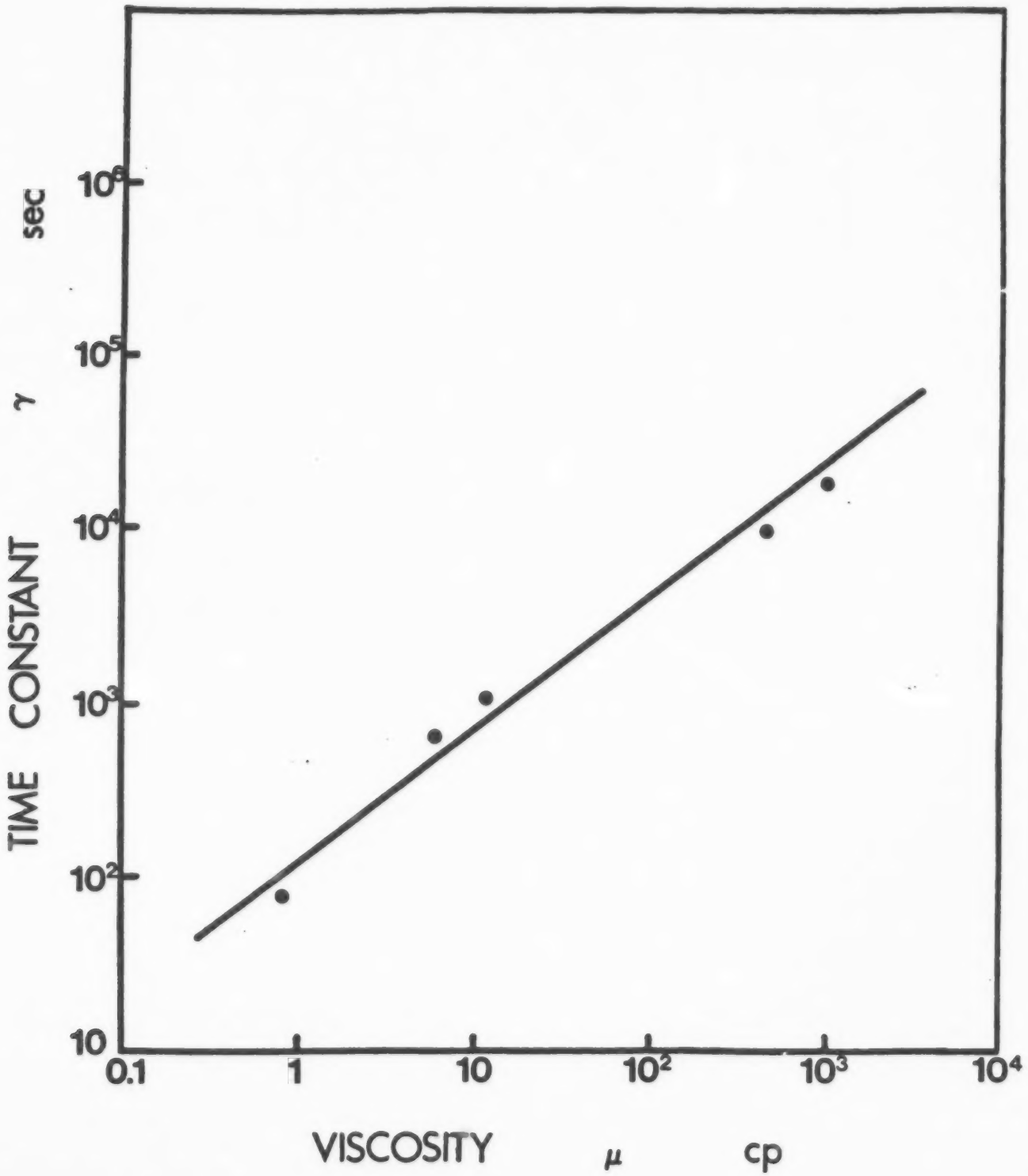

ie. an increase in spill volume, snow depth and density and the chemical viscosity results in an increase in the spreading time constant.

These results were, again, expressed in a dimensionless form:

$$\frac{\gamma V^{1/6}}{g^{.5}} = 0.18 \frac{V^{.62} d^{.6} \rho_s^{1.1} \mu^{.78} g^{1.425}}{\rho_c^{.065} \sigma^{1.815}} \qquad (5.7)$$

The constant 0.18 was determined from the average of the individual constants which ranged between 0.13 and 0.27, for the 18 experiments. Equation 5.7 is presented with the experimental data in Figure 5.5.16.

An equivalent dimensional version is:

$$\gamma = 5700\, V^{.45} d^{.6} \rho_s^{1.1} \mu^{.78} \qquad (5.7a),$$

in which γ is in seconds, V in m^3, d in m, μ in kg/m s, and ρ_s in kg/m^3.

Figure 5.5.16 shows that equation 5.7 was more successful in correlating the snow experimental spreading time constants than equation 5.3 for the ice time constants. This suggests that the factors which were not studied, but were thought to influence the spreading rates on ice, such as chemical-ice surface interactions are not important for spills on snow surfaces. Therefore, equations 5.7 and 5.7a may be used with more confidence than the corresponding equations for ice surface spills.

It was surprising that the snow density parameter, which was required to correlate the spill area data was not required for the correlation of the time constants for experiments 17 and 18. The actual constant in equation 5.7 for these experiments were 0.27 and 0.18, respectively. From the results discussed in Section 5.5.5, a decrease in time constant was expected for the "lower flow resistance" snow crystals employed in experiments 17 and 18. However, close inspection of the experimental area-time profiles revealed that the increase in the rate of spreading was not able to influence the time constants due to the large final areas attained. Since the time constant is the time when the spill area reaches 63% of the now larger final area, the constant was not significantly affected by the type of snow crystal.

As stated previously, an "effective time", which was corrected for the time required for penetration of the chemical to the bottom of the snowcover, was used in the spill area-time profiles to determine and correlate the spreading time constants. There is no doubt that the penetration time can be

Figure 5.5.16 Correlation of Snow Spreading Time Constant

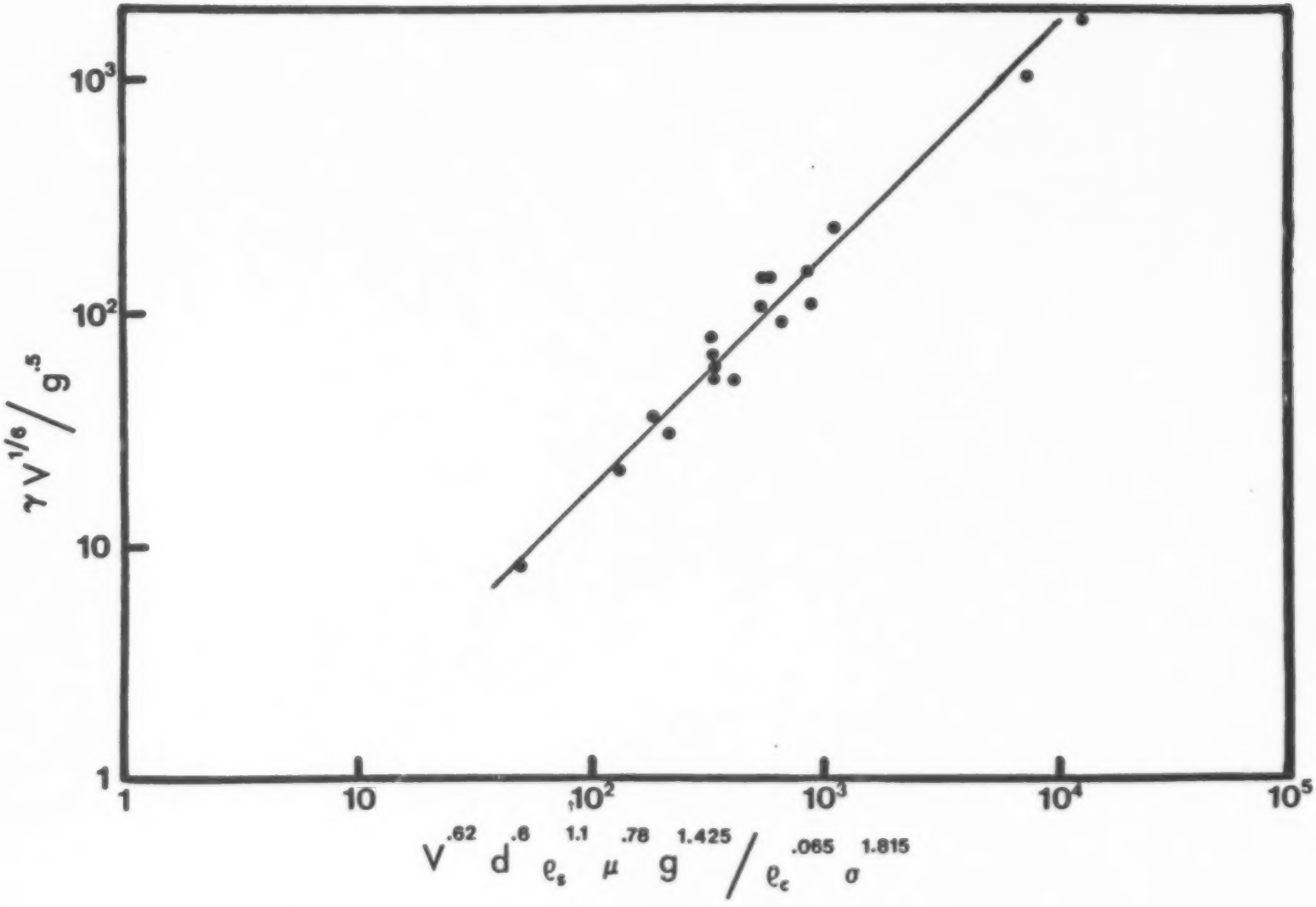

Figure 5.5.17 Snow Spreading Kinetics of Pentanol

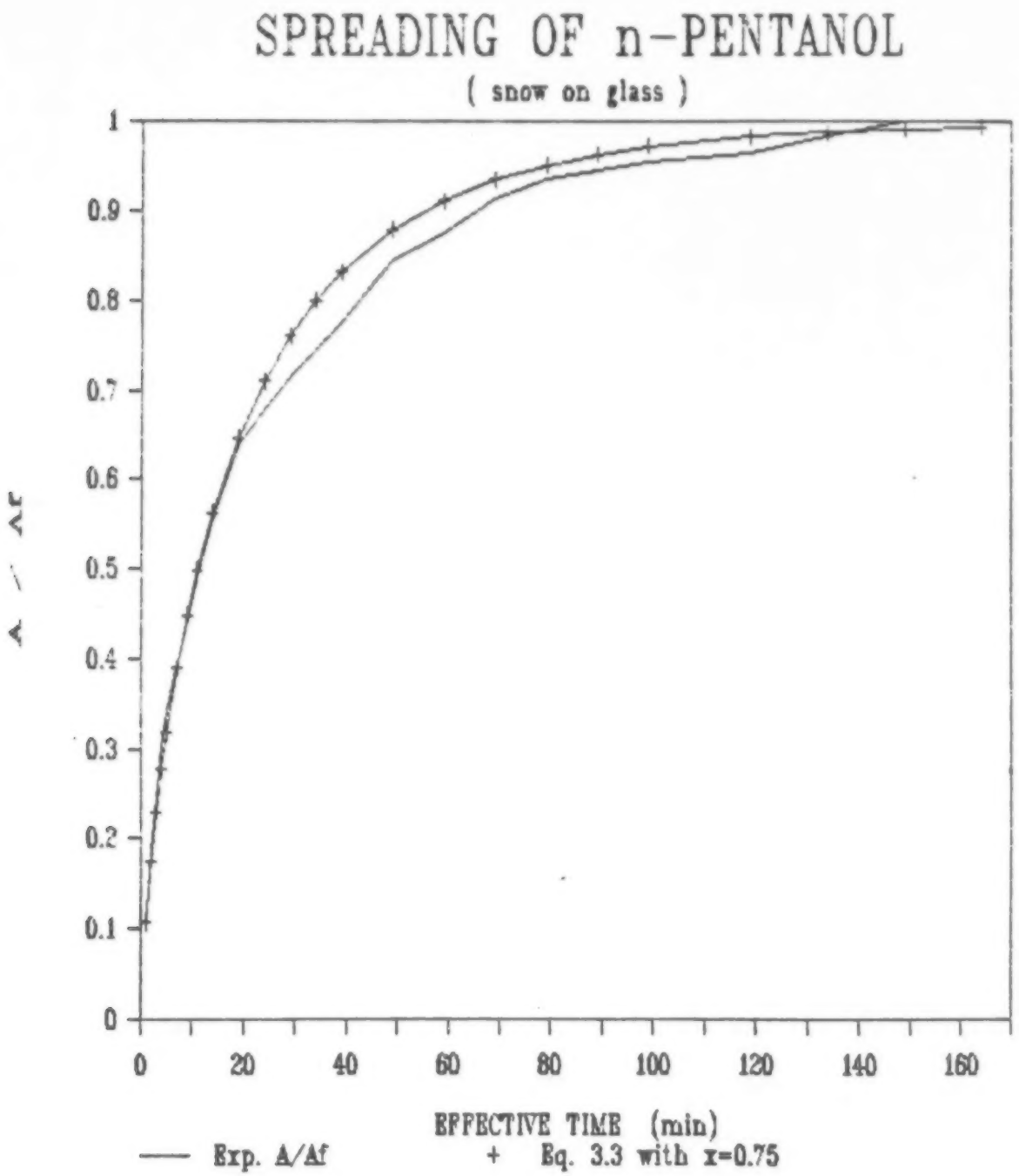

Figure 5.5.18 Snow Spreading Kinetics of Heavy Mineral Oil

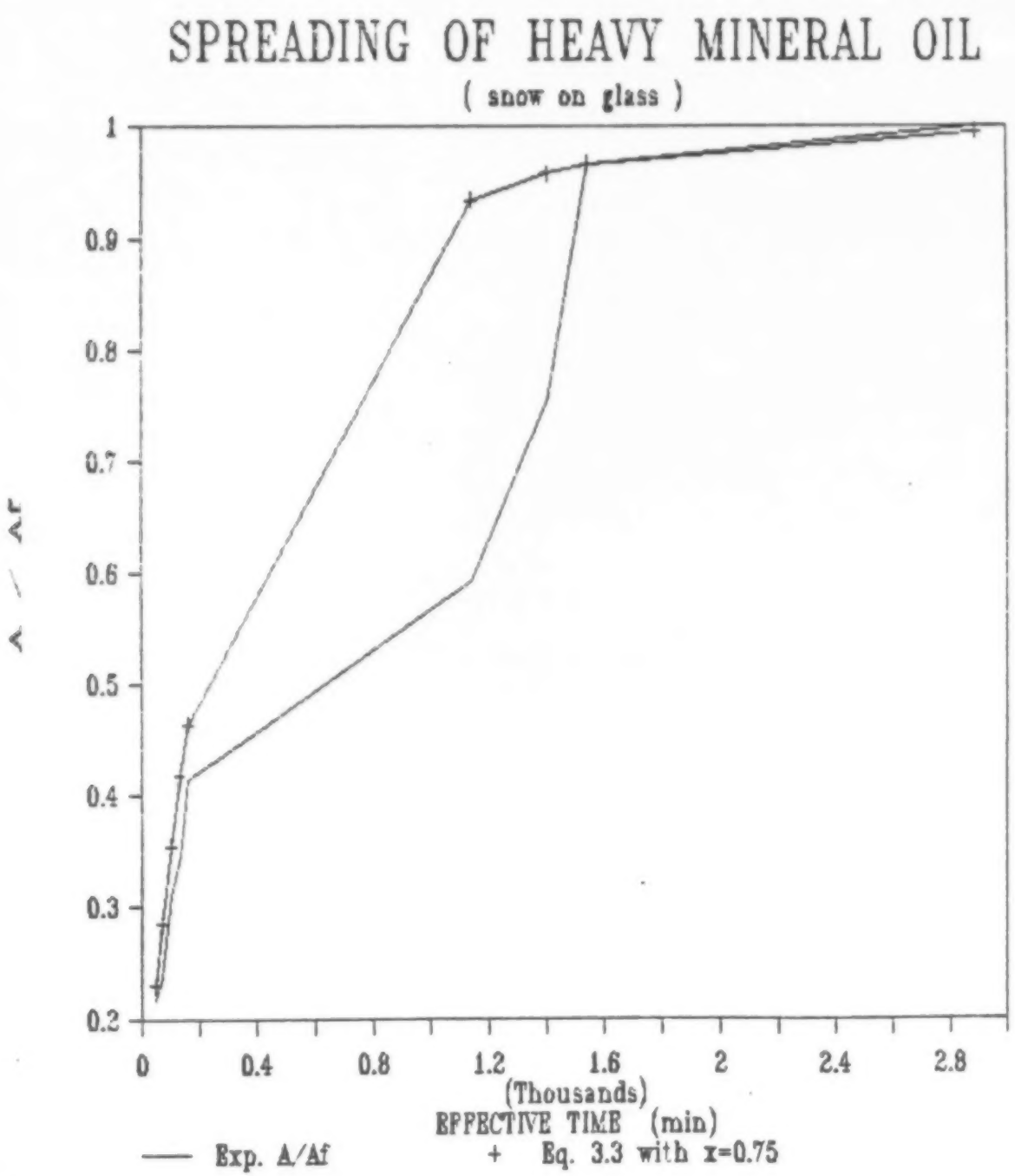

Figure 5.5.19 Spreading Kinetics of Bayol at Snow-Ice Interface

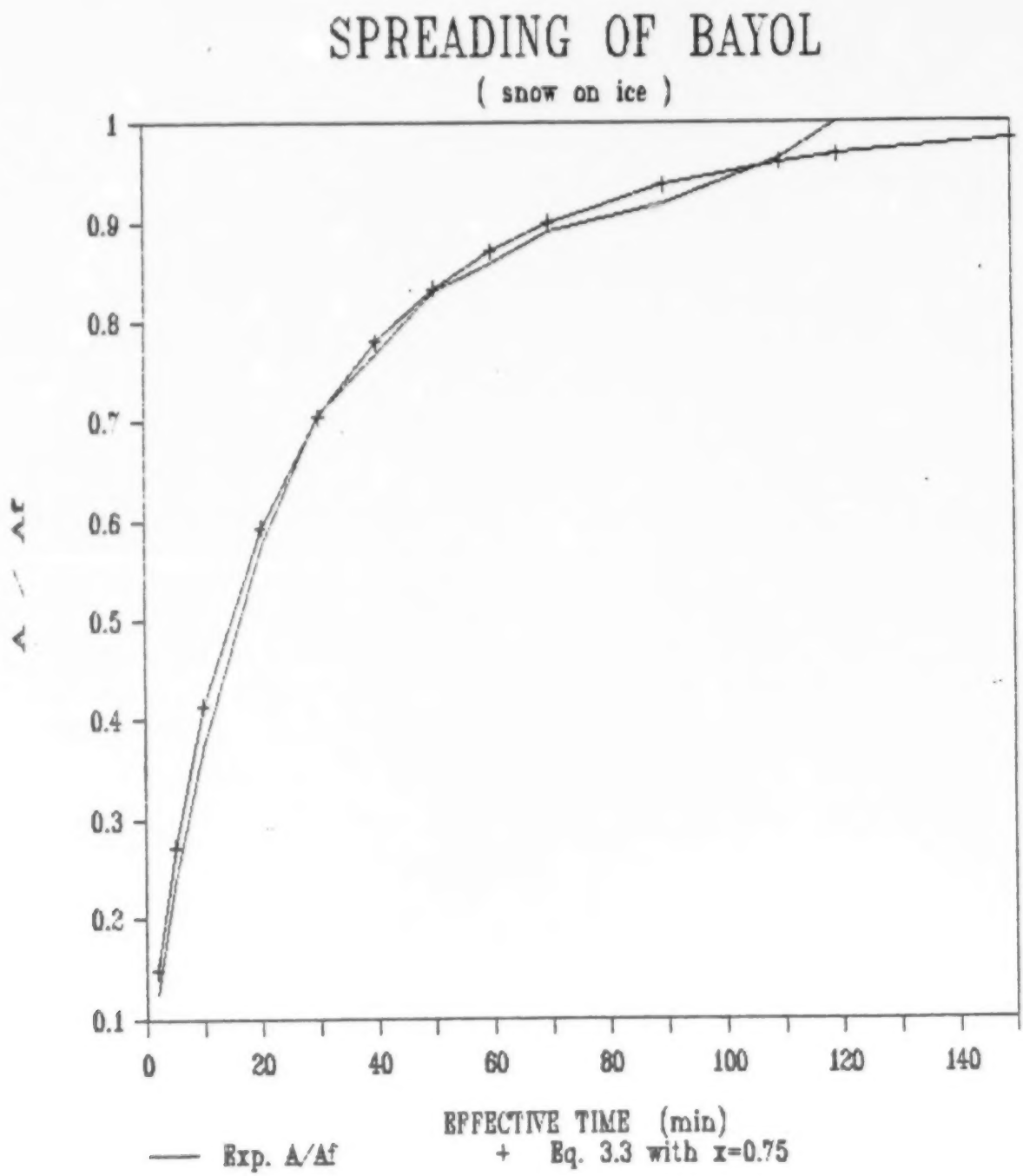

significant for very viscous chemicals, or for deep snowcover. However, the experimental penetration times were very small in comparison to the spreading time constant or the time of spreading. The experimental ratios of the penetration times with respect to the final spreading times never exceeded 0.06 for all snow experiments. (The average was found to be 0.013.) It was the result of this calculation and the fact that an accurate prediction of the penetration time would require accurate values of snow depth and properties, which favored the decision to neglect the penetration time in the spreading rate correlation.

The value of x in equation 3.3 was determined for experiments 12-16 and 18, using the same procedure employed for the ice experiments. The best value of x for these experiments ranged between 0.5 and 1.0, with an average of 0.75. The experimental area-time and the profile predicted by equation 3.3 (using experimental A_f and τ) with x of 0.75 are presented in Figures 5.5.17, 5.5.18 and 5.5.19 for pentanol, heavy mineral oil (snow on glass) and bayol (snow on ice), respectively. The unusual experimental profile observed for heavy mineral oil is attributed to the temperature fluctuations which occurred during the two days of spreading.

The spreading duration can be estimated by equation 3.12. The time of spreading is:

$$t_f = 8\tau \qquad (5.8)$$

5.5.7 Spreading Behaviour of Water Soluble Chemicals

The spill behaviour of water soluble (Group 3) chemicals on snow was observed to be different in many ways, in comparison to Group 1 and 2 spills. Instead of draining through the snow, these chemicals dissolved the snow on contact, with no surface spreading at the discharge area to produce a hole to the bottom of the snowcover, as was seen in Figure 4.12. Since the hole was formed almost instantaneously, the time of penetration for these chemicals was very small, ie. of the order of a few seconds.

Immediately after the discharge of chemicals onto the snow, a pool of liquid was observed at the base of the snowcover, as seen in Figure 5.5.20, for all experiments. For the experiment involving 1L of ethanol onto snow, with ice as its base (experiment no. 22), the initial liquid pool depth was 3 cm. As the spill spread radially along the snow-ice interface, the pool depth decreased, and completely disappeared after 30 minutes. By this time, a small "cave" had been formed around the perimeter of the discharge area.

A decrease in temperature of the pool of chemical/chemical-

snow-slush was also observed for all experiments. The maximum temperature depression usually occurred several minutes after the spill and this temperature was maintained until the disappearance of the liquid pool. At this point, continual measurements of the temperature of the chemical-snow slush revealed that the temperature gradually increased until the termination of the spreading at which the temperature was again approximately equal to the pre-spill temperature. Table 5.9 lists the lowest temperatures observed for three of the four experiments performed.

Table 5.9 Temperature of Group 3 Chemicals After Spill onto Snow

Exp. No.	Chemical	Average Surrounding Temp. (C)	Lowest Temp. Observed (C)
19	Ethanol	-1	-20
21	Sulphuric Acid	0	-10
22	Ethanol	0	-32

One observed result of the temperature depression was the formation of frost.

A cross section of the snow at the end of the experiment, as seen in Figure 5.5.21, reveals that the chemical did not completely dissolve the snow, and the diluted chemical and snow remained in a slush form at the bottom of the snowcover. A slight "caving in" of the snow at the discharge area was also observed for some experiments. For the spill of ethanol which employed an ice surface under the snow, several large cracks in the ice were observed. The cross section profile and the cracks are seen in Figures 5.5.22 and 5.5.23. The width of these cracks ranged from 1mm to 5mm, and the chemical was able to penetrate to the bottom of the 2 cm thick ice cover via these cracks. The cracking is attributed to the rapid decrease in temperature.

The effect of dissolution of snow on the spreading behaviour of these chemicals is tabulated in Table 5.10, which lists the proportionality constants calculated for the final snow spill area correlation (equation 5.6).

Comparison of the spill area correlation constant in Table 5.10 to the average constant of 0.45 for Group 1 and 2 chemicals reveals that the final spill area is much larger (8 to 10 times) for Group 3 chemicals than for similar spills of insoluble chemicals. A similar comparison can be made for the spreading time constant. Since the average constant for Group 1 and 2 chemicals was 0.18, the spreading rates and durations for experiments involving ethanol and ethylene glycol were much

slower and longer than for Group 1 and 2 chemicals, but sulphuric acid had a much faster rate of spreading.

Table 5.10 Constants for Equations 5.6 and 5.7.

Exp. No.	Equation 5.6 (Spill Area)	Equation 5.7 (Time Constant)
19	4.25	3.76
20	3.50	1.94
21	4.51	0.08
22	3.70	3.19

(The physical-chemical properties used in these equations were based on pre-spill properties)

These observations can be explained in part by the magnitude of the temperature depressions observed in the four experiments. Energy is required in the melting of the snow, which is one of the processes that occur during the snow dissolution. To obtain this energy, the system self cools, which results in the temperature drop. The magnitude of the temperature decrease depends on inter-related factors such as the rate of dissolution of snow and the heat of mixing of the chemical. The latter is believed to be the reason for the relatively small temperature drop for sulphuric acid, since it has the highest (exothermic) heat of mixing. From Rossini et al. (1952), the actual heat liberated (cumulative) when one mole of chemical dissolves in 10 moles of water is 67 kJ/mol for sulphuric acid, 7.4 kJ/mol for ethanol and 5.0 kJ/mol for ethylene glycol.

Since all Group 3 chemicals will, if given sufficient energy, melt and dissolve an infinite amount of snow and ice, the extent of dissolution and spreading must be a heat transfer influenced process. The spreading will probably stop when the chemical can no longer draw heat from the surroundings to melt additional snow. Since snow is a good insulator, the heat flux is limited. Therefore, under similar spill conditions, the chemical with the highest exothermic heat of mixing is thought to dissolve the greatest amount of snow, and hence, spread the farthest. This was confirmed by the results presented in Table 5.10, in which the largest value of the spill area correlation constant was observed for sulphuric acid. The smallest value was for ethylene glycol, which has the lowest heat of mixing.

The rate of spreading of these chemicals can also be explained by the heat of mixing property. The spreading rate of ethanol and ethylene glycol, was found to be much slower than for Group 1 and 2 chemicals. This is probably due to the combination of the slow rate of snow dissolution, which is aided by the relatively small heats of mixing and limited heat flux to the chemical-snow mixture, and the increase in chemical

viscosity as result of the temperature depression. On the other hand, the small value of the constant in equation 5.7 for sulphuric acid, as seen in Table 5.10, indicates a very fast rate of spreading. This behaviour is attributed to the release of significantly large amounts of heat at the beginning of the experiment, which caused the temperature of the sulphuric acid to rise to +10 deg C during the experimental discharge period. A high initial incremental heat of mixing (-28.1 kJ/mol to dissolve 1 mole of water) in comparison to the heat of fusion of water (+6.0 kJ/mol) is probably the reason for this temperature increase. Although the temperature quickly dropped to -10 deg C immediately after the discharge period, the temporary increase in temperature is believed to be the cause for the rapid initial melting and spreading.

Therefore, it can be concluded that the heat of mixing is an important parameter in describing the spreading behaviour of Group 3 chemicals. Due to the small number of experiments performed, no attmept was made to quantify the effect of this parameter, or the snow dissolution terms (h_s or H_s in equation 3.9). It is recommended that further studies be conducted to correlate the effect of snow dissolution on the spill area and the spreading rate.

Figure 5.5.20 Spill of Ethanol Immediately After Discharge

Figure 5.5.21 Cross-Section Profile of Ethanol in Snow

Figure 5.5.22 Spreading of Ethanol at the Snow-Ice Interface

Figure 5.5.23 Cracks in the Underlying Ice Surface

5.6 Application of This Study to an Actual Spill Situation

It is believed that the results of this study can be used to obtain a reasonable estimate of the general spreading behaviour of chemical spills on snow and ice surfaces. Since the chemical's ability to dissolve snow/ice is a major parameter affecting the spreading and its behaviour, this property should be determined before any calculations are made. This study proposed, and recommends a simple, 3-group classification system of chemicals, which can be used to estimate the extent of dissolution.

If a spill occurs on an ice surface, the final spill area and the spreading time constant can be predicted by equations 5.2 or 5.2a and 5.3 or 5.3a. Chemical viscosity and spill volume were found to be the major variables which affect the spreading behaviour. The spreading time constant serves two purposes: it can be used in equation 3.3 with x of 0.5 and the final area from equation 5.2 to obtain a profile of the increase in spill area with time; and it predicts the time of spreading, which can be approximated to be the product of a factor of 20 and the spreading time constant. Due to the chemicals selected in these experiments, these correlations apply only for chemicals in which water is not completely soluble (Group 1 and 2 chemicals) but they can be used with caution for water-miscible (Group 3) chemicals. It should also be noted that these correlations break down for low viscosity chemicals, such as xylene (0.9 cp), under high wind speeds.

Since ice is virtually impermeable to Group 1 and 2 chemicals, evaporation is the only natural exit route for these chemicals. For Group 3 chemicals, the chemical may migrate through existing cracks in the ice or cracks formed by the temperature drop associated with the spill of these chemicals. This will be of utmost concern if the spill occurs on ice on underlying body of water.

The spreading behaviour of chemical spills on snow are more complicated than for ice spills. For Group 1 and 2 chemicals, the chemical will be absorbed into the snow and will spread radially along the ground-snow interface. The spreading on the surface of the snow will be relatively small under most conditions. Exceptions may be spills of very viscous chemicals and/or spills on crusty or ice covered snow. The extent and the rate of subsurface spreading in snow media is significantly smaller and slower than for a corresponding spill on an ice surface. This area can be estimated by equation 5.6 or 5.6a and the time constant by 5.7 or 5.7a. The final spreading time can be approximated to be 8 times the time constant. The key variables required for these correlations are: chemical viscosity, spill volume, snow depth, density and crystal type. Although specific snow properties are usually not known, typical

values could be used.

Equations 5.6, 5.6a, 5.7, and 5.7a are believed to provide a reasonable estimate of the spreading behaviour of Group 1 and 2 chemicals in snow. However, these correlations are not recommended for a ground surface with a significant slope (ice surface is not a problem since it is usually formed horizontally), and in the presence of highly stratified snow and ice layers.

Spills of Group 3 chemicals are characterized by a "hole" in the snow at the point of discharge. Although the subsurface spreading extent and rate for these chemicals were not quantified explicitly in this study, the final area was found to be significantly greater than predicted by equation 5.6 or 5.6a, by a factor of 8 to 10 times. The results of these experiments suggest that the spreading characteristics for these chemicals are controlled by the various heat transfer processes that occur in the chemical- snow system. Further studies should be conducted to quantify the spreading behaviour of water soluble chemicals in snow media.

5.7 Sample Calculations

The final spill area and the time of spreading were calculated for a hypothetical spill of 1000 Litres of toluene on: relatively smooth ice surface; and snow-covered ice surface. The following conditions were assumed:

Ambient Temperature: -10 deg C
Initial Chemical Temperature: -10 deg C
Snow Depth: 30 cm of fresh snow.

The physical-chemical properties of toluene at -10 deg C:

Viscosity: 0.8 cp
Density: 0.9 g/mL
Surface Tension: 33 dynes/cm.

a. Spill on Ice

The final spill area can be estimated by equation 5.2 or 5.2a.

Equation 5.2:

$$\frac{A_f}{V^{2/3}} = 6.0 \frac{V^{.18} \rho_c^{.33} g^{.21}}{\mu^{.24} \sigma^{.09}}$$

Using SI units,

$$\frac{A_f}{(1)^{2/3}} = 6.0 \frac{(1)^{.18} (900)^{.33} (9.81)^{.21}}{(0.8\ E\text{-}03)^{.24} (0.033)^{.09}}$$

$$A_f = 690\ m^2.$$

The final spill area is approximately 690 m^2.

Equation 5.2a:

$$h_f = 0.008\ V^{.15} \mu^{.24}$$

kg-m-s units must be used for this equation.

$$h_f = 0.008\ (1.0)^{.15}\ (0.8\ E\text{-}03)^{.24}$$

$$= 0.0014\ m.$$

$$A_f = V/h_f = 1/0.0014 = 710\ m^2.$$

Using equation 5.2a, the predicted area is 710 m^2.

The spreading time, t_f, can be calculated by equation 5.4:

$$t_f = 20\,\gamma$$

Again, one of two equations, 5.3 and 5.3a, can be used to determine the spreading time constant, γ.

Equation 5.3:

$$\frac{\gamma\, V^{1/6}}{g^{.5}} = 2.5\ \text{E-05}\ \frac{V^{7/6}\ \mu^{.5}\ \rho_c^{1.625}\ g^{1.875}}{\sigma^{2.125}}$$

$$\frac{\gamma\,(1)^{1/6}}{(9.81)^{.5}} = 2.5\,\text{E-05}\ \frac{(1)^{7/6}\ (0.8\ \text{E-03})^{.5}\ (900)^{1.625}\ (9.81)^{1.875}}{(0.033)^{2.125}}$$

γ = 14,240 s, or approx. 4 hours.

Therefore, it is estimated that it will take 4 hours for the spill to reach 63% of the final area.

The spreading time is:

$$t_f = 20\ (4) = 80\ \text{h}\ .$$

Similar results are obtained using equation 5.3a:

$$\gamma = 5\ \text{E+05}\ V\ \mu^{.5}$$

$$\gamma = 5\ \text{E+05}\ (1)\ (0.8\ \text{E-03})^{.5}$$

γ = 14,140 s, or 3.9 hours.

t_f = 78 h.

Due to the long spreading time, the effects of evaporation should be considered in this situation.

b. Spill on Snow-Covered Ice Surface

For fresh snow:

ρ_s = 0.28 g/mL (from Table 2.1)
φ = 1.0 (from Table 5.8)

The final subsurface spill area at the snow-ice interface was estimated by equations 5.6 and 5.6a.

Equation 5.6:

$$\frac{A_f}{V^{2/3}} = 0.45 \frac{V^{.2}\ \mu^{.05}\ d^{.2}\ \rho_c^{.8675}\ g^{.4125}}{(\varphi\ \rho_s)^{.48}\ \sigma^{.4375}}$$

$$\frac{A_f}{(1)^{2/3}} = 0.45 \frac{(1)^{.2}\ (0.8\ E\text{-}03)^{.05}\ (0.3)^{.2}\ (900)^{.8675}\ (9.81)^{.4125}}{[(1)\ (280)]^{.48}\ (0.033)^{.4375}}$$

$A_f = 69\ m^2.$

Equation 5.6a:

$$h_f = 5.3\ E\text{-}04\ V^{.13}\ d^{-.2}\ \mu^{-.05}\ (\varphi\ \rho_s)^{.48}$$

$$= 5.3\ E\text{-}04\ (1)^{.13}\ (0.3)^{-.2}\ (0.8\ E\text{-}03)^{-.05}\ [(1)\ (280)]^{.48}$$

$$= 0.014\ m.$$

$A_f = V/h_f = 1/0.014 = 70\ m^2.$

The final spill area is approx. 70 m^2.

The time of spreading is (equation 5.8):

$$t_f = 8\gamma$$

The spreading time constant is:

Equation 5.7:

$$\frac{\gamma\ V^{1/6}}{g^{.5}} = 0.18 \frac{V^{.62}\ d^{.6}\ \rho_s^{1.1}\ \mu^{.78}\ g^{1.425}}{\rho_c^{.065}\ \sigma^{1.815}}$$

$$\frac{\gamma\ (1)^{1/6}}{(9.81)^{.5}} = 0.18 \frac{(1)^{.62}\ (0.3)^{.6}\ (280)^{1.1}\ (.8\ E\text{-}03)^{.78}\ (9.81)^{1.425}}{(900)^{.065}\ (0.033)^{1.815}}$$

$\gamma = 4200\ s = 70\ min.$

The time of spreading is, 8 (70) = 560 min, or 9 hours.

Equation 5.6a:

$$\gamma = 5700\ V^{.45}\ d^{.6}\ \rho_s^{1.1}\ \mu^{.78}$$

$$\gamma = 5700\ (1)^{.45}\ (.3)^{.6}\ (280)^{1.1}\ (.8\ E\text{-}03)^{.78}$$

τ = 5230 s, or 87 min.

This corresponds to a spreading time of 12 hours.

NOMENCLATURE

A	spill area
A_f	final spill area
C_a	absorption constant
C_e	evaporation constant
d	snow depth
Fv	viscous force
g	gravitational constant
h_a	spill depth lost due to absorption
h_e	spill depth lost due to evaporation
h_f	final spill depth (equivalent spill depth for snow)
h_s	spill depth gained due to dissolution
H_s	mean snow depth dissolved
K_a	absorption velocity
K_e	evaporation mass transfer coefficient
P	vapour pressure
R	gas constant
t	time
t_f	final spreading time
T	absolute temperature
v	molar volume
V	spill volume
x	slope term in equation 3.3
ϕ	volume fraction water in snow
φ	snow density parameter
ρ_c	density of chemical

ρ_s	density of snow
θ	contact angle
θ_e	equilibrium contact angle
σ	liquid surface tension
σ_i	ice surface tension
σ_{ic}	ice-chemical interfacial tension
$\Delta\sigma$	net spreading force
γ	spreading time constant
μ	chemical viscosity

REFERENCES

American Petroleum Institute. "Technical Data Book-Petroleum Refining, Chp. 7-14., 2nd ed., 1970.

Banerji B.K. "Physical Significance of Contact Angles" Colloid Polymer Sci. 259. 391-394 (1981).

Belore R., McBean E., Farquhar, G. "Modelling on the Spreading, Infiltration and Evaporation of Chemical Spills on Grass and Impermeable Surfaces" Proc. of the Technical Seminar on Chemical Spills, EPS, Environment Canada, (1986).

Bland W.F. ed. "Petroleum Processing Handbook" McGraw Hill, New York, 1967.

CRC. "CRC Handbook of Chemistry and Physics" 64th ed. CRC Press, Inc. Florida. 1983.

Canadian Transport Commission. "Report on Inquiry into the MacGregor Derailment" Railway Transport Committee, Western Division, (1980).

Chemcentral Corp. "Physical Properties of Common Organic Solvents and Chemicals" (1980).

Chen E.C., Charles D.K. "Surface Tension Spreading of Crude Oil on Ice" Mar. Sci. Comm. 2(1) 1-11, (1976).

Chen E.C., Overall J.C.K., Phillips C.R. "The Spreading of Crude Oil on an Ice Surface" Can. J. Chem. Eng. 52. 71-74, (1974).

Collins R.E. "Flow of Fluids Through Porous Materials" Reinhold Publishing Corp. New York, 1961.

Environmental Protection Service. "Manual for Spills of Hazardous Materials" Tech. Serv. Branch, Env. Canada, March, (1984).

Fay J.A. "Oil on the Sea" Hoult D.P., ed., Plenum Press, 1969.

Gardon J.L. J. Phys. Chem. 67, 1935, (1963).

Gerson D.F. "An Empirical Equation of State for Solid-Fluid Interfacial Free Energies" Colloid and Polymer Sci. 260, 539-544, (1982).

Good R.J. "Surface and Colloid Science" Good R.J., Stromberg R.R., ed., Vol.11, Chp.1, Plenum Press, New York, 1979.

Gray D.M., Male D.H. "Handbook of Snow" Pergamon Press, Toronto, 1981.

Horvath A.L. "Halogenated Hydrocarbons" M.Dekker, Inc., New York, 1982.

Hoult D.P., Wolfe S., O'Dea S., Patureau J.P. "Oil in the Arctic" Dept. of Transportation, US Coast Guard, Washington D.C., CG-D-96-75, (1975).

Kawamura P., Mackay D. "Evaporation of Volatile Liquids" Paper Submitted to the Journal of Hazardous Materials. (1986)

Klein G.J., Pearce C.D., Gold L.W. "Method of Measuring the Significant Characteristics of a Snowcover" Tech. Memo 18, Assoc. Comm. Soil Snow Mech., Nat. Res. Counc. Can., Ottawa, Canada, (1950).

Kuz'min P.P. "Snowcover and Snow Reserves" (English Transl. by Israel Proj. Sci. Transl., Transl. 828) Gidrometerologicheskoe, Izdatelitvo, Leningrad, (1960)

Magono C., Lee C.W. "Meterological Classification of Natural Snow Crystals: J. Faculty Sci., Hokkaido Univ., Ser. VII (Geophysics) Vol 2, pp 321-325, (1966).

McMinn T.J. "Crude Oil Behaviour on Arctic Water Ice" Dept. of Transportation, US Coast Guard, Project 734108, Sept. (1972).

National Research Council. "Classification for Snow" Int. Assoc. Hydrol. Sci. Tech. Memo No. 31., Nat. Res. Counc. Can. Ottawa, Canada, (1954).

Neumann A.W. Personal Communication, University of Toronto, 1986.

Neumann A.W., Good R.J. "Surface and Colloid Science" Good R.J., Stromberg R.R., ed., Vol. 11, Chp.2, Plenum Press, New York, 1979.

Overall J.C.K. "A Study of Terrestial Crude Oil Spills in Arctic Winter Conditions: Field Experiments and Computer Simulation" MASc Thesis, University of Toronto, 1976.

Polak J., Lu B.C-Y. Can. J. Chem., 51, 4018, (1973).

Raisbeck J.M., Mohtadi M.F. "The Environmental Impacts of Oil on Land in the Arctic Regions" Water, Air, and Soil Pollution, 3, 195-208, (1974).

Rossini F.D., Wagman O.D., Evans W.H., Levine S., Jaffe I. "Selected Values of Chemical Thermodynamic Properties" Nat. Bureau of Std. 500, US Govt. Printing Office, Washington D.C. 1952.

Spelt J.K., Absolom D.R., Zingg W., van Oss C.J., Neumann A.W. "Determination of the Surface Tension of Biological Cells Using the Freezing Front Technique" Cell Biophyns. 14, 117, (1982).

The Toronto Star. "Crews Try to Stem Leak After Acid Cars Derail", February 13, p. A7, (1986).

Zukovs G., Metcalfe D.E., Mackay D. "Modelling of the Short Term Behaviour of PCB Spills" Proc. Tech. Seminar on Chemical Spills, EPS, Environment Canada, (1986).

ACKNOWLEDGEMENTS

The authors are grateful to Environment Canada and the Natural Sciences and Engineering Research Council for financial support.

APPENDIX A: SOLUBILITY DATA

Chemical	Solubility of Water/Ice in Chemical (wt %)	Temperature (deg C)	Source
GROUP 1			
Aniline	4.0	- 5	exp
1,3 Butadiene	0.0213	- 5	6
	0.017	- 10	6
	0.0093	- 20	6
Butylene	0.0201	6	6
Carbon Tetrachloride	0.00354	0	2
	0.00217	- 10	2
	0.00131	- 20	2
Chloroform	0.11	- 5	exp
	0.92	- 10	exp
1,2 Dichlorobenzene	0.0334	25	2
Ethyl Acetate	2.2	- 5	exp
Ethylbenzene	0.0178	0	1
Ethylene Dichloride	0.0968	0	2
	0.0716	- 10	2
	0.0504	- 20	2
Fluorochloromethane(R11)	0.00451	0	2
	0.00282	- 10	2
	0.00167	- 20	2
Fluorochloromethane(R21)	0.05347	0	2
	0.03546	- 10	2
	0.02307	- 20	2
Gasoline	0.0005 *	22	1
n-Hexane	0	- 5	exp
1-Hexanol	2.9	- 5	exp
	3.7	- 10	exp
Isopropylbenzene	0.0152	0	6
Methyl Isobutyl Ketone	0.67	- 5	exp
	0.57	- 10	exp
Methyl Methacrylate	1.8	- 5	exp
Methylene Chloride	0	- 10	exp
Mineral Oil (USP Heavy)	0	- 5	exp
Naptha Solvent (54.3 deg API)	4.5*	152	6
Perchloroethylene	0.003471	0	2
	0.002071	- 10	2
	0.001258	- 20	2
Styrene	0.032	4	3
Toluene	0	- 5	exp
1,1,1 Trichloroethane	0	- 10	exp
Turpentine	0	- 5	exp
White Mineral Oil (Bayol-35)	0	- 5	exp
m-Xylene	0	- 5	exp
o-Xylene	0.0185	0	1

* solubility given in mole %

GROUP 2

1-Butanol	9.0	- 5	exp
	8.8	- 10	exp
	7.6	- 20	exp
2-Butanol	**	- 5	exp
	20	- 10	exp
	7.8	- 20	exp
Methyl Ethyl Ketone	**	- 5	exp
1-Pentanol	6.7	- 5	exp
	7.3	- 10	exp
	5.0	- 20	exp
2-Pentanol	14	- 5	exp
	6.6	- 10	exp
Propylene Oxide	**	- 5	exp

** two liquid phases formed

GROUP 3

Acetic Acid	-	5
Acetone	-	5
Acrylonitrile	-	5
Ethanol	-5	exp
Ethylene Glycol	25	4
Ethylene Oxide	-	5
Formaldehyde	-	5
Hydrazine	-	5
Hydrofluoric Acid	-	5
Hydrochloric Acid	-	5
Hydrogen Fluoride	-	5
Hydrogen Peroxide	-	5
Methanol	- 5	exp
Methylamines (di & tri)	-	5
Nitric Acid	-	5
Oleum (Reacts with water)	-	5
Phosphoric Acid	-	5
1-Propanol	- 5	exp
Propylene Glycol	-	5
Sulfuryl Chloride (Reacts with water)	-	5
Sulphuric Acid	-	5

- No specified temperature

---

1 Polak and Lu (1973)
2 Horvath (1982)
3 Bland (1967)
4 Chemcentral Corp. (1980)
5 Environmental Protection Service (1984)
6 American Petroleum Institute (1970)

APPENDIX B: CONTACT ANGLE DATA ON GLASS

Chemical/ Solution	Liquid Surface Tension (dynes/cm)	Equil. Contact Angle (deg)
Ethylene Glycol 100% (aqueous solution)	48	11
80%	50	17
60%	54	20
54%	55	14
32%	60	10
Glycerol 100%	63	38
80% (aq)	65	17
47%	69	30
40%	70	14
n-Heptane	20	15
n-Octane	22	16
1-Butanol	25	11
1-Pentanol	26	11
m-Xylene	29	8
Toluene	29	11
38% aq. sucrose	74	19

Temperature: 22 deg C.

APPENDIX C: EXPERIMENTAL DATA - ICE EXPERIMENTS

Chemical	Vol. (mL)	Ice Surface	Temp. (C)	Spill Area (cm2)	Time Constant (s)	Spreading Time (s)
m-xylene	50	smooth	-5	1452	0.25	1.0
m-xylene	25	smooth	-5	887	0.22	40
m-xylene	50	rough (1)	-5	1576	10	180
m-xylene	50	rough (2)	-5	1590	10	120
bayol	50	smooth	-5	1122	10	180
bayol	25	smooth	-5	531	20	120
bayol	50	rough (1)	-5	1555	50	360
bayol	50	rough (2)	-5	1385	40	480
1-pentanol	50	smooth	-5	616	0.2	60
1-pentanol	25	smooth	-5	342	0.25	600
1-pentanol	50	rough (1)	-5	733	5	600
1-pentanol	50	rough (2)	-5	784	10	180
mineral oil (heavy)	50	smooth	-5	330	95	3000
mineral oil	25	smooth	-5	141	50	2760
mineral oil	50	rough (1)	-5	388	210	8040
mineral oil	50	rough (2)	-5	232	120	2280
m-xylene	450	outdoor	-8	5800	9	360
m-xylene	1000	outdoor	-9	25500	55	300
1-pentanol	1000	outdoor	-6	8742	14	270
bayol	700	outdoor	-6	11300	70	1200
mineral oil (light)	2000	outdoor	-7	13900	565	5400

Ice Surface: (1) - surface roughness 0.5-1 mm
(2) - surface roughness 1-2 mm.

APPENDIX D: EXPERIMENTAL DATA - SNOW EXPERIMENTS

Exp. No.	Bottom Spill Area (cm2)	Spr. Time Constant (min)	Penetration Time (min)	Spreading Time (min)	Surface Spill Area (cm2)
1	573	4	0.2	56	252
2	1104	5	0.25	75	415
3	1886	7.5	0.25	105	804
4	2800	8	0.2	60	700
5	2463	7.5	0.25	60	452
6	2946	13.75	0.7	85	254
7	3293	17	1.8	105	284
8	3685	35	3.5	270	180
9	2133	6	0.3	60	42
10	1427	13	0.8	120	140
11	1172	24	1.2	90	420
12	1676	1.3	0.25	20	95
13	1901	11	1.1	75	154
14	2060	18	1.1	150	117
15	2043	170	50	780	1040
16	2830	300	140	3030	1200
17	2800	20	0.2	60	710
18	5675	23	-	120	1200
19	2920	3	-	240	13 *
20	3217	120	-	387	78 *
21	5313	65	-	290	64 *
22	17090	125	-	700	200*

* area of "hole" in the snow